ADVANCED MATERIALS
www.advmat.de

A Comprehensive Review on Intracellular Delivery

*Dorsa Morshedi Rad, Maryam Alsadat Rad, Sajad Razavi Bazaz, Navid Kashaninejad, Dayong Jin, and Majid Ebrahimi Warkiani**

Intracellular delivery is considered an indispensable process for various studies, ranging from medical applications (cell-based therapy) to fundamental (genome-editing) and industrial (biomanufacture) approaches. Conventional macroscale delivery systems critically suffer from such issues as low cell viability, cytotoxicity, and inconsistent material delivery, which have opened up an interest in the development of more efficient intracellular delivery systems. In line with the advances in microfluidics and nanotechnology, intracellular delivery based on micro- and nanoengineered platforms has progressed rapidly and held great promises owing to their unique features. These approaches have been advanced to introduce a smorgasbord of diverse cargoes into various cell types with the maximum efficiency and the highest precision. This review differentiates macro-, micro-, and nanoengineered approaches for intracellular delivery. The macroengineered delivery platforms are first summarized and then each method is categorized based on whether it employs a carrier- or membrane-disruption-mediated mechanism to load cargoes inside the cells. Second, particular emphasis is placed on the micro- and nanoengineered advances in the delivery of biomolecules inside the cells. Furthermore, the applications and challenges of the established and emerging delivery approaches are summarized. The topic is concluded by evaluating the future perspective of intracellular delivery toward the micro- and nanoengineered approaches.

1. Introduction

Introducing small biomolecules, nucleic acids (DNA and RNA), proteins, synthetic nanomaterials, and drugs into cells (coined as intracellular delivery) is a powerful means to monitor and decode the cellular behaviors as well as influence the cellular fates and its biological functions.[1] Efficient intracellular delivery technologies play a crucial role in biomedical discoveries, biomanufacture, and therapeutic applications.[2] Direct delivery of exogenous cargoes requires to surpass the plasma membrane barrier, which protects the intracellular compositions from outside of the cell. However, the precise underlying mechanisms responsible for biomolecule uptake in certain methods are not fully realized.[3,4]

The existing delivery technologies offer the ability to transport the cargo across the cell membrane, which can be broken down into two areas of macro- or micro- (containing both micro and nano) techniques based on their impact resolution, as shown schematically in **Figure 1**. Macro technologies mainly rely on conventional setups to deliver cargoes to the bulk populations of cells.[5] These approaches are primarily categorized into the carrier-based techniques, which involve fusion and endocytic entry pathways, and membrane-disruption-mediated techniques, which include plasma membrane permeabilization and direct penetration mechanisms.[2,6] Carrier-mediated methods are mainly divided into two categories of biological and chemical approaches.[7] The biological approaches broadly rely on the intracellular delivery of genetically engineered viruses into cells called viral delivery or transduction.[8] The chemical approaches utilize carrier molecules that are mostly cationic lipids, calcium phosphate, or cationic polymers to neutralize or impart a positive charge to anionic proteoglycans on the cell membrane and induce endocytosis.[9]

On the contrary, membrane-disruption-mediated methods can proceed via nucleation and further expansion of transient discontinuities in the cell membrane either by chemical, mechanical, or field-assisted methods. Chemical disruption methods are initiated by triggering of phospholipid bilayer followed by membrane deformation, which can occur through oxidation or peroxidation of constituent lipids and insertion of amphiphilic peptides or proteins.[10] Mechanical methods

Dr. D. Morshedi Rad, Dr. M. Alsadat Rad, S. Razavi Bazaz, Dr. N. Kashaninejad, Dr. M. Ebrahimi Warkiani
School of Biomedical Engineering
University of Technology Sydney
Sydney, NSW 2007, Australia
E-mail: majid.warkiani@uts.edu.au
Dr. D. Morshedi Rad, Dr. M. Alsadat Rad, S. Razavi Bazaz, Dr. N. Kashaninejad, Prof. D. Jin, Dr. M. Ebrahimi Warkiani
Institute for Biomedical Materials & Devices (IBMD)
Faculty of Science
University of Technology Sydney
Sydney, NSW 2007, Australia
Prof. D. Jin
School of Life Sciences
Faculty of Science
University of Technology Sydney
Sydney, NSW 2007, Australia
Dr. M. Ebrahimi Warkiani
Institute of Molecular Medicine
Sechenov University
Moscow 119991, Russia
The ORCID identification number(s) for the author(s) of this article can be found under https://doi.org/10.1002/adma.202005363.

DOI: 10.1002/adma.202005363

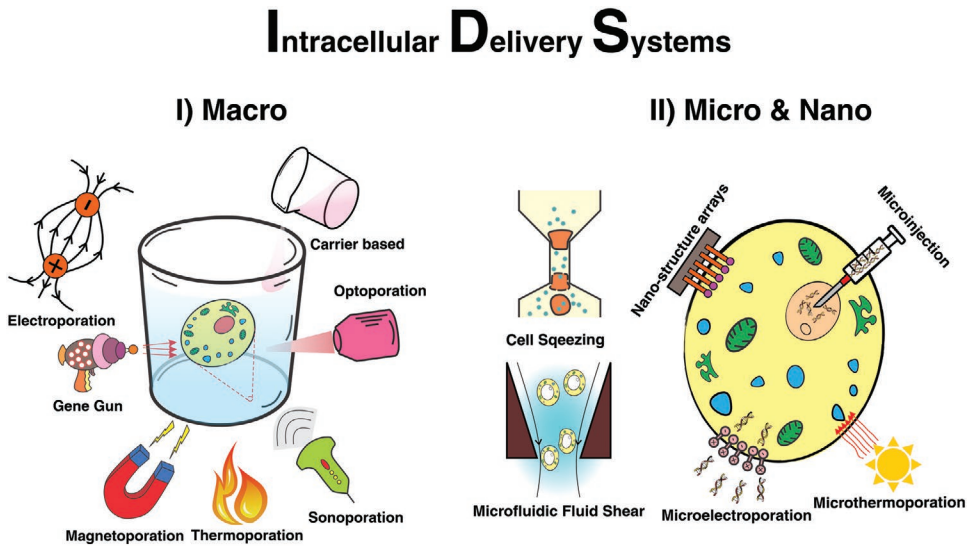

Figure 1. Schematic overview of the scope of the current review paper. Existing intracellular delivery systems can be divided into: I) macroengineered or II) micro and nanoengineered approaches.

of membrane disruption are categorized as particle bombardment,[11] fluid shear,[12] and osmotic pressure.[13] Furthermore, field-assisted delivery methods are those in which an external energy/source is necessary for defect formation in the cell membrane. Depending on the source, these methods are categorized as sonoporation,[14] optoporation,[15,16] thermoporation,[17] magnetoporation,[18] and electroporation.[19] Once chemical modifications, extensive mechanical forces, or high-intensity energies are introduced to the cells, the plasma membrane will experience the perturbation state, which triggers an increase in membrane deformation and permeability of the exogenous cargo.[20] Upon intracellular cargo delivery, the cell would reseal the disruptions through the active membrane and cytoplasmic recovery processes, which largely depend on the cell type, pore size, temperature and the factors presented in the extracellular medium.[21] Studies have proposed up to six different plasma membrane resealing mechanisms (e.g., exocytosis) that are implicated in active membrane repair.[22] For instance, in the case of exocytosis, the lesions with the size of several hundred nanometers or less are extracted, leading to the withdrawal of the disruption into a disposable vesicle for releasing lysosomal signals and further membrane remodeling processes.[23–26]

Despite several advantages of conventional macroscale technologies, they critically suffer from issues such as low cell viability, cytotoxicity, and inconsistent material delivery. Motivated by these shortcomings, micro- and nanoengineered delivery devices have emerged as a promising solution with improved delivery outcomes. The cargo delivery in these devices is mainly based on membrane-disruption-mediated mechanism. In these approaches, microfabrication and nanotechnology have enabled the precise control over the delivery procedure and make previously intractable modalities more feasible for intracellular loading of macromolecular cargoes and exogenous compounds.[27] Furthermore, these platforms gives the biologists the opportunity to perform intracellular delivery even at the single cell level with a high level of efficiency and throughput.[28] Early studies on microengineered approaches have led to the development of the relatively low-throughput methods (e.g., microinjection in the 1980s).[29] The advancements in the development of those intracellular delivery systems are attributable to their limitations, including low-cell viability and low throughput. Recent efforts have focused on reinvigorating the conventional macroscale approaches through nanotechnology, microfluidics, and lab-on-chip devices. Different modalities and platforms have been designed to increase the delivery efficiency and cell viability; e.g., employing micro/nanofluidic devices for localized electroporation.[30] The miniaturization in this context is beyond the simple scale down the model. It adds additional functionalities to the system, which are otherwise impossible.[31] For instance, micro- and nanoscale electroporation devices have been developed to eliminate the shortcomings of conventional bulk electroporation such as changes in the local pH, Joule heating, distortion of the applied electric field, sample contamination through corrosion of electrodes, and the consequent cell damage. While certain intracellular delivery techniques such as electroporation can be implemented either at the macro or microscale, few established techniques such as microinjection are exclusive to the delivery at microscale.

Along with the advances in fabricating the miniaturized devices, a variety of nanomaterials (e.g., carbon nanotubes, nanoparticles, and magnetic nanospears) have been developed to overcome the challenges of conventional techniques.[32] It is envisioned that advances in micro- and nanoscale delivery systems can lead to minimally invasive and highly efficient strategies for effective transportation of biomolecules across the cell membrane. Nevertheless, each delivery modality has its own advantages and limitations, and thus there is a pressing need for further improvements.

Thus far, many studies and review papers have investigated the potential of different delivery modalities. However, there are still some critical issues in this area which have not been tackled properly. Mainly, much less attention has been given

to critically investigate the microengineered approaches for intracellular delivery. Accordingly, there is a lack of a review paper covering the entire established and recently emerging micro- and nanoengineered techniques. Moreover, applications of these delivery strategies are always a missing link in such review papers. This paper is an overview of the classification and applications of various intracellular delivery systems. These approaches can be thought of as macro or microscale (containing both micro and nano) delivery techniques. In particular, micro- and nanoengineered intracellular delivery methodologies are highlighted, and the future perspectives of next-generation intracellular delivery strategies are discussed.

2. Macroengineered Intracellular Delivery

Generally, macroengineered delivery systems can be categorized into two major groups, namely carrier-mediated (divided into the biological and chemical methods) and membrane-disruption-mediated systems (mainly referred to as physical techniques, including chemical, mechanical, and field-assisted delivery systems), as shown in **Figure 2**. In this section, a detailed description of these methods is provided.

2.1. Carrier-Mediated Delivery Systems

For almost half a century, biological and chemical vehicles have been exploited as carrier-mediated means of cargo delivery into target cells. These vehicles encapsulate the exogenous biomolecules to facilitate the intracellular delivery. Once these vectors are attached to the cell membrane, the cargo will be loaded into the intracellular space through either fusion or endocytic entry pathway.[33] Further details on two common approaches of carrier-mediated delivery systems, which are biological and chemical methods, are discussed as follows.

2.1.1. Biological Method

In the biological method, a bioinspired carrier (e.g., viral vector, cell ghost, and extracellular vesicle) is used to introduce nucleic acids such as oligonucleotides of DNA or RNA, plasmid DNA, and mRNA into the intracellular space.[34] The available literature results indicated that viral-mediated gene delivery is the most common solution used in phase I/II clinical trials owing to their high delivery efficiency and specificity.[35] Retroviral, adenoviral, and adeno-associated viral vectors are the most

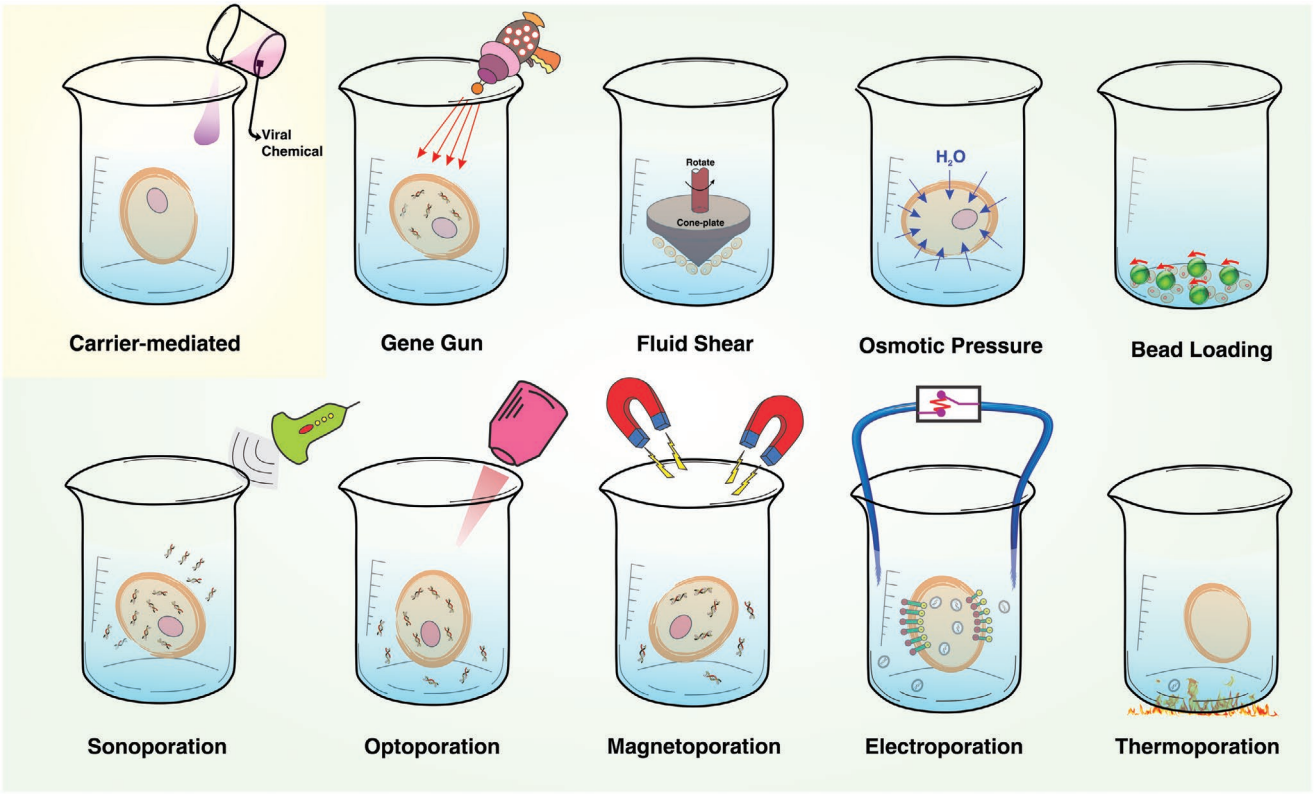

Figure 2. Schematic illustration of commonly used intracellular delivery systems at macroscale. Carrier-mediated delivery systems are highlighted in yellow, and membrane-disruption-mediated ones are highlighted in light green. In carrier-mediated approaches, a mediating carrier is required to transfer the cargo into the cells. This carrier can be either biological- or chemical-based. Membrane-disruption-mediated approaches cause transient damage into the cell membrane through either chemical, mechanical, or field-assisted techniques. Chemical disruption of membrane barrier can take place as a result of modifications in constituent lipids of cell membrane via oxidation, insertion of pore-forming peptides or proteins, or exposure to detergents or surfactants. Mechanical methods include gene gun, fluid shear, and osmotic/hydrostatic pressure. Field-assisted techniques utilize an external field to induce transient membrane rupture as exemplified by sonoporation, optoporation, magnetoporation, electroporation, and thermoporation.

commonly used vectors for the intracellular cargo delivery into mammalian cells.[36] However, major drawbacks of this approach are immunogenicity, cytotoxicity, and the limited packaging capacity of the foreign DNA.[37] Accordingly, several efforts have been devoted to the development of nonviral carriers such as extracellular vesicles. Exosomes are a subpopulation of membrane-derived vesicles, which are released into the extracellular space.[38] These vesicles have been emerged as pivotal mediators of cell–cell communications and regulators of different biological processes, such as tissue regeneration,[39] immune response modulation,[40] and stem cell maintenance over the past decade.[41] Furthermore, exosomes possess numerous advantageous features such as biocompatibility, nonimmunogenicity, and the inherent ability to traverse the blood–brain barrier (BBB).[42] Together these unique features made exosomes suitable carriers for intracellular delivery applications.[43] Early studies have shown the therapeutic potential of unmodified and genetically engineered exosomes in delivery of small molecules, proteins, and nucleic acids.[44] Researchers subsequently used exosomes to deliver curcumin into macrophages,[45] encapsulate paclitaxel and doxorubicin to bypass the BBB in zebrafish embryos,[46] and load doxorubicin into a mouse tumor tissue model.[47]

Along with exosome-mediated delivery of small molecules, researchers began experimenting with exosomes encapsulating proteins. One study has indicated the ability of exosomes in transferring CC chemokine receptor 5 (CCR5) protein from $CCR5^+$ to $CCR5^-$ peripheral blood mononuclear cells.[48] Haney et al. encapsulated antioxidant protein catalase in exosomes followed by intravenous injection to the C57BL/6 mice. Neuroprotective effects in mice with acute brain inflammation was evidenced by the accumulation of this protein in neurons and microglial cells.[49] Besides the intercellular transferring of functional proteins, a growing body of evidence has described the exosome-mediated RNA delivery.[50] Further investigations using exosomes have successfully delivered small interfering RNAs (siRNAs) into various cell types such as T cells,[51] endothelial cells,[52] HeLa cells, and fibrosarcoma cell line.[53] In 2010 Montecalvo and co-workers showcased the first evidence for transferring microRNAs between dendritic cells using endogenously released exosomes.[54] Ohno et al. conducted an investigation into the efficient delivery of let-7a through intravenous injection of $GE\text{-}11^+$ exosomes to xenograft breast cancer cells in $RAG2^{-/-}$ mice. This resulted in the specific binding of $GE\text{-}11^+$ exosomes containing let-7a to the EGFR-expressing tumor cells leading to in vivo inhibition of tumor development and progression.[55] However, the exact mechanisms of exosome-mediated delivery are yet to be extensively explored. The future intracellular delivery applications via exosomes are anticipated to greatly improve the safety and efficiency of drug delivery into different cell types above what is currently achieved through other biological carriers.

2.1.2. Chemical Methods

In chemical delivery strategies, calcium phosphate ($Ca^{2+}P$), polycations (cationic polymers), or lipid-based carriers (cationic lipids and liposome) are used as a reagent for carrier-mediated delivery approaches.[56] These positively charged chemical compounds readily complex with nucleic acids to enable their contact with negatively charged phospholipid bilayer of the cell membrane.[57] The efficiency of this delivery method is determined by various factors, such as the ratio of foreign DNA to the chemical compound and the properties of the target cell (type, density) and the chemical complex (size, charge, and pH).[58–61] Among these methods, calcium phosphate coprecipitation is one of the most cost-effective yet simple chemical delivery methods.[62] This method is suitable for accommodating a high concentration of foreign DNA using calcium chloride and HEPES-buffered saline solution containing sodium phosphate. This method was first used by Graham and van der Eb in 1973 and became a prevalent method since then.[63] Although this method is safe, low-cost, and easy-to-perform, it suffers from $Ca^{2+}P$ nanoparticle aggregation that may significantly reduce the delivery efficiency.[64]

Polycations (cationic polymers) are positively charged polar groups with tunable physicochemical properties, constituting complexes through binding to the negatively charged phosphate groups of DNA molecules.[65,66]

The DNA–polycation complexes with an overall positive net charge are introduced to the cells via nonspecific endocytosis, which leads the cytoplasmic delivery of these complexes followed by transferring DNA into the nucleus.[56] Based on the physicochemical properties of cationic polymers, they are synthesized in different sizes, shapes, and surface charges that form three general structures including linear structure such as spermine, histone (natural DNA binding proteins), and poly-L-lysine (PLL),[67,68] branched structure such as polyethylenimine (PEI) and diethylaminoethyl dextran (DEAE—dextran),[68,69] and spherical structure such as polyamidoamine dendrimers (PAMAM).[68,70]

The lipid-based intracellular delivery takes advantage of highly biocompatible cationic lipids to deliver exogenous DNA or RNA into the cell.[71] This widely used delivery system is mainly based on cationic lipids consisted of one or two hydrocarbon chains and a head group with a net positive charge interacting with the negatively charged phosphate group of the DNA or RNA molecules forming liposomal transfection structure (lipoplex).[56] This complex structure later interacts with the cell membrane through its surface positive charge followed by taking up into the target cell.[72] Taking the benefits of liposomes (phospholipid spherules), this kind of delivery strategy was first reported in the 1980s.[73,74] Lipofection (lipid/liposome-based transfection) introduces DNA molecules with a 5- to 100-fold increase in delivery efficiency compared to the other chemical delivery methods.[72] Delivery efficiency in this strategy mainly depends on a variety of factors, namely pH and type of cell line. In this regard, for each cell line, the optimized operating conditions must be identified, as well.[75]

Commercially available synthetic cationic lipids include Lipofectamine (Life Technologies), [76] Nanojuice (Merck Millipore),[77] and FuGene 6 (Promega), which can condense nucleic acids into compact nanoparticles.[78] Although cationic lipids provide efficient delivery of certain cargoes, the core weakness is cytotoxicity of this setup that directly affect the cell viability. Thus, maltose-based cationic liposomes with different

hydrophobic chain lengths have been developed recently to reduce cytotoxicity and improve delivery outcomes.[79]

2.2. Membrane-Disruption-Mediated Systems

Membrane-disruption-mediated modalities refer to the introduction of an intended cargo to the target cell through transient discontinuities created in the phospholipid bilayer of the cell membrane. Unlike carrier-mediated delivery strategies that are limited to the restricted combination of cargoes and cell type, membrane-disruption-mediated approaches enable temporal control and instantaneous delivery as they are less dependent on cargo properties.[80] Here, we categorized membrane-disruption-mediated systems based on chemical, mechanical (particle bombardment, scrape/bead loading, fluid shear, or osmotic/hydrostatic pressure) and field-assisted (acoustic, optical, thermal, magnetic, or electrical) methods.

2.2.1. Chemical Methods

There are some permeabilization approaches depending on biochemical agents to permeabilize cell membranes. Generally, chemical disruption of lipid barriers is achieved via 1- exposure to certain non-ionic detergents (e.g., Triton X-100, Tween-20, sodium dodecyl sulfate (SDS), lauryl maltoside, octyl glucoside, saponin or digitonin), or organic solvents (such as DMSO, ethanol, or other alcohols), 2-insertion of pore-forming peptides, and 3-oxidation or peroxidation of constituent lipids.[81,82] Saponin and digitonin (a prototype member of the saponin family) are steroid and triterpinoid glycosides that permeabilize cell membrane by preferentially interacting and complexing with cholesterol- and hydroxysterol-rich membranes.[83] In one study, it is demonstrated that delivery of targeted optical contrast agents in the range of 1–150 kDa into the live cells can take place by controlling the mole ratio of Triton X-100 to the number of treated cells.[84] Also, the concentration effect of this material on the permeability of HeLa cell plasma membrane was investigated by monitoring the ferrocyanide (≈0.2 kDa) via electrochemical microscopy.[85] Nevertheless, in permeabilization by detergents, critical curvature stress causes membrane perforation, and the consequent concentration gradient enables cargo molecules to diffuse into the target cells while some cytoplasmic contents and intracellular organelles are lost. Hence, the effect of the detergents on permeabilization of live cells is challenging and hard to control due to their heterogeneous nature.

Dimethyl sulfoxide (DMSO) is an example of a nontoxic, low molecular weight organic solvent which is applied to improve the solubility of small molecular cargoes or drugs and increase their penetration across the plasma membrane.[86] It has been revealed that this organic solvent increases the occurrence of nanoscale membrane damages while it improves the solubility of small cargoes.[87] Yu and Quinn investigated the effect of DMSO concentration on phospholipid bilayer using X-ray diffraction (XRD) technique. They showed that DMSO could increase the distance between polar lipid head groups of phospholipid molecules and decrease the membrane thickness.[88] Ethanol as another example of organic solvents is a short-chain alcohol, which makes it less hydrophobic compared with DMSO. O'Dea et al. used ethanol as a permeabilizing agent for intracellular delivery purposes and demonstrated that the 25% v/v concentration of this alcohol provides the optimal permeabilization condition.[20] Studies have shown that ethanol remains at the water–lipid interface to induce disordering effect on phospholipid acyl chains leading to partially destroy the plasma membrane bilayer structure.[20,89]

Amphiphilic peptides (pore-forming agents) with the hydrophobic tail and hydrophilic head structure are able to integrate into the membrane barrier while buckling the phospholipid bilayer. Followed by the insertion of pore-forming peptides into the membrane, the conformational stress is induced to the target cell leading the trigger for membrane disruption and consequently transient formation of pores across the cell membrane.[81] Localized membrane deformation and permeability can occur through oxidation or peroxidation of constituent phospholipids. Oxidized lipids with distorted hydrophobic tails can trigger bilayer thinning, which is associated with a decline in bending rigidity and loss of bilayer integrity.[10,90]

2.2.2. Mechanical Methods

The central principle of the mechanical disruption methods is that the cell membrane is affected by 1-using a vehicle or conduit, 2-fluid pressure gradient, 3-prompt changes in hydrostatic/osmotic pressure, or 4-migration through the narrow constrictions.[91] Here, mechanical methods are divided into particle bombardment, scrape and bead loading, fluid shear forces, and osmotic/hydrostatic pressure. In the following, these methods are described in detail.

Particle Bombardment (Biolistic Particles or Gene Gun): A gene gun or a biolistic particle is a physical delivery strategy that was first employed to deliver genes into plant cells by Sanford and co-workers. In this method, an acceleration system propels DNA-coated heavy metal particles (e.g., gold, silver, and tungsten in the size range 0.5–2 μm) at a sufficient speed into the target cell.[92] Acceleration in this delivery system could be achieved using a helium discharge or a high-voltage electric spark.[11,93] Delivery timing, particle size (<one tenth of the size of the target cells), and the loading of DNA on the particles are the key parameters that determine the delivery efficiency.[94] The efficiency of this method is controlled by certain factors, including the size of the particles employed as DNA-carriers, the gas pressure used to accelerate the particle velocity, and the dosage of the cargo molecules.[95] Commercially available gene gun devices are Helios gene gun (BioRad Laboratories, Hercules, CA, USA) and Accell gene gun (Agracetus, Inc., Middleton, WI, USA).[96]

The significant advantages of gene gun delivery method include fast obtaining of high-level gene expression,[97] long-lasting gene expression,[98] and allowing to reach numerous organs without injury to the surrounding tissues (liver,[99] heart,[100] brain,[101] and muscle).[102] However, this method proves to have a deficiency in transferring genes into the deep tissue. Since the penetration distance of metal particle is limited, the surgery is required to reach any nonsuperficial tissue. Furthermore, as some interactions may take place between the

particle and target cell membrane, irreversible cell membrane break-down and pore formation can happen probably due to the high-velocity particles.

Scrape and Bead Loading: Solid contact between cells and either a rubber spatula or glass beads have been used to form transient openings in the cell membrane. Scrape loading and bead loading are two mechanical permeabilization strategies that pierce and transiently permeabilize the plasma membrane of adherent cells.[103] In scrape loading, a rubber spatula is passed over a surface of adherent cells (cell-laden) leading dislodge of these cells and bring them into the medium containing impermeable cargo molecules.[104] Then, cargoes existing in the surrounding medium diffuse into the cells with optimal amounts of membrane pores of sufficient size. This method has been used to deliver high molecular weight dextrans,[105] antibodies,[106,107] dyes,[108] and plasmids.[109] In a study led by Fechheimer, scrape loading was compared with the ultrasound-mediated permeabilization method. The results show that scrape loading yielded higher delivery of dextran conjugated dyes and DNA plasmids into hepatic tissue cultures, HeLa cells, and mammalian fibroblasts.[109]

In the bead loading method, glass beads are used in a flask with adherent cells and the cargoes to be delivered where shaking the flask causes direct contact between beads and cells; consequently, the impact of cell–bead collision makes the cells dislodged into the medium. This contact leads to the creation of sufficient strains to generate stochastic disruptions in the plasma membrane.[110] Bead loading has been used for antibody loading into fibroblasts and macrophages,[111] intracellular delivery of quantum dots (up to 15 nm),[112] proteins, and antibodies.[113] For instance, to image single mRNA translation in living cells, bead loading was used to transfer antibody fab fragments to the cell interior. Briefly, glass beads with a diameter of 75–200 μm are incubated in a solution containing the protein cargo. Then, adherent cells are incubated with the beads under mild agitation. This leads to the transient pore formation with the dimensions that are large enough for proteins to pass through the membrane but not too large to allow entering the glass beads.[114]

Low cost and accessibility are the benefits of scrape and bead loading methods. In addition, these methods can be performed using common laboratory equipment. Nonetheless, the generation of cellular and biological debris is a challenging aspect of these methods. Besides, the amount of damage to each cell is stochastic, causing inconsistent delivery outcomes.[80]

Fluid Shear Forces: Existing in vivo (e.g., viral) and in vitro (e.g., lipid-based carriers) delivery systems exhibit shortcomings in the delivery of large and structurally complex target molecules. To address the concerns over the delivery of proteins and the growing diversity of alternative synthetic nanomaterials, mechanical shear-based approaches have been emerged. Fluid shear leads to disruption of lipid bilayers, followed by intracellular delivery of the target cargo. The shear force induced by fluid flow is less invasive compared to the disruption of the membrane via solid contact (such as the gene gun). The disruption by fluid shear forces is generated in certain ways. If water with enough amount of rapid velocity flows parallel to the lipid-based membrane, the heads of lipids may be tilted leading to disruption of the bilayer. Similarly, a stream of water perpendicular to the membrane can result in membrane disruption.[80]

Syringe loading is one of the most straightforward approaches for generating zones with high fluid shear force to drive cell suspensions through tight constrictions around the entrance and exit zones of the syringe needle. In this delivery strategy, cell suspensions are mixed with a high concentration of cargo and repeatedly passed back and forth through fine-gauge syringe needles or similar narrow orifices to transiently permeabilize cells. The loading efficiency and the velocity of the cells aspirated and expelled through these constriction zones is determined by the flow rate.[115] In 1992, Clarke and McNeil used a syringe for creating zones of high fluid shear force to drive a liquid through tight constrictions and further delivery of cargoes with the sizes up to 150 kDa (i.e., fluorescein isothiocyanate (FITC)-labeled dextran) in several mammalian cells. Furthermore, it was shown that pluronic F-68 (poloxamer 188) increased cell survival and loading efficiency during syringe loading, compared to both scrape and bead loading methods.[116] In addition to the delivery of DNA plasmids into mammalian cells,[117] this method was widely applied for different applications in various cell lines (e.g., mouse Ltk(-), CHO, immune, endothelial and neural cells)[118–120] and different cargoes (e.g., antibodies, proteins, guanosine diphosphate (GDP), and guanosine triphosphate (GTP)).[121,122] In order to investigate the effect of viral and bacterial proteins inside the cells, human skin fibroblasts were syringe-loaded with human immunodeficiency virus type 1 protease (HIV-1 PR), and it was revealed that it affects intracellular architecture and nuclear organization.[123]

In addition to generating fluid shear forces by driving cell suspension through the narrow constrictions, later, Blackman and co-workers utilized cone and plate viscometers to produce and control hydrodynamically applied shear stress over endothelial cell monolayer.[12] In their work, a controlled cell shearing device integrated with a fluorescence microscopy apparatus was developed to enable real-time monitoring of cellular responses to mechanical stimuli. Since in this method the flow is controlled manually, improved precision and reproducibility could be achieved by combining this strategy with acoustic sonoporation or optoporation, both of which are described in the hybrid methods, Section 4.

Osmotic/Hydrostatic Pressure Gradients: In the pressure change-mediated system, a hypo-osmotic shock is induced by rapid changes in osmotic and hydrostatic pressure across the cell membrane, resulting in osmolality-dependent permeabilization.[124,125] Hence, cells experience significant stress since their membranes face the differences in osmotic potential between the intra- and extracellular environment (gradients of osmotic pressure), leading to the membrane perturbation, and consequently, delivery of cargoes.[126] The geometry of these gradients may vary between the intracellular contents of target cells and the extracellular environment, facilitating the entrance of osmolytes or impermeable electrolytes through the membrane or aquaporin channels.[127] When a cell is exposed to a low osmolarity environment, hypotonic swelling will soon change the cell volume, which unravels the unfolding of membrane reservoirs and consequently results in lipid bilayer rupture.[128] This technique was first used in conjunction with other methods to access the intracellular organelles and prepare

membrane ghosts (e.g., red-blood-cell ghosts) with minimal membrane damages.[129,130]

In 2010, Andersen et al. used this method to induce intracellular delivery of siRNA and gene silencing in human vein endothelium.[131] Okada and Rechsteiner proposed a method named osmotic lysis of pinosomes to exploit a brief hypertonic treatment followed by a hypotonic shock for the successful delivery of target proteins. In this method, first, endosomes are preloaded with the target proteins to be delivered, and then, internalized endosomes are ruptured by osmotic pressure gradients.[13] However, compared to other delivery systems, this low-cost strategy has not gained much reputation due to its limited delivery capacity by the extent of endocytosis and lack of sufficient reports on delivery of plasmid DNA and mRNA.[127]

2.2.3. Field-Assisted Methods

Ultrasound-Assisted Delivery System (Sonoporation): Ultrasound-assisted delivery method, called "sonoporation" in the context of delivery, is a technique based on the cavitation and microbubble formation, mostly implementing a low-frequency ultrasound wave (20 kHz) to shock the target cell and achieve the enhanced level of cell permeability.[132,133] Vapor-filled microbubbles or cavities in the delivery solution are formed as a result of applying acoustic pressure waves.[134,135] A significant amount of energy after the collapse of these microbubbles is released, which further causes the temporary disruption of the cell membrane, facilitating the entrapment of surrounding macromolecular cargoes (e.g., plasmid DNA) inside the target cell.[136,137] Several studies have shown that increase in the cell permeability mediated by ultrasound shares some similarities to those achieved via electroporation.[138,139]

Sonoporation has been applied for the intracellular loading of a variety of small and large cargoes since the mid-1980s.[109,140–142] However, due to the gene therapy motivations, this noninvasive method is mostly used for the introduction of DNA into the target cells. Wyber et al. demonstrated the ultrasonic delivery of plasmid DNA into the yeast cell suspension (as a model system) by applying 20 kHz ultrasound waves and introduced cavitation as the primary underlying mechanism of membrane disruption.[14] As an example of other cargoes rather than DNA, Fechheimer and Taylor demonstrated the intracellular delivery of proteins and fluorescently labeled dextrans (MW: 40 000 Da) into the cytoplasm of amoebae.[141] For more than a decade, there existed only one commercially available sonoporation device (Sonidel SP100). Nevertheless, it seems that further in vitro use of this method was not fully explored so far due to the cavitation-related side effects including free radical formation, reactive oxygen species (ROS) production, consequent DNA damages, high local temperatures and reduced cell viability.[143,144]

Laser-Assisted Delivery System (Optoporation): Optoporation, also known as optical transfection, optoinjection, photoporation, and laserfection, is a term defined as directly influencing the high-intensity light on the cell membrane.[145] In optoporation, combinations of thermal (applying heat in a focal spot), chemical, and mechanical effects are used to assist the delivery of cargoes inside the target cell.[146] This method has gained a significant level of attention specifically for transfection purposes, in which a tightly focused laser beam (<1 μm spot size) is applied to the cell membrane, and consequently, smaller sized pores (1–5 μm) are created.[147] DNA delivery by optoporation was first reported in 1984 by Tsukakoshi et al. The nanosecond laser pulses (Nd:YAG UV laser) with a wavelength of 355 nm, spot size of ≈0.5 μm, and energy of 1 mJ were focused on the surface of kidney epithelial cells, generating hole of several microns in the cell membrane for the plasmid DNA delivery.[148] This method alleviates the throughput limitations by transfecting thousands of cells with a single laser pulse while maintaining subcellular organelles intact. Since both diameters of the pores formed at the surface of the target cells and duration of the pore opening could be adjusted through laser intensity modulation, this strategy is considered as the most suitable and accurate way of delivering small amounts of mRNA into the discrete subcellular regions.[147]

To date, different types of lasers have been used for the cell membrane poration, including nanosecond-, femtosecond-, and microsecond-pulsed lasers as well as continuous-wave laser.[149] It is noteworthy that the mechanism of laser–cell interaction depends on the type of laser, which shows different perforating mechanism. The femtosecond-pulsed lasers have a high-intensity near-infrared light (wavelength 800 nm). The longer laser wavelength allows deeper penetration into the target cells with inducing minimal photodamages as single pulses of these lasers have lower energy compared to the UV and blue lights. This delivery method has been used for several mammalian cell lines, especially hard-to-transfect cells such as stem cells[150] and neurons[151] and for in vivo gene delivery purposes.[152] However, optoporation is not without its drawbacks. The lasers and optical equipment used in optoporation are expensive and rely heavily on precise positioning and alignment of the laser focal spot with the target plasma membrane. Furthermore, local ablation and heating of cell membrane have limited the in vitro applications of this technique.[153,154] In one study, Zeira and co-workers demonstrated the delivery of plasmid DNA into tibial muscle of BALB/c mice using femtosecond lasers.[153] Their results suggested low penetration-depth of focused laser beams (≈2 mm), which is a major obstacle for cargo delivery into deeper tissues limiting the translation of this technology for non-invasive in vivo applications.[155] More recently, the femtosecond laser-assisted delivery system have been used in combination with laser tweezers to precisely internalize delivery materials (microbeads or nanoparticles) from the extracellular space into subcellular regions.[156,157] These hybrid systems are described in detail in the Section 4.

Thermally Assisted Delivery System (Thermoporation): The permeability of the plasma membrane can be triggered by temperature. In the thermally assisted delivery method, cells either experience multiple cooling-heating cycles or a bulk supraphysiological heating situation (above 37 °C) resulted in membrane disruption and phospholipid bilayer dissociation.[158] Since early 1980s, thermal shock has been commonly used for bacterial transformation to introduce plasmid DNA into "competent" bacteria. During this mechanism, competent bacteria are exposed to consecutive thermal shocks by incubating at 0 °C, followed by a brief heat pulse at 42 °C and chilling on ice. [159] These cooling–heating cycles rapidly reduce the membrane potential and induce formation of transient ruptures in the membrane, which increase its permeability to the exogenous DNA. Upon heat

shock, transformed bacteria are screened from the nontransformed ones through culture in growth media containing a specific antibiotic. After cell division, the selected bacterial colonies replicate the exogenous DNA using their replication enzymes to a sufficient copy number.[160] Accordingly, this method has been used for amplification and isolation of DNA plasmids from log phase bacteria as a key step for gene editing and cloning applications.[161]

Another approach of thermally assisted delivery is heating the cell membrane to reach a temperature above the physiological range. As a result, kinetic energy of the constituent molecules becomes greater than forces maintaining the membrane integrity and thus, spontaneous disruptions happen in plasma membrane.[162] The formation of these stochastic thermally driven defects directly depends on factors such as temperature changes, pH, hydrostatic pressure, and ion concentration. Despite the relative simplicity of this delivery system, it has not been widely used for delivery purposes in animal cells due to concerns like unspecificity, off-target damages, and difficulties in spatiotemporal control of temperature exposure.[163,164]

Magnetically Assisted Delivery System (Magnetoporation): Magnetoporation is a well-established magnetically guided delivery combining either chemotherapeutics or nucleic acids (e.g., anionic DNA molecules) with the cationic magnetic nanoparticles (MNPs) (commonly superparamagnetic iron oxide nanoparticles (SPIONs)) via noncovalent bonds.[165–167] By this means, first cargoes are mixed with MNPs, which are coated and tightly bonded with polyelectrolytes (i.e., polyethyleneimine). Afterward, the field-induced transport of magnetically labeled complexes takes place through the membrane to concentrate the cargo–MNP complexes in the target cells within a few minutes.[167] Polymer nanoparticles with iron oxide cores used in this approach are preferable as they enable real-time noninvasive monitoring of DNA delivery via magnetic resonance imaging (MRI). Accordingly, Kievit and co-workers illustrated that SPION core coated with a novel copolymer (CP-PEI) transfection agent is a suitable contrast enhancing agent for MRI to provide earlier detection of lesions and enhanced spatial resolution.[168] Ferucarbotran (Resovist, particle size ≈ 60 nm) and Fridex (ferumoxides, particle size 120–180 nm) are examples of clinically approved SPIONs used as contrast enhanced agents in MRI of the liver.[169,170] The technique of magnetofection was first used for in vivo selective targeting and concentrating drug bearing MNPs. Widder et al. indicated 77% of the Yoshida sarcoma-bearing rats exhibited complete tumor remission after a single subcutaneous treatment with magnetic microspheres carrying low-dose doxorubicin.[171,172] Thereafter, several studies demonstrated that this delivery method is an appropriate approach for both in vivo and in vitro gene- and nucleic acid-based therapies. Accordingly, Scherer et al. exploited paramagnetic iron oxide nanoparticles in complex with viral or nonviral vectors as drug carriers to achieve an improved level of gene delivery in vitro and in vivo.[133] Compared to the other techniques, magnetofection requires a low number of vectors, shorter incubation time, and a higher chance of local gene delivery to non-permissive cells and surgically accessible tissues (i.e., stomach). Together these unique characteristics facilitate the severe overcoming obstacles such as low throughput gene screening in vitro, low concentration of the vector in target cells or tissues, and low delivery efficacy in vivo. On the other hand, safety concerns regarding the rapid systemic clearance and cytotoxic effects of concentrated MNPs on target cells are current challenges for in vivo applications of magnetofection. [173]

Electrically Assisted Delivery System (Electroporation): The electric-assisted delivery system, otherwise known as electroporation, employs a homogenous electric field to make a series of high-intensity electrical pulses, which are applied to the millions of cells mostly in suspension.[174] This phenomenon leads to reversible destabilization when the external electric field and therefore potential difference across the membrane exceeds a threshold voltage.[175–177] It leads to the temporary formation of electric field-induced nanopores (with minimum 1 nm radius) and thus increases the cell membrane permeability.[178] Hence, the cell membrane becomes highly permeable to a variety of cargo molecules presented in the surrounding medium.[179,180] The efficiency of electroporation mostly depends on several physical (e.g., strength of electric field, duration, and number of pulses) and biological (e.g., cell size and concentration of cargo) factors. Since different pulse durations are required for molecules with different sizes, it is believed that longer pulse durations will lead to the formation of larger pores staying open in a more extended period of time.[181] A pulse generator and an applicator (e.g., an electrode) are the required instruments for electroporation.[178] As the electroporation technique provides the benefits of simplicity, cost-effectiveness and potential of permeabilizing millions of cells, simultaneously, it has become a valuable method for both in vitro and in vivo delivery applications.[182] In 1982 Neumann et al. reported an efficient plasmid DNA transfer into the mouse lyoma cells deficient in TK gene (LTK^-) in vitro by applying high electric fields.[19] Electroporation has subsequently shown utility for gene delivery effectively into mouse skin,[19] early chicken embryos,[183] rat liver,[184] murine melanoma,[185] and mouse muscles.[186] Different types of electrodes are developed for various applications, including surface electrodes, needle electrodes, and electroporation catheters.[187] The main drawback of the procedure, however, is the cell death post treatment due to the Joule heating that induces excessive thermal damage to cells.[188]

Nucleofection, also called nucleofector technology, was introduced in the early 2000s and quickly gained traction as a type of advanced electroporation-based delivery system.[189] Nucleofection uses specific electrical parameters and a combination of specialized solutions to achieve direct delivery of plasmid DNA into the cell nucleus, resulting in enhanced gene expression. This situation becomes more pronounced when primary neurons, as an example of postmitotic cells, are available for the purpose of gene transfer.[190] Nucleofection was applied for transfecting the primary cells (stem cells), which are resistant to the gene transfer via conventional delivery systems.[191] In Amaxa Nucleofector technology (invented by Amaxa company), direct delivery of DNA into the nucleus of target cell takes place, which dramatically revolutionizes further investigations about gene expression in primary cells.[192] Although the signs of progress in electroporation are significant, there is an unmet demand for further studies on the precise mechanism of electropermeabilization and the subsequent procedure of pore formation.

In this section, we limit our approach to bulk or conventional electroporation. Other types of this delivery strategy such

as microcapillary-based electroporation (MCEP), microchannel-based electroporation (MEP) and nano-localized single cell electroporation (NLSCEP) are classified in micro-engineered approaches and explained in the Section 3.6.

3. Micro- and Nanoengineered Intracellular Delivery

Recent advances in micromachining and nanotechnologies led to the emergence of micro- and nanoscale delivery approaches. These methods have enabled single-cell manipulation as well as universal delivery of any cargo biomolecules into different cell types with better delivery outcomes, greater precision and higher throughput. It is imperative to note that micro- and nanoengineered approaches mainly deploy a membrane-disruption mechanism to create transient pores and transport the cargo of interest across the cell membrane. Here, we focus on micro- and nanoengineered intracellular delivery approaches and present state-of-the-art advances in this field. **Figure 3** summarizes the most widely used micro- and nanoscale techniques which are briefly introduced in the following section.

3.1. Microinjection

Microinjection is one of the major direct penetration strategies for intracellular delivery. This technique employs either a miniaturized pipette-like vehicle or conduit with sharp ends to break down the cell membrane and inject fluid containing delivery cargo inside the cell of interest.[193] The equipment required for the microinjection procedure includes an inverted microscope for cell visualization, a glass injection micropipette filled with the nucleic acid solution, and a micromanipulator controlling the movement of injection micropipette and the pressure injector.[194] In some cases, for automated injection, the glass micropipette is coated with a carbon film, called "carbon nanopipette", used for electrical measurements and detection of cellular and nuclear penetration.[195] Though not suitable for a bulk population of cells, this method is beneficial for single-cell intracellular delivery.

Microinjection was first proposed by Barber for the injection of a single bacteria into the cytoplasm of a plant cell.[196] Since then, this method has been mainly employed for intracellular delivery of large cargoes (e.g., mitochondria and sperm), nucleic acids, and proteins.[193,197] Microinjection was also utilized for initial experiments of nuclear transplants. During these experiments, the nucleus was departed from blastula cells and directly injected into the enucleated eggs of frogs giving rise to produce a normal frog.[198,199] The generation of transgenic animals by the pronuclear microinjection is one of the most critical applications of this approach that led to the birth of Dolly as the first cloning instance of the mammalian species.[200] Furthermore, transgenic mice were produced using the pronuclear microinjection of transgenic DNA construct to the nucleus of fertilized oocytes followed by transferring the injected embryos to the oviducts of pseudo pregnant surrogate mothers.[201] Microinjection was also deployed to replace the mitochondrial genome and transfer spindle–chromosomal complex in mature nonhuman primate oocytes (metaphase II/MII) and abnormally fertilized human zygotes to correct mutations in mitochondrial DNA.[202,203] Artificial delivery of sperms into oocyte cells (in vitro fertilization or

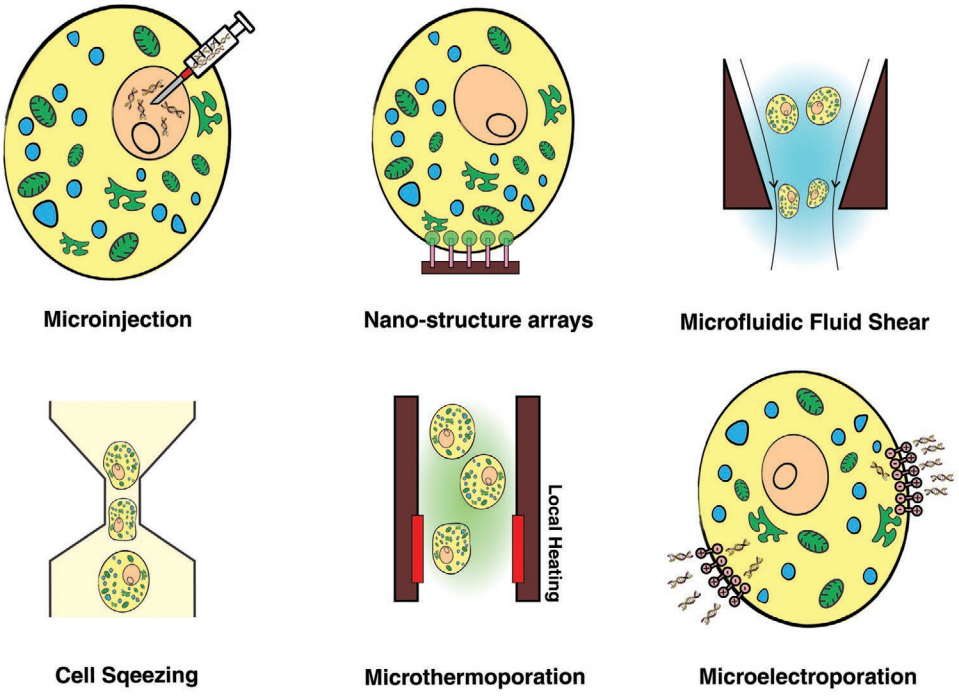

Figure 3. Schematic illustration of the most widely used intracellular delivery systems at the micro- and nanoscale. Some of these techniques such as fluid shear, thermoporation, and electroporation can be applied at both macro and micro (containing both micro and nano) scale. Other techniques, such as microinjection, nanostructure arrays, and cell squeezing are exclusive to micro- and nanoengineered platforms.

IVF)[204,205] and transferring artificial chromosomes for transgenic studies are other applications of this approach.[206,207] A novel quantitatively managed microinjection technique for single cell transfection utilizes microfluidic chips to form suspended cells in an array for easy injection and precise measurement of the delivered materials. This technology, which allows the microinjection of multiple components into a single cell, can be applied for investigating the effect of various dosages of the delivered cargo on the delivery efficiency and cell responses.[28] Fixed cells, low-throughput analysis, and slow process are considered as the major drawbacks of this approach.

3.2. Microfluidic-Induced Shear Stress

Inducing a sudden velocity gradient in the flow of cells can generate shear stress and temporarily permeabilize the cell membrane, thereby facilitating the intracellular loading of cargo macromolecules.[208] Manual pipetting through hypodermic needles is the simplest possible form to induce shear stress for intracellular delivery.[116] However, the method is highly subjective and nonrepeatable, and due to lack of any control over the flow rate and the size of the needle, it requires individual skills. Hence, microfluidic devices can be utilized to precisely control the shear stress by controlling the device dimension and fluid flow of cell suspension. Surprisingly, this topic has received less attention from the microfluidic community, and to the best of our knowledge, except only one microfluidic study in this field, which was conducted more than 10 years ago, there are no other similar studies. The authors used laser micromachining to produce either a single cylindrical channel (with a diameter of 50 μm), a single conical channel or an array of conical microchannels with 300 μm inner diameter and 50 μm outer diameter. They showed that different-sized macromolecules (0.6-2000 kDa) were loaded into more than one-third of the DU145 cells (prostate cancer cell line) with 80% cell viability at the optimized values of shear stress (e.g., >2000 dynes cm^{-2}) and exposure duration.[209]

In 2019, Kizer et al. developed a new vector-free platform for intracellular delivery at the throughput of more than 1 million cells min^{-1} based on rapid hydrodynamic cell deformation and inertial microfluidics. Hydroporator with the new design also utilized the inertial-based effects to mix the cell suspensions with delivery material and focus randomly distributed cells into the center of the cross-junction microchannel, wherein the cells undergo stretching as a result of shear stress. With this method, they demonstrated the clogging-free delivery of different dextran sizes (3–2000 kDa) and vanilla DNA origami nanostructures (nanotube and donut-shaped), which revealed to maintain their integrity for nearly 1 h after loading into the K562 cells (**Figure 4**A). While this system is highly efficient for cytosolic loading of nanomaterials (up to 50 nm), a notable weakness is the limited delivery of larger cargoes.[210] To address this open challenge, in a follow-up study, Kang et al. introduced a novel spiral hydroporation platform designed with a cross-junction and two opposing T-junction microchannels to induce cell deformation sequentially. In this PDMS microfluidic device, as the mixture of cell suspension and delivery nanomaterial passed the cross junction and T-junction microchannel, they experienced inertial focusing, spiral vortex (see Figure 4B), and cell-wall collision, respectively that resulted in rapid membrane poration. Considerable delivery efficiency of loading different FITC-dextran sizes (3–2000 kDa), gold nanoparticles, doxorubicin-loaded mesoporous nanoparticles, and EGFP mRNA have been achieved using spiral hydroporation.[211]

In 2019, Indee labs introduced a microfluidic vortex shedding (μVS) device that takes advantage of hydrodynamic conditions at Reynold's number of 146 to induce and sustain vortex shedding (Figure 4C). The 2D chip consisted of a flow chamber (960 μm width, 40 μm depth) with arrays of circular microposts spacing greater than the target cell diameter. In this platform, a mixture of human $CD3^+$ T cells and EGFP mRNA constructs was driven through the chip to pass the ion-etched microposts, which interrupt and split the flow suspension to generate vortices around. These hydrodynamic vortices facilitate the rotation of the cells as well as membrane disruption giving rise to the μVS-based cytosolic loading of constructs encoding EGFP mRNA into the $CD3^+$ T cells. This highly efficient intracellular delivery device with minimal effects on cell viability, recovery, and growth after delivery procedure holds promise for commercial manufacturing of engineered primary human cells and gene-modified cell therapy at clinically relevant scales.[212] Considering the advances in microfabrication and sample delivery, it is expected to develop more microfluidic platforms for shear-induced loading of target cells with controlled flow through microchannels.

3.3. Microthermoporation

Microthermoporation makes the use of thermal energy to induce local heat shock and destabilize phospholipid membranes. This strategy was reported by Li and co-workers, where an on-chip local heat shock microfluidic device (consisting of a 50 μm microchamber along with channels and a double-spiral platinum microheater) was used for transformation of plasmid DNA into *Escherichia coli* bacteria. They employed thermal stimulation (from 0 to 50 °C within 5 s and maintain at 50 °C for 90 s) to deliver plasmid DNA into competent bacterial cells. This study reported a significant decrease in the required volume of bacterial cells (one-thousandth) as well as an increase in delivery efficiency compared to the conventional heat shock procedure.[213] However, in most of biochemical applications, bacterial transformation using macroscale thermoporation is preferred over the microthermoporation due to its simplicity and relatively high throughput.[214]

In another work, Kavaldzhiev and co-workers fabricated microthermoporation system, in which cell membrane was permeabilized by induced localized heating of arrays of highly biocompatible gold microneedles with diameter of 1.5 and 5 μm height.[215] Remotely activating and wirelessly induced heating of microneedles was generated by an alternating magnetic field of 360 Oe and 425 kHz (**Figure 5**A). In this study, the HCT116 colon cancer cells were used to grow on top of microneedles (Figure 5B) and wrap around them to form focal adhesion points on the micropillars. Next, the magnetic field was applied for co-localization of calcein AM and ethidium homodimer-1 (EthD-1) fluorescent dyes into the HCT116 cells

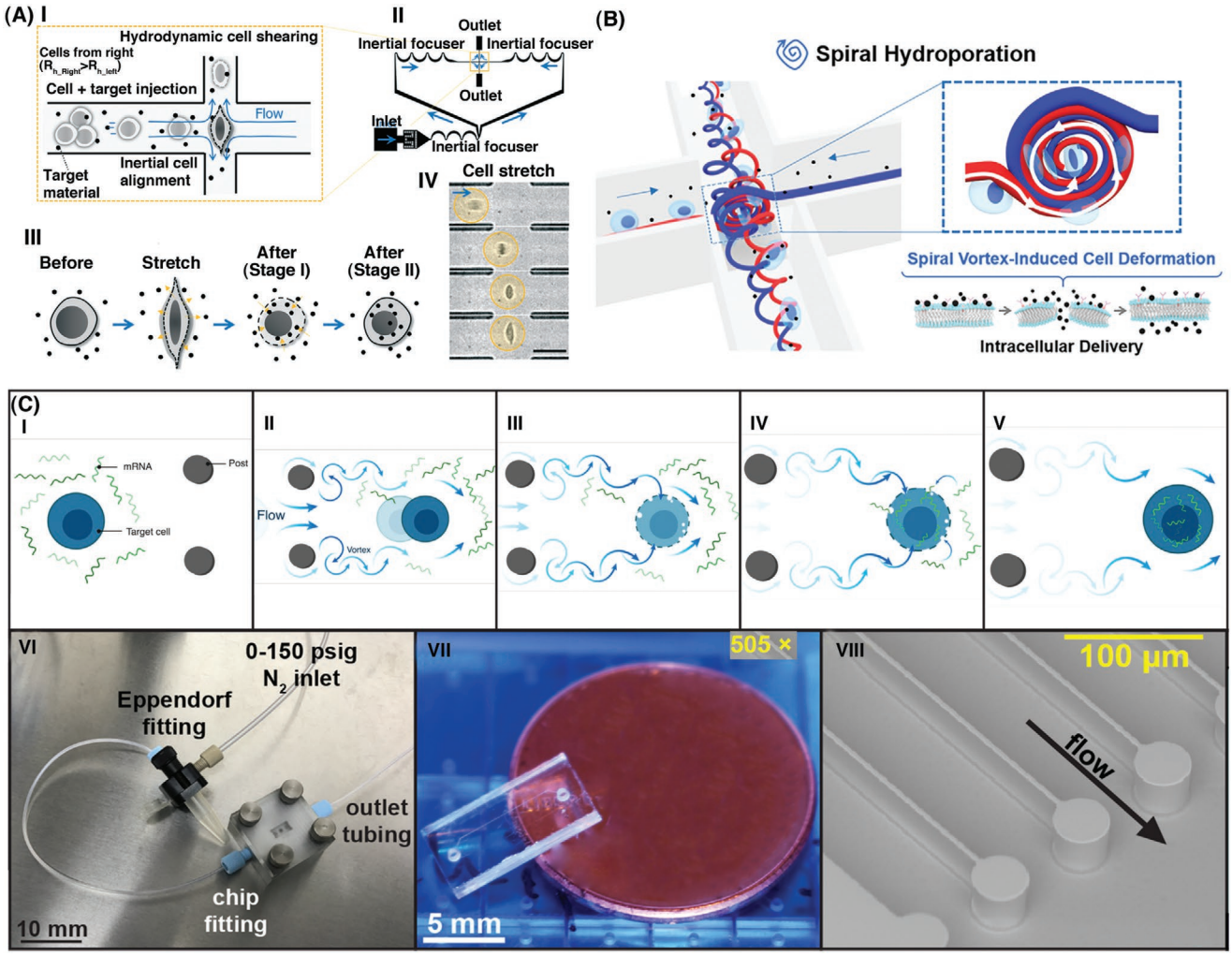

Figure 4. Schematic representation of microfluidic-induced shear stress platforms used for intracellular cargo delivery. A) Hydrodynamic cell shearing device. I,II) This plan represents the schematic design of hydroporator, which hydrodynamically induces shear stress resulted in creating several disruptions in the cell membrane. III) Delivery approach in this design consists of sequential steps including: inertial focusing of target cells, hydrodynamically induced stretching and deformation of plasma membrane at the cross junction point of the microchannel, cargo uptake through both diffusive and convective transport mechanisms, and membrane resealing within a few minutes. IV) Time-lapse images of the cell stretching process at the extensional flow point taken every 7 µs via high-speed camera. A) Reproduced with permission.[210] Copyright 2019, Royal Society of Chemistry. B) The spiral hydroporation device takes advantage of spiral vortex and vortex break down to induce sequential membrane deformations in cells passing through the cross- and T-junction channels of the microfluidic chip at moderate Reynolds numbers. Reproduced with permission.[211] Copyright 2020, American Chemical Society. C) The mechanism of the microfluidic vortex shedding delivery. I–V) First, target cells and exogenous cargoes are mixed and forced to pass through the flow chamber. Upon impacting circular miscroposts, the flow of cells and cargoes was interrupted creating vortices that temporarily permeabilize the cell membrane. Later, during the membrane recovery process, target cargoes were loaded into the cell cytosol by passive diffusion. VI) The driving hardware unit uses compressed nitrogen (120 psi) to drive the cell suspensions and delivery cargoes through the microfluidic chip and induce membrane permeabilization followed by cargo uptake. VII) Image of the fabricated pneumatic pressure-driven microfluidic device. VIII) The close-up architecture of the flow cell chamber with regularly-spaced microposts. Adapted under the terms of the CC-BY Creative Commons Attribution 4.0 International license (https://creativecommons.org/licenses/by/4.0).[212] Copyright 2019, The Authors, published by Springer Nature.

and fluorescence imaging was performed at three different times of 1, 5, and 15 min. For specific treatment times of 1 and 5 min, the delivery efficiency of calcein and EthD-1 dyes was reported 35% and 75%, respectively. However, the duration of field application is an essential factor determining the cell viability as a longer magnetic field application (i.e., for a time of 15 min) overexposed the cells on the top of heated microneedles and caused cell death of the entire population. The advantages of microthermoporation to its counterpart include smaller sample volume, higher throughput, fast and uniform heating profile, and increased precision by controlling the influx of molecules into desired cells. It is noteworthy to mention that this method is still under development and available in specialized labs only.

3.4. Microsonoporation

As discussed in the Section 2.2.3, sonoporation is a technique to gain the benefit of ultrasound waves to permeabilize cell

membranes both in vitro and in vivo.[216] Compared to the macroapproaches, microsonoporation has superior advantages such as application for both adherent and suspension cells, high-throughput manipulation, and easy tracking of single cells during and after cavitation event. For instance, Le Gac et al. reported the sonoporation of human promyelocytic leukemia suspension cells (HL60) in a microfluidic system.[217] In this study, the formation of a rapidly expanding cavitation bubble (10–100 µm radius) occurred as a result of light absorption at 532 nm and further energy deposition of the laser pulse. Next, this single laser-induced cavitation bubble located in a microchamber was expanded and collapsed, which gave rise to the creation of cavitation-induced shear stress, loss of membrane integrity and further membrane poration of cells in the vicinity. They indicated that the creation of membrane pores was related to the distance between the target cell and the center of the cavitation bubble. Accordingly, they showed that while the cells at the distance of 0.75 R_{max} (the maximum bubble radius) from the center of a cavitation bubble were permeabilized with a probability of >75% other cells located farther away (>four-times R_{max}) remained unaffected. In another work, high lateral-resolution ultrasonic microtransducer arrays (UMTAs) were fabricated for the site-specific sonoporation (Figure 5C).[218] A monolayer of green fluorescent protein (GFP)-expressing human melanoma cells (LU1205) was cultured on the top of a UMTA-biochip, and 100×10^{-9} M of carboxylic-acid-derivatized CdSe/ZnS core/shell quantum dots (QDs) were added to the cell culture media to be delivered to the cell interior. Afterward, ultrasonic microtransducers were activated by applying 30-MHz sinusoidal signals (for low, medium, and high RF powers) to induce site-specific cellular sonoporation and QDs transport into the LU1205 cells. The results indicated that this delivery strategy increased the intracellular distribution and transportation of QDs as the enhanced factor for LU1205 cells was higher than 100 at an applied pressure of 0.29 MPa compared to endocytosis-driven QD-uptake. They also reported a threshold pressure (≈0.12 MPa) at which the LU1205 cells undergo ultrasound-induced mechanical stress and become permeable enough for the transportation of QDs through the transient pores in the cell membrane. Moreover, the ability of ultrasonic standing wave fields to control the position of the cell and induce sonoporation has been explored in several studies.[219–221] In contrast agent-free adaptation of this delivery approach, Carugo et al. used a non-inertial ultrasound microfluidic device for the intracellular loading of therapeutic agents (apigenin, luteolin, and doxorubicin) into the H9c2 cardiac

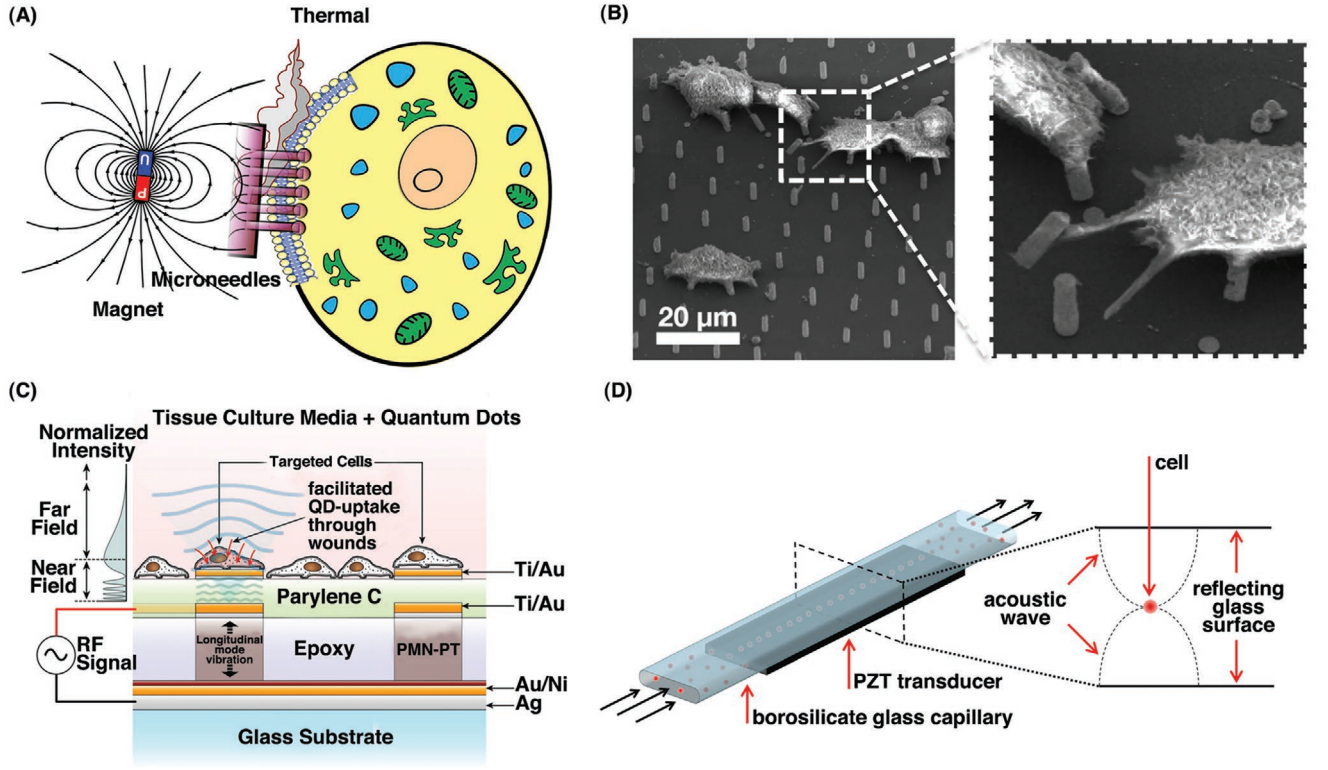

Figure 5. A) Schematic illustration of microthermoporation method in which arrays of gold microneedles are inductively heated (below 45 °C) by applying an alternating magnetic field, which further resulted in intracellular delivery via heat energy. B) Electron microscopy image showing HCT116 cells that are attached on top of 5 µm long microneedles. Reproduced under the terms of the CC-BY Creative Commons Attribution 4.0 International license (https://creativecommons.org/licenses/by/4.0).[215] Copyright 2018, The Authors, published by Springer Nature. C) Cells seeded above the active area of the PMN-PT microtransducer (lead magnesium niobate–lead titanate, piezoelectric coefficient $d_{33} \cong 2500 \times 10^{-12}$ C/N), and ultrasonic waves were created by an RF signal across the transducer pillar near the cells. Reproduced with permission.[218] Copyright 2011, Elsevier. D) While cells are moving through a capillary glass which is coupled to a PZT transducer, they are exposed to ultrasonic standing wave and acoustic radiation forces, allowing the precise control over the flow and positions of the target cells. Reproduced with permission. [221] Copyright 2011, American Institute of Physics.

myoblast suspension cells (Figure 5D). This device contained a disposable borosilicate glass microcapillary which is acoustically coupled to a piezoelectric (PZT) transducer to generate acoustic microstreaming and allow the migration of cells towards a single nodal plane. The real-time single cell analysis demonstrated that at peak-to-peak voltage>20 the CA-free sonoporation facilitated the loading of membrane-impermeable fluorescent probes (5-chloromethylfluorescein diacetate and FITC-dextran) and therapeutic agents while maintaining high cell viability.[221] In recent work by Belling et al. sonoporation has been integrated with microfluidics (coined as acoustofluidic sonoporation) to deliver Cy3-DNA into the Jurkat cells. They also achieved successful delivery of EGFP plasmid into the Jurkat, PBMCs, and CD^{34+} cells using this delivery approach at a scalable throughput of 200 000 cells min^{-1} without compromising the cell health.[222]

3.5. Mechanoporation

Mechanoporation or rapid mechanical deformation of cell shape through microfluidic constrictions can provide intracellular loading of structurally diverse materials into different cell types. Filtroporation is a simple yet efficient mechanoporation technique, which induces membrane discontinuities in the cells driven through uniformly sized filter micropores smaller than the cell diameter. A major advantage of filtroporation is its applicability for a bulk population of cells, which facilitates higher-throughput experimentation. As a proof of concept, Williams et al. induced transient membrane perturbation in Chinese hamster ovary (CHO) cells traversing the micropores of track-etched polycarbonate filers, coined the procedure as filtroporation. By tuning the treatment parameters, they achieved nearly 50% delivery efficiency for loading of 10, 70, and 500 kDa dextran-conjugates and luciferase reporter DNA plasmid into CHO cells forced through the polycarbonate microporous membranes. In the reported study, at a constant micropore size, the loading efficiency and loss of cell viability were directly proportional to the magnitude of the hydrodynamic shear forces caused by tangential strain. However, they proposed a strain threshold for the cells forced to pass through a confined space, as further strengthening the applied pressure at a constant pore size was predicted to rupture the plasma membrane.[223] Followed by this study, Yen et al. developed a highly efficient delivery device based on membrane filtration (called transmembrane internalization assisted by membrane filtration or TRIAMF) to deliver Cas9/sgRNA RNPs into primary human $CD34^+$ hematopoietic stem and progenitor cells (HSPCs) derived from bone marrow. Their experiment revealed the potential of TRIAMF for clinical scale gene-editing as they successfully loaded Cas9 RNPs with sgRNAs targeting human β-globin into ex vivo expanded $CD34^+$ HSPCs.[224]

Cell squeezing, as one imperative subcategory of microfluidic-based mechanical deformation of cells, is a robust vector-free platform. In this delivery system, which was first introduced by Sharei and co-workers, cells experience rapid mechanical deformation as they pass through parallel constrictions with a minimum dimension smaller than the cell diameter, resulting in the formation of transient pores.[225] In this platform, HeLa cells were resuspended in the desired delivery buffer, mixed with the quantum dots as a model molecule, and then placed into the inlet reservoir of the silicon-based microfluidic device (**Figure 6**A). Afterward, a constant pressure (0–70 psi) was used as a driving force to run the HeLa cells through constrictions 30–80% smaller than their diameter which further induce compression and shear forces to the cells. As a result, transient micropores are formed giving rise to the diffusion of unaggregated quantum dots into the HeLa cell cytosol and the collection of loaded HeLa cells in the outlet reservoir.[225] To better understand the kinetics of plasma membrane repair mechanisms and cell viability post-treatment, Sharei et al. reported on the development of a new cell-squeezing-based microfluidic platform with more treatment homogeneity and higher throughput (≈6×, 50 000—500 000 cells s^{-1}) than the previously reported ones. To do this, they designed different microfluidic devices with two access pores (as inlet and outlet reservoir), 15 parallel channels and 5 subchannels with different geometries and numbers of constrictions in series. They used this parallelization strategy to increase the efficiency of loading cascade blue dextran (3 kDa), FITC dextran (70 kDa), and APC conjugated IgG1 isotype control antibody into HeLa cells and primary murine naïve T cells. The results suggested the dependency of the membrane repair process upon the constriction geometries, flow rate, and calcium concentration of the surrounding buffer (recovery time ≈30 s with calcium versus ≈5 min without calcium).[226] To further demonstrate independency of cell squeezing process on cell type and delivery cargo, cytosolic loading of small and large biomolecules including, CdSe/CdS core–shell quantum dots,[227] siRNA,[228] antigen,[229] recombinant IFN regulatory factor 5,[230] fluorescently labeled tRNAs,[231] Janus kinase inhibitors,[230,232] fluorescent tris-N-nitrilotriacetic acid probes (≈1kDa),[233] and cascade blue dextran polymer[234] was observed in several mammalian cell types. A significant outcome of microfluidic cell squeezing platform is maintaining the cell functionality in $CD34^+$ HSCs and T-cells in vivo as well as minimal delivery-mediated effects on cell phenotype including global gene expression and cytokine secretion, which highlighted the therapeutic potential of this delivery modality.[235] Although cell squeezing is a user friendly and minimally invasive platform that only requires a pressure source and a regulator to precisely control the flow rate, the application of each device with a specific geometry is limited to the target cell size and narrow range of flow rate.

In another study of parallelization strategy, Han and co-workers introduced multiple microfluidic devices consisting of 14 similar cell-scattering and deformation zones, each of which contains 10 arrays of microconstrictions (Figure 6B). The rationale behind the design of these zones is to induce rapid mechanical deformation to the dispersed cells passing through the microconstrictions with different patterns of the diamond, circle, and ellipse. The authors reported higher cell viability when the diamond-patterned constrictions with 4 μm width were used for loading the FITC-labeled single-stranded DNA and GFP encoding plasmids into HEK293T cells. Moreover, they achieved high-efficiency CRISPR (clustered regularly interspaced short palindromic repeats)-Cas9-mediated gene-editing in MDA-MB-231 and SU-DHL-1 lymphoma cells by loading plasmids encoding EGFP-targeting single guide RNAs

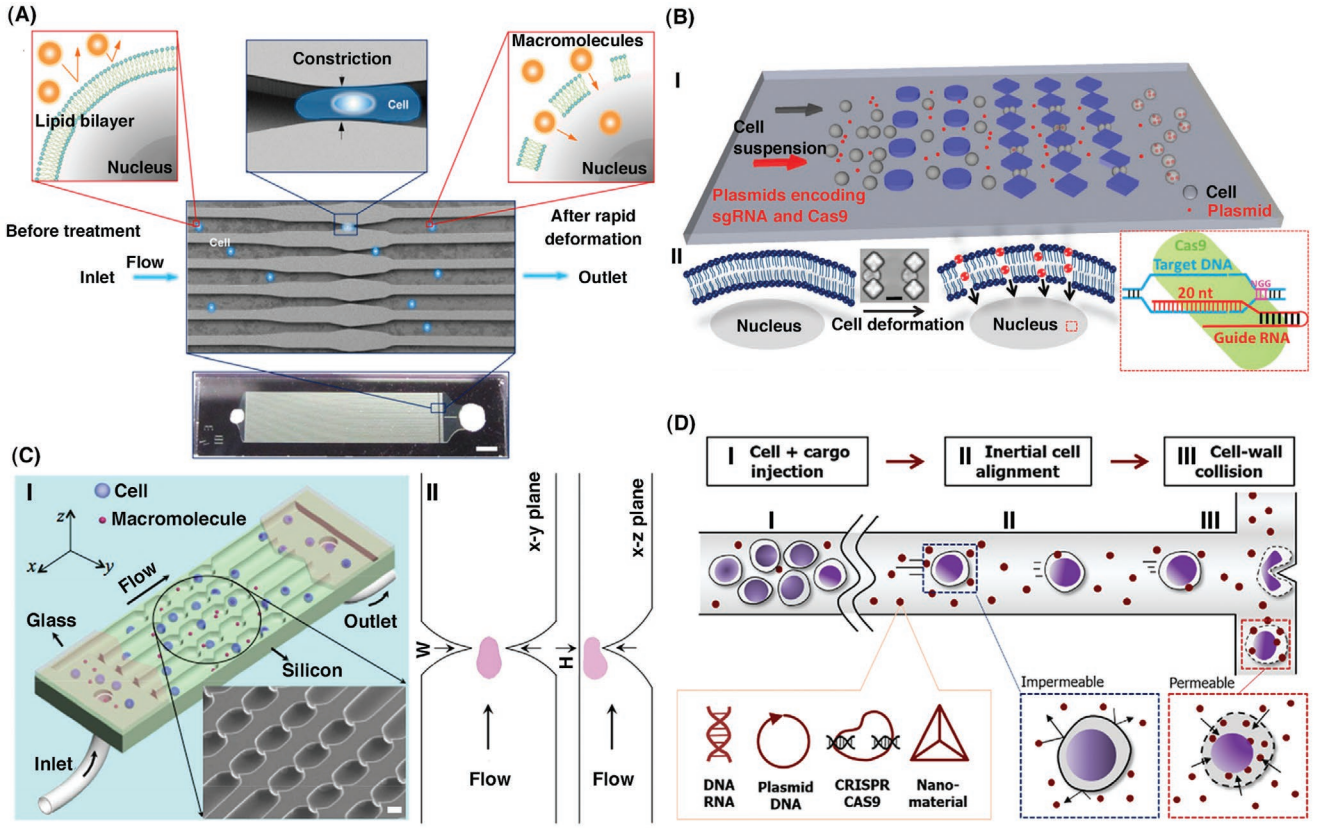

Figure 6. Different variations of mechanoporation devices for cytosolic delivery. A) The original cell squeezing platform. This microfluidic squeezing strategy induces rapid disruptions in cell membranes by forcing them through small rectangular constrictions. This cell squeezing device has one inlet and one outlet, wherein a mixture of cell suspensions and exogenous cargo is loaded in the inlet reservoir, and then the treated cells are collected from the outlet. Reproduced with permission.[229] Copyright 2020, The Authors, published by National Academy of Sciences, USA. B) Schematic of the membrane-disruption-based delivery device for CRISPR/Cas9 gene-editing. I,II) In this platform, the cells experience rapid stretching upon passage through a series of microconstrictions in the deformability zone. Transient membrane discontinuities created during the treatment process would be large enough for the cytosolic loading of CRISPR plasmids. Reproduced with permission.[236] Copyright 2015, The Authors, published by American Association for the Advancement of Science (AAAS). Reprinted/adapted from ref. [236]. © The Authors, some rights reserved; exclusive licensee American Association for the Advancement of Science. Distributed under a Creative Commons Attribution NonCommercial License 4.0 (CC BY-NC) http://creativecommons.org/licenses/by-nc/4.0/. C) A single cell squeezing microfluidic device. I) The flow chamber in this chip is fabricated with a series of parallel microchannels, each featuring a set of highly localized semicircular microconstrictions for single cell squeezing (scale: 20 µm). II) While single cells cross a point constriction, they are forced in 2 dimensions that further induces shear stress and membrane disruption. Reproduced with permission.[240] Copyright 2018, American Chemical Society. D) Schematic illustration of the microchannel design and the mechanism of intracellular delivery of macro (e.g., DNA, RNA, and plasmid DNA) and nanomaterials (e.g., DNA origami nanotubes, tetrahedrons, and nanospheres) via inertial microfluidic cell hydroporator (iMCH). The presented microfluidic device takes advantage of inertia-based cell focusing. Upon collision of the cells to the sharp tip protruding from the microchannel wall, they could uptake the impermeable cargoes via passive diffusion. Reproduced with permission.[241] Copyright 2018, American Chemical Society.

(sg-EGFP1, sgEGFP-2) or Cas9 protein. Rather than CRISPR/Cas9 delivery, they also made other attempts for genome editing through siRNA mediated knockdown of akt1 resulted in suppressing the growth of PC-3 cells.[236] To improve the delivery efficiency of Cas9/sgRNA ribonucleoproteins (RNPs) into human T-cells, Han et al. optimized the microfluidic chip by changing the pattern of microconstrictions to curved tunnels. In the new design, each chip consisted of 10 arrays of cell passage tunnels (4–8 µm width, 15 µm depth) that formed the deformation zone. Although the new chip showed nearly similar cell viability as the previous one, it takes advantage of increasing membrane deformations over an extended time of passing through the microconstrictions. Using this new cell-deformation design, they achieved efficient delivery of 70 kDa FITC-dextran and siRNA together or separately into the luminal-like SK-BR-3 and neutrophil-like HL-60 cells. This microfluidic device has shown promise for Cas9/sgRNA RNP delivery to SK-BR-3 and hard-to-transfect human $CD4^+$ T-cells while reducing the off-targeting and the reaction time.[237] In a follow up study performed in Qin lab, an integrated microfluidic chip was designed with repeated fishbone-shaped arrays of constrictions to achieve on-chip siRNA-mediated gene knockdown as well as on-chip cell migration assay.[238]

Based on this approach, Ma et al. proposed a hematopoietic stem cell (HSC)-specified chip (nanoblade chip, NB-chip) with an asymmetrical microchannel in the deformation zone featuring a nanoblade constriction only in one side. They used silicon as the nanoblade substrate material to increase

nanofabrication accuracy and the sharpness of the constriction that induce more contact pressure on cell membranes. By optimizing the treatment conditions, they reported ≈70% efficiency of loading 70 kDa FITC-dextran into the hard-to-transfect primary human $CD34^+$ HSCs while maintaining high cell viability (≈80%). Although the delivery efficiency of their method was similar to that of electroporation, they were of the opinion that the device is more capable of inducing minimum stimuli to maintain the inherent pluripotency of the HSCs for a longer time than other delivery methods as well as high cell viability. They conducted further investigations into the gene-editing ability of the NB-chip by delivering Cas9 protein and EGFP-targeting sgRNAs/Cas9 RNP into the HSCs and MDA-MB-231 cells, respectively.[239]

Building on the parallelization strategy, Xing et al. fabricated a microfluidic device with 15 main flow channels (with 300 µm width, 21 mm length) and 75 evenly distributed subchannels. Each array of subchannels (with 20 µm width, 7 mm length) contained a cascade of either 2, 4, or 8 single cell point constrictions, making semicircular deformation regions. Unlike other cell squeezing devices, this low backpressure system with a unique constriction profile forced the cells to migrate in two dimensions, which yielded to form rapid membrane deformations and increase the cytosolic delivery (Figure 6C). By tuning the applied pressure, constriction number, and constriction size, they achieved effective delivery of 3 kDa dextran conjugated with cascade blue into the HCT116 cells at 3 bar using a specific design with a cascade of 4 constrictions each sized 8 by 12 µm. They also verified the delivery performance of this modality by codelivery of 3 and 70 kDa labeled dextran to NIH3T3, HEK293, and hard-to-transfect MDCK cells under a constant set pressure (0.25–4 bar). While this platform showed effective delivery of the antitubulin antibody (≈150 kDa) and anti-EGFP siRNA into the HCT116 and HeLa cells, respectively, notable weakness is failing to return detectable loading of large dextran molecules (500 kDa) and plasmids (gWIZ-GFP, 5757 bp) into HCT116 cells.[240]

Another mechanoporation approach uses cell-wall collision to force the cells to collide with the wall of the microchannel featuring a single spike-like structure at the T-junction. Deng et al. proposed a robust high throughput approach based on inertial microfluidic cell hydroporator (iMCH) for intracellular loading of various nanomaterials into the different cell types, as illustrated in Figure 6D. In this approach, the sequential delivery steps include (1) the injection of the cell suspensions mixed with cargo to pass through the microchannel; (2) inertial focusing of the randomly distributed cells at the centerline of the microchannel; (3) collision of the cells with the sharp tip at the T-junction, which induces rapid mechanical deformation and membrane disruption; (4) passive diffusion of nanomaterials through the transient nanopores during the membrane recovery process. Using iMCH, significant delivery efficiencies and high cell viability were achieved for loading of FITC-dextran (3 and 70 kDa) and DNA nanostructures (e.g., DNA nanotube, nanosphere, and tetrahedron) into MDA-MB-231 cells. The results illustrated the potential application of this method in siRNA-mediated gene knockdown and CRISPR/Cas9-mediated gene knockout after loading of siRNAs and Cas9/sgRNA RNPs in different cell lines with nearly 50% efficiencies. This inertia-based approach takes advantage of simplicity; no external moving parts needed, and it executed a low-cost syringe pump for the entire delivery process. Compared to the cell squeezing modalities, iMCH devices offer improved delivery efficiency with minimal cell damage in intracellular loading of large molecules like plasmid DNA into the target cell. However, the core weakness of this design is partial cell clogging, lowering its delivery efficiency.[241]

3.6. Microelectroporation

Concurrent with the advancement in microengineering, microscale electroporation has been emerged with improved delivery efficiency and viability to address the potential problems that exist in its counterpart. These shortcomings include local distortion of the electric field, solution contamination via corrosion of electrodes, microbubble formation, Joule heating, deviations from the local pH, and difficulties in maintaining high cell viability. As the field currently stands, several studies have been published on the subject of microscale electroporation, which initially raised by Kurosawa's group. In this study, they aimed to measure the dynamic response of myocytes, which are in contact with micro-orifice or an array of orifices to the external stimuli.[17] Later more studies, however, have classified this method into different categories; microelectrode, microcapillary, and microchannel electroporation. In microelectrode- and microcapillary-based electroporation, intracellular delivery of cargoes happens inside a chamber under the static flow conditions while in microchannel-based electroporation the biomaterials are loaded into the target cells within a channel under controlled dynamic flow conditions. Thus, microelectrode-, microcapillary-, and microchannel-based electroporation can be described according to the following.

3.6.1. Microelectrode-Based Electroporation

This technique takes advantage of fabricated microelectrodes that are embedded inside a microfluidic chip to generate the required voltage for electropermeabilization of the cell membrane. The geometry of microelectrodes ascertains the distribution and the uniformity of the electric field that significantly affect the delivery efficiency.[27,242] Accordingly, a variety of microelectrode designs have been used for electroporation purposes on microchips. Published examples include parallel plate,[243] coplanar,[244] wire,[245] and 3D electrodes.[246] The parallel plate electrode system is one of the most straightforward architecture that mimics the conventional electroporation to permeabilize the cells within a microchannel sandwiched between two parallel electrodes.[243] In coplanar electrode system, electric field distribution varies upon different microelectrode geometries including parallel strip electrodes,[247] interdigitated electrodes (with rectangular,[244] castellated,[247] circular,[248] curved[249] or saw-tooth[250] strips), and circular/square electrode arrays. Microelectrodes fabricated in wire geometry are inserted in open reservoirs that are connected to the microchannels of a chip. These microelectrodes not only provide uniformity in electric field distribution but also address

the weaknesses of the previously reported geometries including microbubble formation and Joule heating. Although in this system interelectrode distance is longer than the other microfabricated electrodes, the surface area of the wire electrodes is small, which brings about a considerable reduction in the cell death rate.[251] Followed by these studies, 3D microelectrodes were fabricated with different geometries and then placed vertically in sidewalls of the reaction chamber to generate a more uniform electric field which covers three dimensions.[252]

3.6.2. Microcapillary-Based Electroporation (MCEP)

Microcapillary-based electroporation (MCEP) is a term that addresses the intracellular delivery within the disposable reaction microchambers under the controlled conditions.[253] Based on the applications of MCEP, this approach is divided into two major groups. The first method is based on creating localized electric fields by placing electrolyte-filled capillaries (EFC) in the close vicinity of cells that selectively treated target cells without affecting the surrounding ones.[254] Hence, this method can be applied specifically to better focus an electric field on target single cells while neighboring ones remained unaffected. The second method is based on tip-type microcapillary electroporation integrated with laboratory pipettes for improving both sample handling speed and delivery efficiency with the same sample loading method as the conventional pipettes. In this method, the electroporation process occurs within the reaction chamber consisted of a long and narrow capillary integrated with a wire-type electrode. Major advantages of the tip-type capillary electroporation compared to EFC are enhanced cell viability (70–80%) and delivery efficiency (up to 80% in cell lines), minimized local pH level variations during the delivery procedure, and shortened processing time (into 15 min).[255]

3.6.3. Microchannel-Based Electroporation (MEP)

Microchannel-based electroporation (MEP) system applies a precisely controlled low-voltage electric field (less than 10 V) focused in the microscale channels to drive electropermeabilization of the cell membrane.[256] MEP can be useful for electroporation of single or multiple cells in a gentler environment under dynamic conditions. This device consists of an inlet and outlet reservoir, a microchannel called reaction chamber, and an electric pulse generator that might be connected to the microfabricated electrodes. In this technique, a mixture of cell suspensions and cargoes to be delivered are loaded in the inlet reservoir. Next, the pulse generator perforates the membrane at the microscale (without the complete disruption) through the delivery of the low-voltage pulses to the cell suspensions. After the application of the electric field, the electroporated cells are collected from the outlet reservoir. The confined region of microscale pores created during the MEP causes the selective diffusion of biomaterials (based on their size) into the target single cell.[27,257]

This technique not only offers a potential application to be used as a high throughput lab-on-chip platform but also provides the benefits of real-time detection and cell manipulation, simultaneously, followed by intracellular delivery. However, significant weaknesses of this system are the inability to dosage control and difficulty in the manipulation of the electroporated cells as they are fixed within the reaction microchamber. To cope with these challenges and provide more controllable delivery, MEP system can be combined by micropore array on polyethylene terephthalate (PET) track-etched membranes, planar microelectrode arrays (MEA) and 3D microelectrodes, microfluidic hydrodynamic focusing, and single cell isolation techniques.[258,259]

Membrane Sandwich MEP: Fei and co-workers introduced a novel method providing better confinement of target genes near the cell membrane to facilitate the cargo loading into mammalian cells called membrane sandwich electroporation (MSE). In the reported study, they fabricated a microfluidic-based MSE device with a pair of cross channels (one on the top and the other on the bottom with 500 μm width and depth) connected via a center hole, and a center reservoir where the track-etched PET membranes are embedded within the device. Using this delivery approach, the immobilized cells are sandwiched between two track-etched PET membranes with randomly distributed pores.[260,261] Then, a low voltage current is required for breaking down the cell membrane and cytoplasmic loading of the biomaterials.[261] In a subsequent study, the group modified their device architecture to provide more uniform electric field distribution generated by randomly distributed pores on the track-etched PET membranes through utilizing micronozzle array and nanofiber.[260,262]

Microelectrode-Array-Assisted MEP: Microelectrode arrays (MEAs) are designed to achieve parallel cytosolic loading of exogenous biomaterials into different cells and simultaneous cell-based screening of multiplex parameters affecting electroporation efficiency as well as cell viability.[263] More recently, Ouyang et al. developed a microscale symmetrical electroporator array (μSEA), which is an on-chip vortex assisted electroporation system equipped with real-time visualization of the sequential delivery processes (**Figure 7**A). This device with micropatterned planar electrode array and lower voltage requirement enables simultaneous enrichment of cells at single cell resolution, and either single cargo delivery or codelivery of various cargoes (multi-molecular delivery) with the controlled dosage that results in enhanced delivery efficiency and cell viability.[264]

3D Microelectrode-Assisted MEP: The MEP method combined by 3D microelectrodes utilizes a low-voltage electric field in the same direction as the intracellular delivery process, but in a vertical direction (*Z*-direction) of thousands of cells on a planar membrane (*X, Y* directions) for membrane poration. Accordingly, Dong et al. developed a pyramid pit-shaped micropore array chip for single cell patterning and 3D microelectroporation in situ. This controllable delivery platform consisted of a bottom (Cr/Au) and a top electrode that were placed in the lower and upper chamber, respectively, a silicon chip with micropore array, and a PDMS spacer. In this approach, cells were injected into the upper chamber to be cultured onto the silicon-based micropore array, and delivery cargoes were loaded into the bottom chamber. By applying a voltage as low as 1 V between the two electrodes, membrane damage was induced to the cells that allowed cytosolic loading of cargoes into the cells.

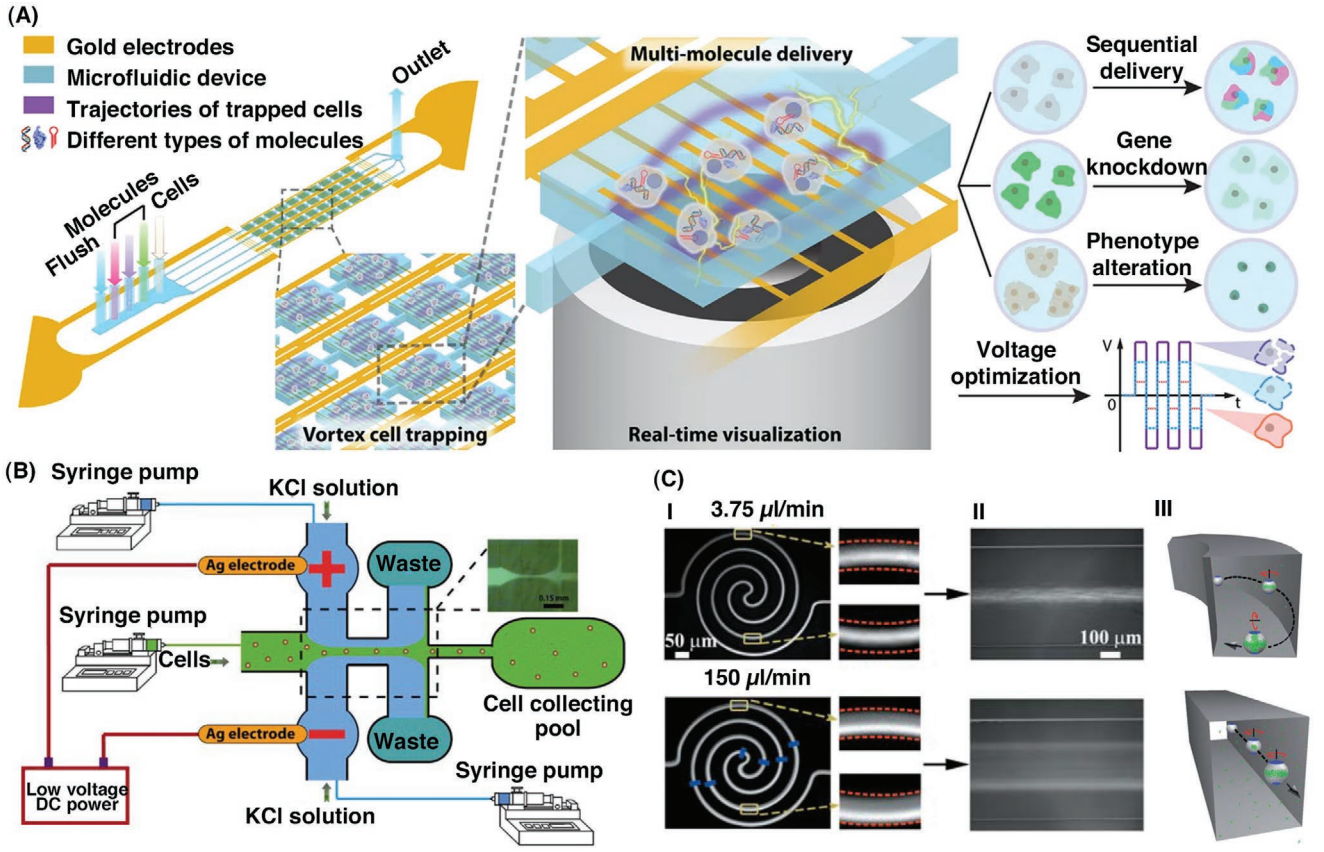

Figure 7. Schematic representation of recent advances in microelectroporation techniques. A) Illustration of the vortex-assisted electroporation system that trap the cells in the vortex chamber containing micropatterned Au electrodes. Reproduced under the terms of the CC-BY Creative Commons Attribution 4.0 International license (https://creativecommons.org/licenses/by/4.0).[264] Copyright 2017, The Authors, published by Springer Nature. B) A continuous DC voltage is applied to the highly conductive KCl solution on the side channels, which squeeze the central flow into a stream of the thin layer. The cells in the central flow layer experience hydrodynamic focusing, and a short electric pulse leading to the electropermeabilization of the cell membrane. Reproduced with permission.[266] Copyright 2009, Springer Nature. C) Microfluidic electroporation device with the spiral-shaped channel. This device mainly consists of one narrow part with spiral design (4.7 mm length, 35 µm width) and two wide parts with 3 cm length and 500 µm width. I) Fluorescent microscopy of labeled CHO cells passing through the spiral microchannel at two different flow rates of 3.75 and 150 µL min^{-1}. II) Although CHO cells are loosely focused at the center of the spiral-shaped channel at a low flow rate (3.75 µL min^{-1}), in higher flow rates (75–150 µL min^{-1}) Dean flow results in drag forces that shift the focused CHO cells to the multiple locations across the channel centerline. III) Cells passing through curved paths or spiral-shaped microchannels (top) are subjected to a complex combination of transverse advection and rotation when compared to straight (bottom) ones. C) Reproduced with permission.[269] Copyright 2001, Royal Society of Chemistry.

The device showed up to 90% delivery efficiency of CRISPR/Cas9 plasmids into the A375 cells while maintaining the cell viability.[265]

Recently, researchers presented an advanced form of 3D MEP that is guided by magnetic tweezers generating a uniform magnetic field for high throughput intracellular delivery of biomaterials into target cells.[259] In this system, four orthogonal electromagnets (*X, Y* directions) and a solenoid (*Z* direction) make the magnetic-tweezers set up to perform magnetic-field assisted manipulation of cells, and a combination of a planar and bottom electrode creates the required electric field for membrane permeabilization. The magnetic tweezers-based MEP systems offer the opportunity for high-throughput (≈40 000 cells cm^{-2}) and uniform intracellular delivery with more than 90% cell viability and simultaneous manipulation of cells at single cell resolution. In 2014 Chang et al. used this platform for on-chip parallel manipulation, delivering of GATA2 molecular beacon into single or an ordered array of leukemia cells on MEP chip and transportation of GATA2-loaded cells for further analysis.[68,259]

Hydrodynamic MEP: Favorable hydrodynamic conditions can manipulate cells in microfluidic channels to enhance the delivery efficiency of microscale electroporation. Hydrodynamic focusing of fluids with different conductivities has shown the potential to be a broadly utilized method in which sheath flow from two lateral channels squeezes the central flow into a thin stream layer. Accordingly, Zhu et al. developed a microelectroporation method based on hydrodynamic focusing of yeast cell suspension using a low voltage direct current (DC) power supply (Figure 7B). In this device, a highly conductive KCl solution was pumped from the lateral channels, and the yeast cell suspension was pumped from the central one (called sample channel). The microelectrodes were then placed in the inlets of the KCl solution channels to create a constant DC voltage (<3 V) for high throughput cytoplasmic delivery while protecting the cell suspension from local heat generated in lateral

channels. This microfluidic-based system not only dissipates the local heat but also prevents any deviations from local pH and the formation of microbubbles during the electropermeabilization process.[266]

On the other hand, hydrodynamic effects associated with Dean flows that arise in microfluidic devices can create inertial forces along curved flow paths or spiral-shaped microchannels. Under the optimal conditions, these curvature-induced forces become strong enough to generate a transverse vortex resulting in transverse advection and continuous rotation of the cells passing through the spiral microchannels. In such a scenario, enhanced delivery efficiency is achieved as the exogenous biomaterials have more access to a larger fraction of the entire membrane surface that is experiencing a complex combination of inertial lift and drag forces to become uniformly permeabilized. Wang et al. were among the first to use spiral microfluidic electroporation devices to induce vortex-assisted electropermeabilization of CHO cells and further uptake of pEGFP-C1 plasmids (Figure 7C). It is imperative to note that previously reported vortex-based microfluidic systems designed with straight microchannel have been used to experimentally verify the intracellular delivery of a wide variety of exogenous cargoes to different cell types.[264,267,268] However, Wang et al. illustrated that electropermeabilization of CHO cells in this system, along with empirical optimizations, enhanced the delivery of pEGFP-C1 plasmids nearly twofold over devices designed with straight microchannel while the cell viability is almost similar (≈90%).[269] In another case, Yun et al. developed a vortex-assisted microfluidic device with embedded electrodes for electropermeabilization of preselected MDA-MB-231 and K562 cells based on their size. In this setup, as the heterogeneous population of cells was passing through the microchannels, they experienced shear-gradient and wall lift force giving rise to inertial focusing of cells based on their biophysical characteristics. Next, an extracellular electric field (E_i = 0.4 kV cm^{-1}) was applied to load two different membrane-impermeable dyes (PI and YOYO-1) into the target cells with uniform size. The proposed device provides enhanced efficiency with precisely controlled delivery of multi-molecules while preserving viability.[268]

Single Cell MEP: Single cell MEP technique takes advantage of creating a highly focused electric field in the local region of the single cell to achieve high delivery efficiency and cell viability without affecting surrounding ones.[270–272] This technique offers dosage control, manipulation of single cells to a specific position, real-time monitoring, and spatio-temporal control over the delivery process. However, its core weakness is time-consuming and high-cost fabrication of the single cell MEP chips. Different strategies of MEP at single cell resolution include isolation of an individual cell from others and focusing an electric field on a single cell coined as nanolocalized single cell electroporation (Section 3.9). Single cell electroporation in microscale devices can be categorized into two groups according to the way that cells move through the device, either the cell trapping-based or droplet microfluidic-based approach, which are described as follows.

Cell trapping-based approach: Cell trapping-based MEP devices at single cell resolution usually consist of a micropore or an array of planar microconstrictions smaller than the cell diameter. In these devices, negative pressure and an inhomogeneous local electric field are applied to induce membrane disruptions in trapped individual cells. In the following, some cell trapping-based microfluidic devices applicable for MEP at single cell level are described.

One of the first cell trapping-based microfluidic setups for single cell MEP was proposed by Huang et al. in 1999. This vertically stacked device consisted of a top and bottom chamber filled with saline and separated by a 1 μm thick silicon nitride middle layer with a microhole sized between 2 to 10 μm. In this device, top and bottom transparent layers are fabricated using n^+ polysilicon layer with metal like properties, which make them ideal to be used as electrodes. These two saline-filled chambers had different pressures. As the pressure in the top chamber was higher than that in the bottom one, the cells tend to flow from the top to the bottom chamber leading the trap of individual cells in the microhole that connects the two chambers and electrodes. Plugging the microhole and providing a constricted electric field using a continuous DC power supply with the pulse duration and amplitude of 2 μs to 100 ms and 0–120 V, respectively, can finally cause the electropermeabilization and further cytosolic delivery of the exogenous compounds into the trapped single cells.[273]

In a follow up study, they took advantage of the flow-through microfluidic chip for high throughput manipulation and highly efficient single cell MEP in two separate studies in 2001 and 2003.[274,275] In their investigation in 2003, they developed a microfluidic chip with higher widths compared to the cell dimensions, in which the cells are mechanically confined and focused at the centerline to pass through the microchannel individually and reach the microhole region. Since the applied pressure in the bottom chamber is lower than that in the top one (negative pressure), the single cells are easily trapped in the microhole region. Then, reversible electropermeabilization of the trapped single cell and further cytoplasmic delivery of cargoes take place after supplying an external electric field with an appropriate pulse (10 V, 10 ms). In order to release the electroporated single cell from the microhole and substitute the next cell for the electropermeabilization process, the lower pressure of the bottom chamber should be withdrawn.[275]

An improved cell-trapping-based microfluidic setup for single cell electroporation was proposed by Khine et al. in 2005 (**Figure 8**A). This multiplexed patch-clamp array chip had two wider trapping microchannels with a width of 3.1 μm (equal to one-third of the cell diameter), which were used for cell input and output. In this microfluidic device, an Ag/AgCl electrode was connected to each microchannel, and the main inlet channel was linked with many microchannels to laterally capture the single cell in the small region coined as trapping channel. Applying negative pressure to the microchannels caused the release of cells from the primary inlet to the middle circular section to laterally trap a single cell at the microhole region and locally electropermeabilize the individual cells at the end of microchannels using a low voltage electric pulse (≈0.76, 6.5 ms).[276] This microfluidic device was later bonded to a disposable 96-well plate for manipulation and real-time monitoring of individual cells (Figure 8B).[277]

Later, Ionescu-Zantti et al. developed a cell-trapping-based microfluidic device for single cell electroporation that takes advantage of electrophoresis to deliver exogenous anionic

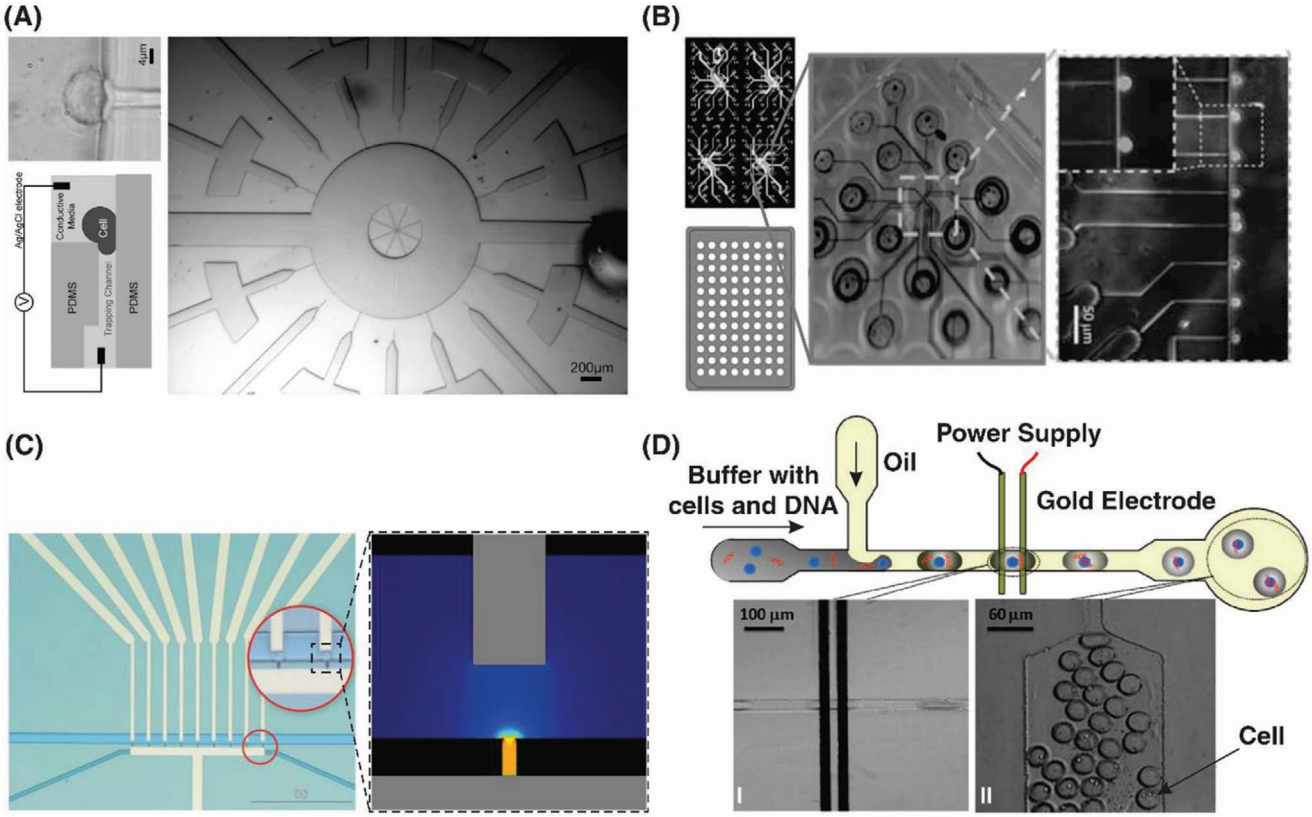

Figure 8. Different variations of single-cell MEP, which is mainly divided into the two groups of cell trapping- and droplet microfluidic-based approach. A) In multiplexed patch-clamp array cells are laterally immobilized and hydrodynamically trapped in the trapping channel (4 μm × 3.1 μm) by applying negative pressure. Next, they are locally electroporated using low applied voltages (<1 V). Reproduced with permission.[276] Copyright 2001, Royal Society of Chemistry. B) In this single cell MEP setup, microfluidic cell-trapping devices are bonded to a standard 96-well plate, which is divided into 4 quadrants. Each quadrant consists of multiple trapping sites which allow the lateral trapping of single cells within 20 μm distance from each other. Reproduced with permission.[277] Copyright 2001, Royal Society of Chemistry. C) This microchip (20 × 15 × 1 mm) has nine trapping sites and a localized electroporation spot to expose the individual cells with biomolecules or dyes. After localizing the cells at the trapping sites, a low voltage electric field is required to electropermeabilize the trapped cells. Reproduced with permission.[278] Copyright 2001, Royal Society of Chemistry. D) Droplet microfluidic-based device with nearly 33 μm depth for single cell microelectroporation. I) The water-in-oil droplets contain individual cells and delivery cargoes were produced in the T-junction part of the microchannel and then rapidly flowed through the two microelectrodes (with 25 μm depth) leading the electropermeabilization of the cells encapsulated within the droplets. II) After electropermeabilization process and consequent cytosolic loading of cargo molecules, these droplets can be collected at the exit site of the droplet-based microfluidic device. D) Reproduced with permission.[288] Copyright 2009, American Chemical Society.

impermeant molecules. This electrophoresis-driven MEP device had lateral microchannels terminating in 3 × 3 μm capillaries to focus the external electric field (50–200 mV) and further trap the single cell through the capillary microchannels by utilizing the negative pressure. In this method, first, the exogenous impermeant cargoes were preloaded in capillary microchannels, then a short high-intensity pulse (0.5–2 V) and a slight negative pressure were applied to increase the cargo concentration at the channel interface and trap the individual cells, respectively. Next, the electroporation process was initiated by applying larger amplitude electric pulses (5–30 ms) to electropermeabilize the cell membrane. Afterward, to enhance the rate of intracellular delivery, a low electric field was used to electrophoretically drive exogenous molecules into the cell cytoplasm in addition to the diffusion loading during the release of the cell membrane.[277]

Moreover, Valero et al. designed a microfluidic device for single cell MEP that takes advantage of using parallel channels as cell trapping arrays (Figure 8C). This device consisted of two main microchannels connected via microholes and an array of nine independent trapping sites to electroporate nine single cells at the same time. One characteristic of this microfluidic set up is that the electrodes generate a highly focused electric field that merely electropermeabilize the cells at the nine trapping sites while the neighboring ones remain unaffected. The device showed up to 75% delivery efficiency of vector DNA encoding EGFP-ERK1 into C2C12 cells and MSCs.[278] Along with recent advances in cell-trapping based single cell MEP, Punjiya et al. fabricated a flow-through microfluidic chip using a single AC excitation source for negative dielectrophoresis (nDEP) trapping and electroporation of individual cells. Transient expression of a plasmid DNA encoding FusionRed fluorescent protein (RFP) that flowed into the electropermeabilized HEK-293 cells from the culture media was achieved using this device.[279,280]

Droplet Microfluidic-Based Approach: Droplet-based microfluidic devices focus on manipulating, screening, and transporting

single cells encapsulated within water-in-oil droplets, which provide an environment to investigate the cellular response and conduct single cell genomics and differential gene expression analysis. These droplets act as monodisperse carriers of single cells and biomolecules in the aqueous phase within the droplet-based microfluidic devices. In this setup, on-demand and continuous droplets are created as a result of implementing electric fields (coined as active method) and pressure-driven flow (called passive method), respectively.[281–284] The specific design of microfluidic devices allowing uniformly sized-droplet production in a passive approach, which is the most commonly used method, includes T-junction,[285] flow-focusing,[286] and coflowing.[287] In all of these cases, the prime mechanism is shearing of the aqueous phase through the inert oil phase, which creates aqueous droplets surrounded by oil. Zhan et al. reported the transfection of EGFP encoding plasmid into CHO cells via a droplet microfluidic-based single cell electroporation device. This device was fabricated with PDMS using a standard soft lithography process and designed with T-junction channels. As illustrated in Figure 8D, the device contains two inlets, one outlet, and two microelectrodes with 150 nm thickness and 20 μm electrode gaps. Once the electroporation buffer with CHO cells and pEGFP-C1 plasmid were loaded in one inlet channel, the cells were encapsulated in aqueous droplets. Simultaneously, hydrocarbon oil was introduced from the other inlet, facilitating the flow of cells to downstream where the microelectrodes were located. To avoid the cells from settling down while they were spinning, the droplets were introduced by a syringe pump with magnetic stirrer making a stir bar to rotate in the medium. Then a constant DC voltage was applied between the pair of the microelectrode. As a result, electric current acted on the conductive buffer and electropermeabilized the cells inside the flowing droplets within the microchannel. The cytosolic loading of cargoes occurred during the membrane resealing process with nearly 11% efficiency and then the cells were released from the droplets, which were immediately transferred to the culture media. The electrode gap (≈20 μm), applied voltage (5–9 V), dimension (60–386 μm in length), and velocity (1.38–8.86 m min^{-1}) of the droplets were the key factors defining the intensity and duration of electroporation process.[288] A major weakness of using hydrocarbon oil in conventional droplet-based microfluidic devices is low cell survival and delivery efficiency due to its low gas permeability and loss of organic reagents used in chemical delivery methods.

However, fewer reports exist on the cytosolic loading of cargoes inside droplets for single cell MEP purposes, possibly due to low delivery efficiency, highlighting the urgent need for further investigations using different sizes of droplets. While microdroplet based systems require high DNA concentration to achieve higher delivery efficiencies, at lower DNA concentrations bulk electroporation would be a better option to obtain higher delivery efficiency.[253]

3.7. Microchemoporation

Although cationic liposomes are considered as one of the highly efficient approaches in carrier-mediated intracellular delivery systems (Section 2.1.2.), multicomponent liposome and target DNA complexes (called lipoplexes) prepared by bulk self-assembly are highly toxic to the cells. To address this concern, Digiacomo et al. scaled down the reagent volumes required for chemical delivery via microfluidic mixing in NanoAssemblr benchtop system. In this microchemoporation setup, multicomponent liposomes were mixed with pGL3 luciferase reporter vector at a total flow rate of 4 mL min^{-1} followed by overnight dialysis. The authors suggested that the lower delivery efficiency but higher cytocompatibility was achieved using lipoplexes prepared by microfluidic mixing. More advanced studies used the droplet microfluidic approach to achieve microlipofection in single cells.[289] Accordingly, Chen et al. in 2011 proposed a microfluidic chip for the generation of aqueous droplets in fluorocarbon oil to encapsulate CHO-K1 cells, chemical transfection reagents (a cationic dendrimer called PolyFect), and pEGFP-C1 plasmids for single cell chemical transfection. In this setup, the aqueous phase (containing target cells, plasmid DNA, and transfection reagents) came into the device from the center flow while fluorocarbon oil came in from two side flows. Tiny aqueous droplets were then generated as a result of flow focusing to provide microscale confinements that increase the probability of interactions between cells and PolyFect/plasmid complexes. Fluorocarbon oil has a number of advantages when compared to that of hydrocarbon, which includes high biocompatibility and gas permeability that brings about high viability of cells inside the droplets. They obtained results suggesting that delivery efficiency in smaller droplets was higher than that in bigger ones. It is thought that enhanced delivery efficiency (≈25%) in smaller droplets could be due to the high surface-to-volume ratio and high probability of interactions between target cells and loading cargoes in microscale confinement.[289] In a recent study by Li et al. designed a droplet-based platform working with coflowing the mixture of cell suspension and plasmid DNA with lipofectin solution. The monodisperse droplets encapsulating lipofectin, plasmid DNA, and single cells were then generated at the flow-focusing pinch-off orifice, wherein shear stress at this junction induced membrane disruption in target cells. Moreover, as droplets were passing through the serpentine microchannel, they experienced chaotic mixing and advection resulted in lipoplex formation, lipoplex-cell collision, and efficient transfection. Using the droplet lipofection platform, they achieved up to 50% efficiency of loading pcDNA3-EGFP plasmid into hard-to-transfect K562, THP-1, and Jurkat cells. Additionally, the results indicated 81% ± 8% knockout efficiency of TP53BP1 gene in K562 cells through droplet lipofection delivery of pLentiCRISPR.v2-sgTP53BP1 plasmid.[291] Yet delivery challenges including lack of user-friendly design, the complexity of circulating flow within the droplet, and dependency of transfection efficiency on the size of lipoplexes retarded their deployment in clinical applications.

3.8. Nanoengineered Structures

In recent years, nanotechnology has been employed to fabricate nanostructures for further investigation of the intracellular environment and cellular manipulation. A variety of nanoscale structures have been developed in which either high mechanical

pressures (e.g., nanotubes or nanospears) or localized electric shock (e.g., nanostraws, nanofountain probes, nanospikes, and nanochannels) is induced to the nano–bio interface.[292] Carbon nanotubes (CNTs),[293] mesoporous silica nanoparticles (MSNs),[294] gold nanoparticles (AuNPs),[295] quantum dots (QDs),[6] silicon nanoneedles,[296] and silicon nanowires[297] (**Figure 9**A,B) are examples of nanostructures, which have been widely used for the intracellular cargo loading applications. The chemophysical properties of these nanostructures such as size, charge, and displayed ligands on their surface can be tuned for intracellular delivery purposes. More specifically, they can be used for cytosolic loading of proteins while they protect these proteins from denaturation via proteolysis. Among these nanostructures, biocompatible and water-soluble functionalized CNTs have been broadly used in numerous intracellular delivery applications.[298,299] Single-walled carbon nanotubes (SWCNTs) embedded with needle-like geometry can penetrate through the cell membrane with minimal damage. In particular, Li et al. have shown the use of CNTs for the cytosolic delivery of biotinylated proteins into the cells by near-infrared (NIR) light irradiation.[300] In another study, Cai et al. used nickel-embedded nanotubes coined as a nanotube spearing approach to achieve highly efficient cytosolic loading of pEGFP-c1 into the Bal17 cells. In this approach, first, the nanotubes are driven by a magnetic actuation resulted in spearing of the cell membrane and then they are pulled into the cell cytosol by applying a static magnetic field.[301] Using magnetically drived nanospears, Xu et al. achieved successful intracellular loading of GFP-expressing plasmid with high throughput.[302] MSNs are mostly used for encapsulating proteins and protecting them from denaturation and proteases

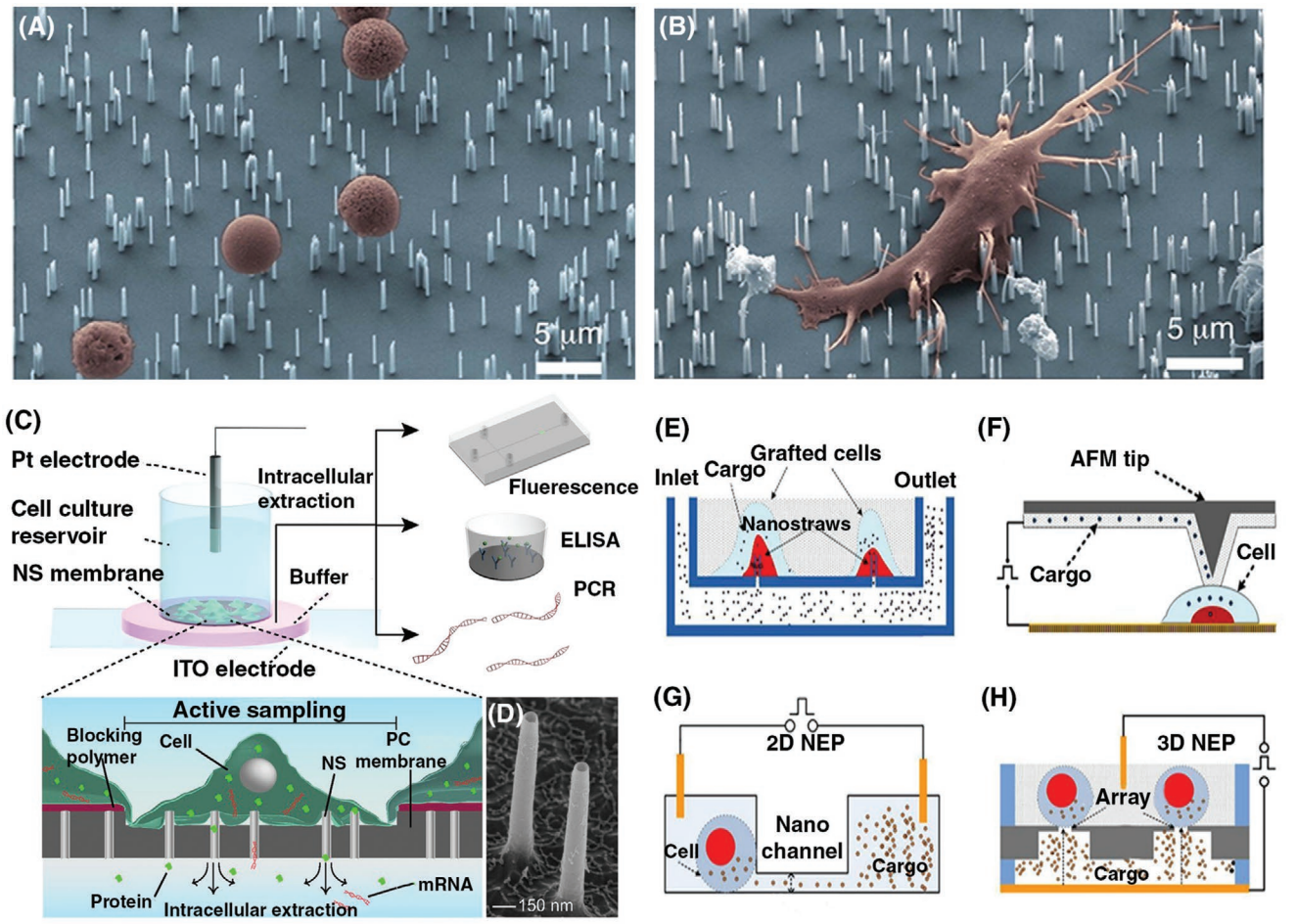

Figure 9. Modes of various nanoscale intracellular delivery techniques. A,B) Nanowires are able to load molecular cargoes ex vivo into immune cells. The scanning electron microscopy of B cells and dendritic cells after 24 h of culturing on top of nanowires is shown in (A) and (B), respectively. A,B) Reproduced with permission.[297] Copyright 2012, American Chemical Society. C) In the nanostraw electroporation platform, the highly localized electric field is induced to the nanostraw–cell interface to either load biomaterials into the intracellular space or extract cargoes (e.g., proteins, and RNA) out of the target cells. D) Scanning electron microscopy of nanostraws with the height of 1.5 µm and diameter of 150 nm. C,D) Reproduced with permission.[312] Copyright 2020, The Authors, published by National Academy of Sciences, USA. E) Nanostraw EP system with enhanced delivery efficiency facilitates the penetration of biomolecules through piercing the cell membrane and creating nanopores. F) In situ delivery of biomolecules into the target cells through the flexible movements of hollow AFM tips and highly localized transportation in the nanofountain probe electroporation system. G) The basic design of nanochannel electroporation in 2D (2D NEP) that leads the precise dose control of cargo to the target cell. H) High-throughput 3D nanochannel electroporation (3D NEP) takes advantage of the parallelization strategy to handle up to millions of single cells per wafer-scale. E–H) Reproduced with permission.[327] Copyright 2009, Royal Society of Chemistry.

during the cytosolic protein delivery. Accordingly, Lin et al. used MSNs for cytosolic loading of FITC-labelled cytochrome c into the HeLa cells.[303] AuNPs can readily be conjugated to nucleic acid strands, which are modified with thiols (SH-PEG-SH) to deliver them into the target cells.[304] In addition to the nucleic acids, proteins and peptides can be loaded into the cells using the AuNPs.[305] In the reported study, Bhumkar and co-workers have confirmed functionalized AuNPs as carriers of insulin. In this work, chitosan, a non-toxic biopolymer, was coated on AuNPs to absorb insulin on their surface.[306] In nanoneedle mediated cytosolic loading, which is also known as nanoinjection, an array of vertical porous silicon nanoneedles is used to enhance the internalization of molecular cargoes. Accordingly, in a recent study, Gopal et al. achieved rapid nanoneedle-mediated delivery of fluorescently labeled transferrin, albumin, cholera toxin, dextrans and GAPDH-siRNA into the cultured hMSCs on the array of biodegradable nanoneedles.[307] QDs ranging from 2 to 10 nm are semiconductor nanocrystals that their size increases up to 5–20 nm in diameter after polymer encapsulation. In this work, drug-loaded silicon QD aggregates were presented by using amine-modified silicon QDs with visible photoluminescence. Accordingly, the selective intracellular release of the loaded drugs occurred due to silicon QD aggregates which broke down as a result of a decrease in endosomal PH.[308]

3.9. Nanoscale Devices for Localized Single Cell Electroporation

Nanoscale devices for localized electroporation at single cell resolution apply and focus a low-voltage electric field to a small area of a cell for local poration of plasma membrane without affecting the neighboring cells. These devices can provide certain promising advantages such as low power input, small sample volume, and negligible heat and ion generation resulting in higher compatibility and lower cytotoxic effects. These parameters are important to achieve better delivery outcomes while maintaining cell viability.[309,310] Indeed, nanoscale devices that rely on localized electric field such as nanostraw, nanofountain probe, nanospike, and nanochannel electroporation can precisely and selectively deliver cargoes into a single cell. A key advantage of these nanoscale delivery devices is that they are in direct contact with cells, which allows the induction of stronger and highly localized stimuli to the region of interest in the plasma membrane.[33] In the following, the nanoscale electroporation platforms are highlighted with more details, as depicted in Figure 9C–H.

3.9.1. Nanostraw Electroporation

Nanostraws are vertical hollow metal-oxide nanowires that pierce the cell membrane without perturbing vital cell functions to provide direct and continuous intracellular access for external fluids (Figure 9C–E). In this method, cells are cultured on the microporous track-etched membrane, with a number of protruding nanostraws that are in contact with the fluid beneath the membrane. Then, by applying a low electric field focused on the plasma membrane, cultured cells are locally disrupted at the cell–nanostraw interface. This technique was developed as a powerful tool for spatio-temporal controlling of intracellular delivery and sensing, which enabled further investigations on a real-time molecular transfer in situ and longitudinal cell monitoring.[311,312] Nanostraw electroporation system took advantage of electrophoretic injection of any freely diffusing cargo biomolecules besides the passive diffusion process to increase the delivery efficiency at the nanoscale during pulsing. Reducing the required voltage for electroporation and increasing the homogeneity over a large area that enables precise control over the concentration of delivery biomaterials are the further advantages of this approach. Nanostraw electroporation membranes were fabricated using track-etched polycarbonate nanoporous membranes with 3×10^7 pores cm^{-2}, each pore was ≈100 nm in diameter. The surface of these membranes was then coated with alumina (10–30 nm thickness), which created nanostraws within the nanopores extending through the polymer and protruding from the membrane surface with a typical height of 1–2 μm. Afterward, the nanostraw membranes were integrated within two microfluidic compartments and placed over the microchannels to allow culturing the cells on the nanostraw membrane and provide the direct access of the fluidics to the intracellular space through an array of nanostraws. In this setup, the microfluidic channel was bonded on top of a glass slide coated with indium tin oxide to act as an anode (bottom electrode) and a platinum electrode was placed in cell suspensions to serve as a cathode (top electrode). By applying a localized electric field between these two electrodes, Xie et al. achieved more than 80% efficiency for cytosolic delivery of PI dye and pm-Cherry-C1 plasmids into CHO cells without compromising the cell viability.[313,314] Recently, Cao et al. reported nanostraw electroporation system as an accurate dosage-controlled delivery system for loading plasmid DNA, mRNA, and protein into cell lines as well as primary cells. Using this delivery system, they codelivered GFP encoding plasmid and mCherry mRNA with different concentration ratios between 250:15.6 to 15.6:250 into the HEK 293 cells. They could successfully achieve 75–90% delivery efficiency while maintaining the cell viability. The results indicated that the expression levels of delivery cargoes in target cells can be precisely controlled by varying the cargo concentrations in delivery buffer.[315] However, the potential drawback of this system is high potential differences required for electroporation of target cells that may generate reactive oxygen species, which are harmful for cell health. Moreover, fabrication of electroconductive nanostraws requires complex and costly procedures including atomic layer deposition and etching.[316]

3.9.2. Nanofountain Probe Electroporation

Fabricated nanofountain probe (NFP) microchips are designed with an array of cantilever tips connected to microreservoirs through build-in microchannels and dispensing fountains to deliver cargoes into individual cells directly. This device is coupled with a micro/nano manipulator or AFM for precise force and position control (Figure 9F).[317] In this setup, externally applied pressure drives the biomolecules within the microreservoirs to the microchannels to reach the cantilever tip region. When the cantilever tip is in contact with a single cell,

an electric pulse is applied to trigger nanopore formation and induce electropermeabilization in a region of interest in the target cell.[318–321] The system was used to load PI and plasmid DNA into single HeLa and HT1810 cells, which demonstrated a high delivery efficiency (>95%), single cell selectivity, precise dosage control without affecting the cell viability (>92%). In this study, NFP chips were then coupled with optical imaging and electrical detection to control single cells precisely and reduce cell stress and damage upon the contact force applied by the probe. Furthermore, the dosage of the injected biomolecules into the cells was controlled by the amplitude and duration of the electric pulses. Direct delivery and large-scale nanopatterning of biomolecules (including proteins, DNA, and RNA) in a liquid are among the significant applications of NFP chips. The primary benefit of this method is the potential of loading cells with molecules of various sizes and charges without affecting the cell viability.[317] This method was also applied for localized loading of bovine serum albumin (BSA) to either cytoplasm or nucleus by positioning the probe away from or on top of the nucleus.[309] In follow up applications of this system, Yang et al. carried out CRISPR-based gene editing to knockout EGFP in HEK293 cells and generate a monoclonal cell line. In this platform, HEK293 cells are patterned on an array of 100 μ micropillars and allowed to grow for 24 h. Applied electric field to the cell–probe interface increased the transmembrane potential leading to generation of nanopores in plasma membrane and molecular cargo transfer.[322]

3.9.3. Nanospike Electroporation (NSP-EP)

The nanospike electroporation system was developed recently in order to reduce the required voltage to permeabilize the plasma membrane of the target cell. In this technology, nanospike chips were initially designed with top and bottom aluminum electrodes, which were separated by a spacer with 100 μm length to form the electroporation chamber. Next, arrays of nanospikes were fabricated on the bottom aluminum electrode using anodization and etching processes. In a follow-up study, the same researchers upgraded the nanospike electroporation by fabricating arrays of highly ordered 3D aluminum nanospikes through the same electrochemical processes. The efficient electroporation process at reduced voltages has occurred as a result of high-aspect-ratio 3D nanostructures generating the enhanced electric field. The nanospike EP systems were designed in chips and wafer levels for handling and manipulation of small (100–500) and large (10^4 to 10^5) cell populations, respectively. This electroporation method is reproducible and cost-effective, revealing high delivery efficiency without affecting the cell viability (>93 ± 6%). Low pulse duration and amplitude applied in this setup allow the electroporation at the nanoscale without undesirable electrochemical reactions and electrolysis occurred due to applying high voltages.[323]

3.9.4. Nanochannel Electroporation (NEP)

Nanochannel electroporation (NEP) has been designed recently as an efficient platform to achieve high-throughput cytosolic delivery, high cell viability, and precise dosage control.[324] A micro/nanofluidics setup based on 2D NEP for cargo loading and single cell analysis consisted of microchannels connected with arrays of nanochannels was presented by Zhao et al.[325] In this setup, each microchannel is linked to a specific reservoir and filled with either the target cells or delivery cargoes. The target cells were first positioned in one microchannel (lying against the nanochannel) via an optical tweezer, and then an extremely high voltage (between 220–250 V) was applied to the nanochannel. These high voltage pulses induced nanopore formation in the small area of interest in the membrane of AML cell lines (Kasumi-1 and KG1a) to facilitate the cytoplasmic uptake of pIRES-EGFP plasmids encoding miR181a as well as wild-type/mutated CEBPA genes. This device could handle the cell population from a single cell to more than a hundred cells. There has been no evidence of cell death reported during the NEP process yet. In this regard, the cell viability and delivery efficiency of this approach are estimated to be near 90%.[325–327] Gallego-Perez et al. developed a nanochannel electroporation device to topically deliver *Etv2, Foxc2*, and *Fli1* transcription factors to reprogram skin cells into induced endothelial cells. They further achieved successful delivery of these factors followed by reprogramming of fibroblasts into the induced neuron cells using NEP system.[328] More recently, Yang et al. demonstrated the ability of nanochannel electroporation in stimulation of attached cells by generating transient nanopores in the plasma membrane. In this study it was found that NEP significantly triggered the formation and release of the multivesicular bodies (e.g., exosomes) from the treated cells, which is assumed to be initiated by increased intracellular concentration of Ca^{2+}.[329] While NEP chips with the 2D planar design are able to electropermeabilize less than a hundred individual cells per run, 3D NEP devices with parallel nanochannel array allow high throughput cytosolic loading of cargoes into more than 40 000 cells cm^{-2}. The schematic design of 2D and 3D NEP chips are depicted in Figure 9G,H, respectively. Despite the recent efforts on applying nanoengineered structures for both research and clinical purposes, the challenge of the limited number of cells loaded with these structures is yet to be extensively explored.

4. Hybrid Intracellular Delivery Systems

Hybrid intracellular delivery systems are defined as methods in which two or more techniques are combined synergistically, to gain the efficiencies of all subsection devices and achieve enhanced intracellular delivery performance. Escoffre et al. demonstrated that in a combined system of electric and ultrasound fields, the efficiency of loading pEGFP-C1 plasmid DNA into CHO cells was increased sixfold compared with electropermeabilized cells; **Figure 10**A. In this system, the plasma membrane was first disrupted using electric fields, and plasmid DNA migrated toward the permeabilized membrane. Then, an ultrasound-assisted modality with gas microbubbles further introduced the plasmid DNA into the cell cytoplasm rapidly.[330] Another early study demonstrated enhanced delivery efficiency of pcDNA3Luc or pCAGGS-mIL-12 plasmid using an electric field combined with ultrasound waves in C3H/HEN Crj mouse skeletal muscles.[331] Also, a flow-through microfluidic

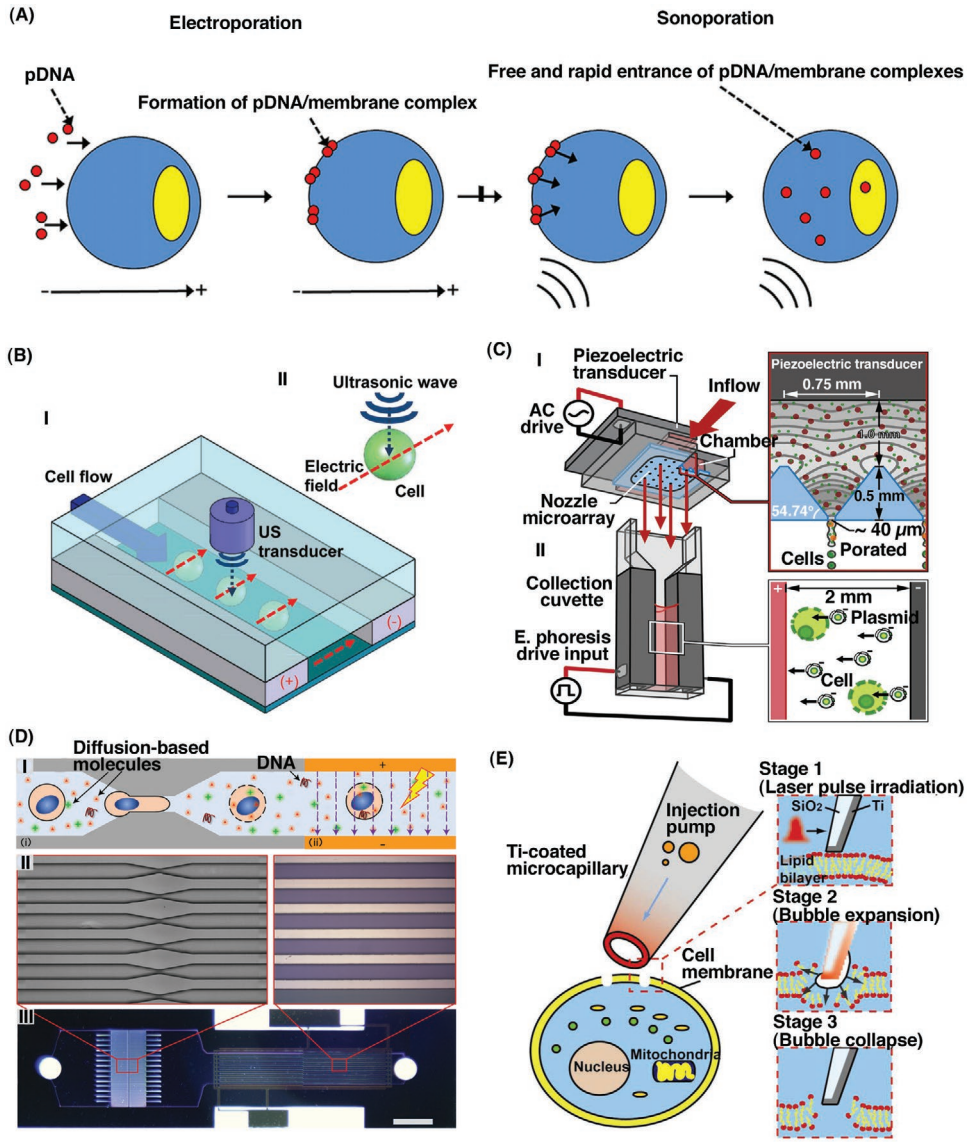

Figure 10. Schematic presentation of various hybrid systems for cytosolic delivery. A) Mechanism of electrosonoporation system. First, an electric field was applied to induce membrane disruption and subsequent transfer of plasmid DNA across the permeabilized membrane. Afterward, the cells experienced sonoporation that created gas microbubbles to further assist the cytoplasmic delivery of plasmid DNA. Reproduced with permission.[330] Copyright 2010, Elsevier. B) A microfluidic-based hybrid intracellular delivery system by combination of electroporation and sonoporation. The applied electric field to the microelectrode pair drove the cells through the microchannel. In addition, the acoustic wave was applied perpendicular to the electric field and formed the transient nanopores along both axes of the cell membrane at the same time. Reproduced with permission.[332] Copyright 2001, Royal Society of Chemistry. C) A combination of electrophoresis gene transfer method and mechanoporation for cytosolic delivery purposes. This system consists of a piezoelectric transducer for acoustic wave generation and an electrophoresis collection cuvette. The resonant acoustic field drove cells into orifices of a nozzle microarray for cell mechanoporation. Then, an electric field transported the negatively charged DNA into cells. Reproduced under the terms of the CC-BY Creative Commons Attribution 4.0 International license (https://creativecommons.org/licenses/by/4.0).[333] Copyright 2018, The Authors, published by Springer Nature. D) This mechano-electroporation device combined a set of parallel microfluidic constriction on a silicon wafer and deposited electrodes on a Pyrex wafer. The mechanical disruption of cells occurred when the cells passed through the constriction region. Next, electric pulses were applied to drive DNA molecules into the cell cytoplasm and nucleus through the locally disrupted membrane. Reproduced with permission.[334] Copyright 2017, Springer Nature. E) Schematic representation of a combined optoporation/microinjection system. In this strategy, the laser heated a titanium-coated glass micropipette to make cavitation bubbles and induce transient shear stress. Cargoes inside the micropipette were then delivered into the cell via synchronized laser pulsing. Reproduced with permission.[335] Copyright 2011, American Chemical Society.

electro-sonoporation device has been fabricated using novel 3D microelectrodes for permeabilizing membranes with an average poration efficiency of more than 95%. In this microfluidic system, electric field and ultrasound waves were applied simultaneously in perpendicular directions to provide high-efficiency and high-throughput cytosolic loading of PI into HeLa cells (Figure 10B). The proposed device benefited from the advantages of 3D electrodes, which have two functions;

applying the electric field and serving as a cell flowing channel structure. The obtained results from this device on HeLa cells exhibited a higher delivery efficiency compared with using microelectroporation or microsonoporation, while cell viability was maintained higher than 90%.[332]

Recently, Meacham et al. developed a two-stage shear-based delivery method through coordinating mechanical disruption of the target cell membrane and electrophoretic action of cargo delivery to the target cell (Figure 10C). This acoustic shear poration method not only augments the delivery efficiency and capabilities for active transport of cargo but also preserves the compelling flexibility of shear-based delivery as it does not affect the cell viability. In this approach, a fabricated array of micronozzles was used to focus acoustic waves and create high shear forces to induce transient pore formation and cytosolic loading of small to large biomaterials. In addition to the passive diffusion, adding an electric field could facilitate the active transport of different sized FITC-labeled dextran molecules into the nucleus of HEK293 and Jurkat cells without affecting their viability.[333] In subsequent efforts, Ding et al. developed disruption and field enhanced delivery devices by combining two approaches of cell squeezing and electric-field-driven transport to demonstrate nuclear delivery of plasmid DNA by integrating microfluidic channels with constrictions and microelectrodes (Figure 10D). The applied electric field in this setup facilitates the disruption of both the cell and nucleus membrane which increases cargo delivery into the nucleus. According to their results, cargo delivery efficiency reached above 60% and 90% by applying electric field amplitudes of 8 and 10 V, respectively.[334]

A photothermal nanoblade technology, which is a combination of microinjection, optoporation, and thermoporation, was introduced by Wu et al. to achieve the highly efficient delivery of various cargoes from nucleic acids to 200 nm polystyrene beads and 2 µm bacteria. Interestingly, using this strategy they successfully loaded GFP-labeled *Burkholderia thailandensis* bacteria (the largest and the most fragile cargo to be delivered) into HeLa cells. In this system, a titanium film with 100 nm thickness was coated onto the outer wall of a glass microcapillary pipette tip and coupled with a real-time imaging system to characterize the dynamics of cavitation bubbles. When the cells became in light contact with the photothermal nanoblade, a short laser pulse was applied to heat the titanium tip and the surrounding water layer quickly, which resulted in the generation of cavitation bubbles (Figure 10E). The explosion of these cavitation bubbles could create an ultrafast flow to induce highly localized membrane puncture near the contact area without disturbing the adjacent parts.[335]

5. Combined Cell Transfection and Long-Term Perfused Cell Culture

One of the key advantages of micro- and nanotechnology is the capability of such systems in integrating various procedures on a single chip, resulting in automation, high-throughput analysis, shorter processing time, and higher accuracy.[336] In the context of intracellular delivery, microfluidic platforms can integrate cell seeding procedure, perfused culture platform, and subsequent manipulation for cargo loading inside the cells. The recovered cells from such systems can be further processed using either on-chip or off-chip flow cytometry. Using a modular microfluidic approach, Hufnagel et al. developed a successive platform for both long-term culture and high-throughput protein delivery, as shown in **Figure 11**A. In such a platform, integration of microfluidic cell culture chamber with flow-focusing droplet generator enabled both long-term culture and high-throughput compartmentalization of the cells for gene transduction.[337] To make the microfluidic device more compatible with the concept of "lab-on-a-chip," the microbioreactor can also be integrated with on-chip actuators (e.g., peristaltic micropump) to facilitate the loading of culture media and delivery reagents, Figure 11B.[338] Raimes et al. developed an automated and versatile microfluidic device for on-chip cargo delivery and long-term perfused culture with the application in derivation of induced pluripotent stem cells.[339] In another recent study, Vitor et al. used the droplet microfluidic approach to demonstrate cargo delivery followed by quantitative analysis of loaded CHO-S cells with lipoplexes containing pMAX GFP plasmids. It was illustrated that this system enabled real-time tracking and long-term culture of CHO cells postdelivery at least up

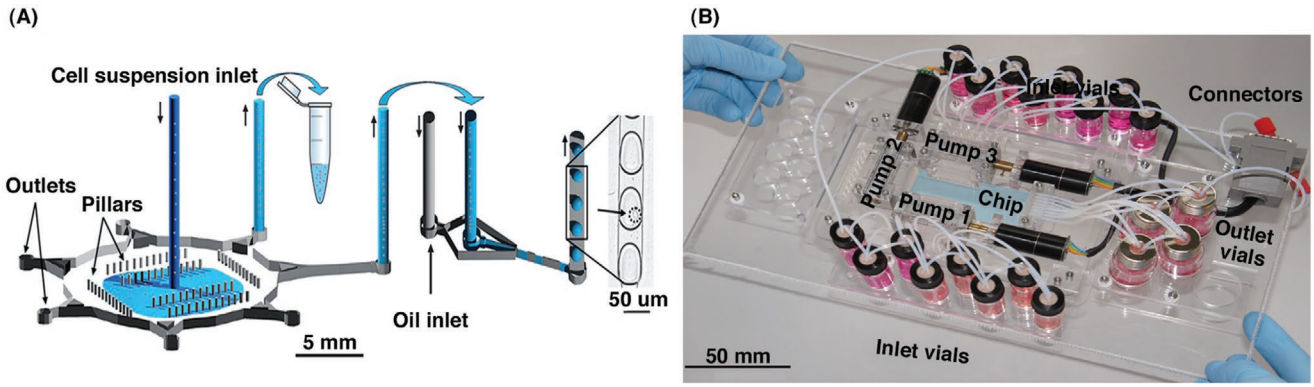

Figure 11. Integrated modular microdevices for cargo delivery and perfused culture of loaded cells. A) Schematic illustration of a modular microfluidic device utilized for the seeding, cultivation, transfection, remobilization, collection, and encapsulation of the adherent mammalian cells. Reproduced with permission.[337] Copyright 2001, Royal Society of Chemistry. B) An image of an integrated parallel microdevice consisted of a microfluidic chip with 16 inlet and 4 outlet vials for automated cell culture. Reproduced with permission.[338] Copyright 2011, Springer Nature.

to 62 h. Compared with the conventional protocol, on-chip delivery platforms not only offer improved loading efficiency, but also provide a more facile means for real-time tracking and manipulation of cells. Such systems hold great promise for gene therapy and regenerative medicine.[340]

6. Application of Intracellular Delivery Systems

A wide range of applications for intracellular delivery systems have been proposed that they are classified into biological research, clinical practice, and drug delivery.[341] **Table 1** summarizes different intracellular delivery strategies including their advantages, disadvantages, and potential applications.

As for biological research, the major applications of intracellular delivery systems are the functional study of a gene and the underlying regulatory mechanisms as well as recombinant protein production for investigations on protein–protein interactions.[365,366] Delivery systems have also been used for clinical approaches such as gene therapy, i.e., loading CRISPR/Cas9 components inside the target cell. In such systems, several parameters, including the delivery efficiency, cell viability, onset, duration, and termination of the gene expression should be controlled precisely to avoid unwanted expression and adverse effects like unspecific cellular and immune responses.[56] Song et al. developed an efficient gene delivery method known as electric-field-induced molecular vibrations for in vivo gene therapy. The device generated vibrational forces upon ultrahigh voltage knocking by the Gene Symphonizer machine. In this method, two electrodes induced vigorous vibrations in the mixture of cell suspension and DNA molecules. This mixture was first placed in a glass dish and further subjected to the vibrations made by two electrodes without any direct contact. As these vibrations exceeded the hydrophobic bonding energy of plasma membrane phospholipid molecules, foreign DNA molecules can bypass the plasma membrane and enter the cytoplasm, regardless of their size. As a result, sustained expression of the foreign DNA molecules is achieved. Accordingly, the delivery efficiency of this method has been evaluated in different cell types, including primary mesenchymal cells, immortalized mouse, and human cell lines. The results showed various advantages for this rapid and reproducible method such as high cargo loading efficiency (more than 74%), low cell mortality without the need for specific sample preparation/reagent. The protected differentiation ability of cells after cargo delivery was an essential point regarding this procedure.[367] Mechanical oscillations are introduced as another novel technique for gene delivery. This method also disturbs cell membrane structure to increase the penetration level of foreign molecules. PASCO Sine Wave Generator machine which oscillates the samples at different frequencies, enables biologists to transfect siRNA into myelogenous leukemia cell line K562. These cell vibrations do not affect cell viability resulted in increasing the delivery efficiency from 30% to nearly 100%, which varies based on oscillation conditions.[368]

The issue of the growing prevalence of diverse cancers has raised the requirement for effective drug delivery systems and gene/cell therapy modalities with the approach of precision medicine. In this regard, the commercialized platforms developed by different companies involved in gene/cell therapy are considered as appealing scenarios to address these demands. The global market of intracellular delivery techniques based on microfluidics is limited to SQZBiotech company, mainly working on cytoplasmic cargo loading through squeezing the cell of interest in a series of microchannels. Most of the commercialized companies in this field are based on either electroporation or viral-based delivery techniques. Hence, there are still plenty of rooms for commercialization of novel, efficient, high-throughput in vitro delivery systems. In current ex vivo cell-based therapies, the modified, reprogrammed, or repaired cells (all manipulated in vitro via intracellular delivery of cargoes) are introduced into a patient's body to restore the lost function or confer a therapeutic effect.[369] In 2017, food and drug administration (FDA) approved the clinical trials recruiting cell-based therapy to introduce modified T-cells with chimeric antigen receptors (CARs) into the patient's body with the aim of adoptive T-cell immunotherapy and producing therapeutic effects against B-cell malignancies.[370,371] Virus-mediated delivery systems and liposomes are commonly used as in vivo carriers for clinical purposes. This approach is preferentially used for in vivo cargo loading into terminally differentiated cells including neurons and cardiomyocytes. In this regard, the overall applications of viral-based platforms consisted of more than 50% of gene therapy submissions to the FDA in 2015.[2,372,373] The recent successful gene therapies using viral-mediated vectors are applied for gene editing in monogenic diseases including severe combined immunodeficiency (SCID), β-thalassemia, and Wiskott-Aldrich syndrome (WAS).[374] A prominent example of ex vivo application of lentiviral delivery modalities is transduction of a transgene to the hematopoietic lineage.[374,375] Among the nonviral transfection systems, liposomes are the most popular and widely used method in cell and biomedical research.[56,348] Since virus-mediated delivery systems and liposomes have some safety issues including immune responses and cytotoxicity, their clinical applications are limited.[376,377] Thus, some other techniques such as microinjection and electroporation have emerged for both in vivo and in vitro applications because of their low level of risks associated with the delivery process.[93,187] Microinjection has a wide range of applications from in vitro fertilization (IVF) to make transgenic mice in animal model studies.[351,378–380] Successful in vitro trials on both animals and patients have been performed using a nonviral delivery system.[260,261] Polycations are nonviral delivery systems that have been used for both gene therapy and drug delivery purposes.[345,381–383] Recent years have witnessed the unprecedented growth of research at the interface of developing novel active or passive polymeric carriers, which has given rise to the targeted drug delivery to cancer cells within solid tumors or tumor microenvironment.[384] FDA has approved more than 20 nanoparticle (NP) formulations (with the size range from 1 to 100 nm) including polymeric carriers, liposomes, and other formulations underlying preclinical or clinical trials for targeted drug delivery in solid tumors.[385] Since NPs have active cellular uptake and localized mechanism of action while reducing the side effects as well as increasing the delivery efficiency, much more research in this area is needed to realize the full potential of NPs in targeted drug delivery to solid tumors.[385] Nano- and microstructures including Doxil

Table 1. Comparison of commonly used intracellular delivery methods.

Delivery method	Advantages	Disadvantages	Applications
Biological method[342,343]	More than 90% delivery efficiency (highly efficient gene delivery)	Limited size of DNA, cytotoxic effects may be induced, labor-intensive, packaging cell lines is an additional required step, and most of the viruses are invasive	Broad application in vivo, introducing a single cloned gene, which should be highly expressed after integration into the host cell genome
Calcium phosphate[344]	High delivery efficiency, cost-effective, applicable to the different type of cells	Minimal changes in pH (±0.1) will alter delivery efficiency, not suitable to be applied for the cells growing in RPMI media due to its high concentration of phosphate	Transfection with the approach of protein purification
Cationic polymers[345–347]	Cost-effective, applicable to different cell types, rapid and easy to perform	Toxicity due to the high concentration of utilized cationic polymers, delivery efficiency depends on cell type, exhibited <10% delivery efficiency in primary cells	Drug delivery coupled with gene therapy
Lipofection[348,349]	High efficiency, minimal required steps, able to adapt with high-throughput systems	Not applicable to all type of cells	Commonly used in the field of cell biology studies
Magnetofection[133,167,350]	Rapid, direct transportation leading to high efficiency, can be performed both in the presence or absence of serum	Requiring additional steps to immobilize suspension cells	Cargo delivery inside adherent mammalian cells and primary cell culture
Microinjection[30,201,351]	A host-range independent physical method with a direct and precise delivery system	Special equipment including inverted microscope and glass pipette are required, induce damages during the injection, low throughput as it only targets a single cell per injection	Broad applications from in vitro fertilization (IVF) to produce transgenic animals in animal model studies, very useful for single cell transfection
Particle bombardment[187,352,353]	Technical simplicity without the need for vector with relatively high efficiency	An expensive method due to the high cost of the required equipment including the microprojectile device, cell membrane break-down, the possibility of particle penetration to the cells without carrying the cargo biomaterial, and random integration	DNA vaccine delivery for studying Alzheimer disease, genetic immunization, and gene therapy
Sonoporation[354–356]	Noninvasiveness, applicable for several cell types, simplicity, high-safety profile	Cell membrane damage, low efficiency in vivo, and costly equipment	Therapeutic and diagnostic applications using sinusoidal probes at megahertz frequencies
Optoporation[357–359]	Noninvasiveness, high efficiency and precision, thousands of cells could be loaded with a single laser pulse	Significant cell death assisted by membrane damage, costly, different loading extents due to distance variety of target cells from the shock wave	The most suitable and accurate way of delivering the transcriptome (population of mRNAs), gene, and drug to single mammalian cells, and genetic manipulation of cells
Electroporation[360–362]	Applicable to different cell types, high efficiency, not altering biological structure and function of target cell	In suboptimal circumstances, cell mortality takes place due to the high level of cell damage	Localized in vivo gene delivery through glass needles, having a reputation for cargo delivery inside primary cell types
Membrane sandwich electroporation[261]	Low applied voltage electroporation, higher cell viability and delivery efficiency (compared with conventional bulk electroporation)	Lack of uniform electric field distribution	Gene delivery into mammalian cells
Microscale electroporation (microchannel and microcapillary EP)[253,256,363]	User-friendliness, visualization at the single cell resolution, loading cargo into a variety of cells more reliably, and minimum electrochemical reactions	Hard to manipulate cargo loaded cells within microchannels, relatively complicated operation procedure	Useful for high-throughput applications in electroporation-based drug delivery
Nanoscale electroporation (nanostraw, nanofountain probe, nanospike, and nanochannel EP)[242,326,364]	Dose control, minimal cell damage, and precise delivery of biomolecules into living cells	Relatively complicated operation procedure and costly	Useful to transfect a large number of cells, active gene delivery system

(the first FDA-approved nanopharmaceuticals in 1995), Caelyx, Myocet, DaunoXome, Onco TCS, and Abraxane are the commercial formulations passed all the clinical trials and widely used in cancer therapy.[386] Unlike small cargo biomolecules, protein therapeutics including antibody-based drugs (monoclonal antibodies), anticoagulants, bone morphogenic proteins,

interferons, hormones, growth factors, and interleukins take advantage of generating surfaces capable of recognizing targets.[80,387] In precision medicine, for the sake of antitumor vaccine preparations, scientists have begun the clinical trials based on intracellular delivery and loading of mutant tumor proteins into dendritic cells activating cytotoxic T-cells to attack tumor cells with the same proteome content.[388–391] Some types of cancers are hard to treat due to their resistance to conventional systemic chemotherapy.[392,393] Developed NP-based delivery systems can be used for addressing these limitations in drug-resistant cancers including pancreatic ductal carcinoma (PDAC).[393,394] Adair and co-workers introduced a novel and efficient technology to deliver phosphorylated metabolites of the chemotherapy drugs 5-FU and gemcitabine to pancreatic tumor cells by encapsulating them into calcium phosphosilicate NPs (CPSNPs) preventing the drug from breakdown and clearance.[394–396] The future intracellular delivery modalities for personalized cancer treatment and gene therapy will go beyond what is currently attained through the current systems due to their higher efficiency and safety.

7. Current Challenges and Limitations

Despite massive efforts and research for the development of new intracellular delivery techniques, the majority of existing systems entail some limitations and challenges. The major challenges include delivery efficiency, cell viability, and technique specificity. The viral delivery technique, which is one of the widely used delivery methods, has some disadvantages including high viral load, subsequent low delivery efficiency, low cell viability, and the limited loading capacity of viral vectors. Furthermore, the complexity of preparation in research applications and lack of patient-specific viral dosage, immune responses, and random gene insertion and mutagenesis are the current problems faced when working with viral-mediated delivery systems.[397] On the other hand, lack of selective targeting of a specific cell type (target specificity) remains as a significant and long-standing challenge of non-viral delivery systems primarily in the case of cargo delivery using chemical polymers.[398]

One of the typical limitations restricting clinical applications of electroporation is the risk of bioelectrical signal interference in central and peripheral nervous systems involving in physiological activities.[399] While field-assisted delivery systems have gained more attention due to their high-throughput, the set-up of the required equipment to achieve uniform magnetic/electrical fields and consequent homogenous cargo loading inside the cells is expensive.[400] Although the limitations of the established delivery technologies have hampered the cell therapy progress, they provide an incentive to develop novel delivery approaches with the maximum efficiency and minimum cytotoxicity. To address the current limitations in existing delivery systems, scientists have come up with a combination of different intracellular delivery systems.[2] For example, Schmidt-Wolf et al. in 2000 introduced a highly efficient protocol by adding cationic liposomes to adenoviral gene transfer inside lymphoma cells for cancer therapy purposes. The results indicated that liposomes considerably increased the expression of transgene delivered through the adenoviral vectors to B-lymphoma cell lines and primary lymphoma cells.[401] Dholakia et al. devised a novel intracellular delivery method by combining a microlens fiber-based optical system with a microcapillary based microfluidic device to achieve higher loading efficiency along with localized drug delivery.[402] Wang et al. presented a highly efficient delivery method with lower cytotoxicity effects through combining sonoporation, low-dose liposomes, and HTERT/CMV chimeric promoter for enhanced delivery of HSP70-shRNA in 22RV1 prostate cancer cells.[403] Hirooka et al. used a combination of the lipid-based delivery reagents including Lipofectamine LTX, FuGENE HD, TransFectin, and Fibroblast Transfection Reagent to transfect primary fibroblasts and hepatoblasts. The attained results indicated an increased delivery efficiency when combination of the mentioned lipid-based reagents were employed.[404] It is envisioned that rapid expansion of combinational intracellular delivery methods will continue to influence biomedical science and medicine.

8. Conclusions and Future Perspectives

We have reviewed and highlighted the established and emerging techniques for delivery of biomolecules into the host cells in the areas of research and therapeutic approaches. We categorized the intracellular delivery systems based on macro (conventional) and micro (containing both micro and nano) engineered approaches. Next, we evaluated diverse delivery systems from the conventional ones including calcium phosphate and bulk electroporation to the novel delivery strategies using microfluidics (cell squeezing, microchannel, and microcapillary electroporation) and nanotechnology (nanostraws, nanofountain probes, nanospike, and nanochannel electroporation). The macroengineered approaches were specifically divided into two areas of carrier-mediated and membrane-disruption-based intracellular delivery systems. We then explored the cutting-edge advances in micro-engineered intracellular delivery techniques. Some of these techniques such as fluid shear, thermoporation, and electroporation can be performed at both macro or micro/nanoresolution. However, some of the mentioned delivery strategies, such as microinjection, nanostructure arrays, and cell squeezing are exclusive to micro- and nanoengineered platforms. Subsequently, the applications of various intracellular delivery systems were presented, and different commercialized technologies in this field were introduced. Furthermore, different intracellular delivery platforms were compared, and finally, the limitations and technical challenges of each approach were briefly discussed.

Recent dramatic improvements in intracellular delivery methods play a pivotal role in achieving higher efficiency, lower cell death, and cytotoxicity sparking renewed excitement in this research field. All existing delivery systems, ranging from macroengineered approaches to nanochannel electroporation, possess some challenges in addition to their advantages.

Future delivery systems should approach the aim of precise biomolecule delivery to the subcellular regions at single cell resolution without affecting the cell viability. This direction will broaden a new field in genetic investigations about the single

cell genomics, differential gene expression, and functional analysis in the target cell. Nowadays, there is a pressing need for developing novel delivery methods minimizing cytotoxicity while maximizing efficiency, cell viability, and applicability in clinical trials.

Collectively, since different delivery systems are evolving rapidly and diversely, the choice of an appropriate delivery modality among the plethora of options heavily depends on the experimental or clinical objectives. Developing an effective and safe intracellular delivery technique targeting specific cell types and directing the materials to a particular organelle such as the nucleus through the combination of different strategies would facilitate both research and clinical approaches in precision medicine with unprecedented accuracy. Advances in micro/nanofluidic devices and a new generation of viral vectors will serve as promising starting points to expand the frontiers of membrane-disruption- and carrier-based delivery techniques, respectively. Meanwhile, it is critical to conduct further investigations and endeavors to develop more advanced delivery technologies that precisely transport the cargo into the target cells with maximum efficiency and minimum adverse effects.

Acknowledgements

D.M.R., M.A.R., S.R.B. contributed equally to this work. The authors thank Dr. Martin Stewart for his helpful advice and comments. M.E.W. acknowledges the support of the Australian Research Council through Discovery Project Grants (DP170103704 and DP180103003) and the National Health and Medical Research Council through the Career Development Fellowship (APP1143377).

Conflict of Interest

The authors declare no conflict of interest.

Keywords

cell-based therapy, genome editing, intracellular cargo delivery, micro- and nanotechnology, plasma membrane permeabilization

Received: August 7, 2020
Revised: September 22, 2020
Published online:

[1] W. Poon, B. R. Kingston, B. Ouyang, W. Ngo, W. C. W. Chan, *Nat. Nanotechnol.* **2020**, *15*, 819.
[2] M. P. Stewart, A. Sharei, X. Ding, G. Sahay, R. Langer, K. F. Jensen, *Nature* **2016**, *538*, 183.
[3] J. M. Meacham, K. Durvasula, F. L. Degertekin, A. G. Fedorov, *J. Lab. Autom.* **2014**, *19*, 1.
[4] A. Sharei, J. Zoldan, A. Adamo, W. Y. Sim, N. Cho, E. Jackson, S. Mao, S. Schneider, M.-J. Han, A. Lytton-Jean, P. A. Basto, S. Jhunjhunwala, J. Lee, D. A. Heller, J. W. Kang, G. C. Hartoularos, K.-S. Kim, D. G. Anderson, R. Langer, K. F. Jensen, *Proc. Natl. Acad. Sci. USA* **2013**, *110*, 2082.
[5] S. Mitragotri, *Nat. Rev. Drug Discovery* **2005**, *4*, 255.
[6] L. Y. Chou, K. Ming, W. C. Chan, *Chem. Soc. Rev.* **2011**, *40*, 233.
[7] J. Shi, Y. Ma, J. Zhu, Y. Chen, Y. Sun, Y. Yao, Z. Yang, J. Xie, *Molecules* **2018**, 23, 3044.
[8] J. A. St George, *Gene Ther.* **2003**, *10*, 1135.
[9] V. V. Sokolova, I. Radtke, R. Heumann, M. Epple, *Biomaterials* **2006**, *27*, 3147.
[10] T.-Y. Wang, M. D. J. Libardo, A. M. Angeles-Boza, J.-P. Pellois, *ACS Chem. Biol.* **2017**, *12*, 1170.
[11] L. Cheng, P. R. Ziegelhoffer, N. S. Yang, *Proc. Natl. Acad. Sci. USA* **1993**, *90*, 4455.
[12] B. R. Blackman, K. A. Barbee, L. E. Thibault, *Ann. Biomed. Eng.* **2000**, *28*, 363.
[13] C. Y. Okada, M. Rechsteiner, *Cell* **1982**, *29*, 33.
[14] J. A. Wyber, J. Andrews, A. D'Emanuele, *Pharm. Res.* **1997**, *14*, 750.
[15] S.-I. Kurata, M. Tsukakoshi, T. Kasuya, Y. Ikawa, *Exp. Cell Res.* **1986**, *162*, 372.
[16] K. Rhodes, I. Clark, M. Zatcoff, T. Eustaquio, K. L. Hoyte, M. R. Koller, in *Methods in Cell Biology*, Vol. *82*, Academic Press, San Diego, CA **2007**, p. 309.
[17] O. Kurosawa, H. Oana, S. Matsuoka, A. Noma, H. Kotera, M. Washizu, *Meas. Sci. Technol.* **2006**, *17*, 3127.
[18] F. Krötz, C. d. Wit, H.-Y. Sohn, S. Zahler, T. Gloe, U. Pohl, C. Plank, *Mol. Ther.* **2003**, *7*, 700.
[19] E. Neumann, M. Schaefer-Ridder, Y. Wang, P. H. Hofschneider, *EMBO J.* **1982**, *1*, 841.
[20] S. O'Dea, V. Annibaldi, L. Gallagher, J. Mulholland, E. L. Molloy, C. J. Breen, J. L. Gilbert, D. S. Martin, M. Maguire, F.-R. Curry, *PLoS One* **2017**, *12*, e0174779.
[21] A. Etxaniz, D. González-Bullón, C. Martín, H. Ostolaza, *Toxins* **2018**, *10*, 234.
[22] A. M. Moe, A. E. Golding, W. M. Bement, *Semin. Cell Dev. Biol.* **2015**, *45*, 18.
[23] A. C. Howard, A. K. McNeil, P. L. McNeil, *Nat. Commun.* **2011**, *2*, 597.
[24] M. Labazi, A. K. McNeil, T. Kurtz, T. C. Lee, R. B. Pegg, J. P. F. Angeli, M. Conrad, P. L. McNeil, *Free Radical Biol. Med.* **2015**, *84*, 246.
[25] J. D. Marks, C.-Y. Pan, T. Bushell, W. Cromie, R. C. Lee, *FASEB J.* **2001**, *15*, 1107.
[26] G. Serbest, J. Horwitz, K. Barbee, *J. Neurotrauma* **2005**, *22*, 119.
[27] T. Geng, C. Lu, *Lab Chip* **2013**, *13*, 3803.
[28] Y. T. Chow, S. Chen, R. Wang, C. Liu, C.-W. Kong, R. A. Li, S. H. Cheng, D. Sun, *Sci. Rep.* **2016**, *6*, 24127.
[29] M. R. Capecchi, *Cell* **1980**, *22*, 479.
[30] S. T. Santra, G. F. Tseng, *Micromachines* **2013**, *4*, 333.
[31] J. Kim, I. Hwang, D. Britain, T. D. Chung, Y. Sun, D.-H. Kim, *Lab Chip* **2011**, *11*, 3941.
[32] A. Tay, N. Melosh, *Acc. Chem. Res.* **2019**, *52*, 2462.
[33] M. P. Stewart, A. Lorenz, J. Dahlman, G. Sahay, *WIREs Nanomed. Nanobiotechnol.* **2016**, *8*, 465.
[34] F. Mingozzi, K. A. High, *Nat. Rev. Genet.* **2011**, *12*, 341.
[35] J. L. Howarth, Y. B. Lee, J. B. Uney, *Cell Biol. Toxicol.* **2010**, *26*, 1.
[36] Y. K. Sung, S. W. Kim, *Biomater. Res.* **2019**, *23*, 8.
[37] M. Ramamoorth, A. Narvekar, *J. Clin. Diagn. Res.* **2015**, *9*, GE01.
[38] O. M. Elsharkasy, J. Z. Nordin, D. W. Hagey, O. G. de Jong, R. M. Schiffelers, S. E. L. Andaloussi, P. Vader, *Adv. Drug Delivery Rev.* **2020**, *159*, 332.
[39] S. Gatti, S. Bruno, M. C. Deregibus, A. Sordi, V. Cantaluppi, C. Tetta, G. Camussi, *Nephrol., Dial., Transplant.* **2011**, *26*, 1474.
[40] J. Ratajczak, K. Miekus, M. Kucia, J. Zhang, R. Reca, P. Dvorak, M. Z. Ratajczak, *Leukemia* **2006**, *20*, 847.
[41] G. Raposo, H. W. Nijman, W. Stoorvogel, R. Liejendekker, C. V. Harding, C. J. Melief, H. J. Geuze, *J. Exp. Med.* **1996**, *183*, 1161.
[42] L. Alvarez-Erviti, Y. Seow, H. Yin, C. Betts, S. Lakhal, M. J. A. Wood, *Nat. Biotechnol.* **2011**, *29*, 341.

[43] X. Luan, K. Sansanaphongpricha, I. Myers, H. Chen, H. Yuan, D. Sun, *Acta Pharmacol. Sin.* **2017**, *38*, 754.
[44] D. E. Murphy, O. G. de Jong, M. Brouwer, M. J. Wood, G. Lavieu, R. M. Schiffelers, P. Vader, *Exp. Mol. Med.* **2019**, *51*, 1.
[45] D. Sun, X. Zhuang, X. Xiang, Y. Liu, S. Zhang, C. Liu, S. Barnes, W. Grizzle, D. Miller, H.-G. Zhang, *Mol. Ther.* **2010**, *18*, 1606.
[46] T. Yang, P. Martin, B. Fogarty, A. Brown, K. Schurman, R. Phipps, V. P. Yin, P. Lockman, S. Bai, *Pharm. Res.* **2015**, *32*, 2003.
[47] Y. Tian, S. Li, J. Song, T. Ji, M. Zhu, G. J. Anderson, J. Wei, G. Nie, *Biomaterials* **2014**, *35*, 2383.
[48] M. Mack, A. Kleinschmidt, H. Brühl, C. Klier, P. J. Nelson, J. Cihak, J. Plachý, M. Stangassinger, V. Erfle, D. Schlöndorff, *Nat. Med.* **2000**, *6*, 769.
[49] M. J. Haney, N. L. Klyachko, Y. Zhao, R. Gupta, E. G. Plotnikova, Z. He, T. Patel, A. Piroyan, M. Sokolsky, A. V. Kabanov, E. V. Batrakova, *J. Controlled Release* **2015**, *207*, 18.
[50] K. O'Brien, K. Breyne, S. Ughetto, L. C. Laurent, X. O. Breakefield, *Nat. Rev. Mol. Cell Biol.* **2020**, *21*, 585.
[51] J. Wahlgren, T. D. L. Karlson, M. Brisslert, F. Vaziri Sani, E. Telemo, P. Sunnerhagen, H. Valadi, *Nucleic Acids Res.* **2012**, *40*, e130.
[52] A. B. Banizs, T. Huang, K. Dryden, S. S. Berr, J. R. Stone, R. K. Nakamoto, W. Shi, J. He, *Int. J. Nanomed.* **2014**, *9*, 4223.
[53] T. A. Shtam, R. A. Kovalev, E. Y. Varfolomeeva, E. M. Makarov, Y. V. Kil, M. V. Filatov, *Cell Commun. Signaling* **2013**, *11*, 88.
[54] A. Montecalvo, A. T. Larregina, W. J. Shufesky, D. Beer Stolz, M. L. G. Sullivan, J. M. Karlsson, C. J. Baty, G. A. Gibson, G. Erdos, Z. Wang, J. Milosevic, O. A. Tkacheva, S. J. Divito, R. Jordan, J. Lyons-Weiler, S. C. Watkins, A. E. Morelli, *Blood* **2012**, *119*, 756.
[55] S.-I. Ohno, M. Takanashi, K. Sudo, S. Ueda, A. Ishikawa, N. Matsuyama, K. Fujita, T. Mizutani, T. Ohgi, T. Ochiya, N. Gotoh, M. Kuroda, *Mol. Ther.* **2013**, *21*, 185.
[56] L. Kaestner, A. Scholz, P. Lipp, *Bioorg. Med. Chem. Lett.* **2015**, *25*, 1171.
[57] T. K. Kim, J. H. Eberwine, *Anal. Bioanal. Chem.* **2010**, *397*, 3173.
[58] L. Salimzadeh, M. Jaberipour, A. Hosseini, A. Ghaderi, *Avicenna J. Med. Biotechnol.* **2013**, *5*, 68.
[59] A. Kichler, W. Zauner, M. Ogris, E. Wagner, *Gene Ther.* **1998**, *5*, 855.
[60] J. P. Yang, L. Huang, *Gene Ther.* **1998**, *5*, 380.
[61] F. Sakurai, R. Inoue, Y. Nishino, A. Okuda, O. Matsumoto, T. Taga, F. Yamashita, Y. Takakura, M. Hashida, *J. Controlled Release* **2000**, *66*, 255.
[62] M. A. Khan, V. M. Wu, S. Ghosh, V. Uskoković, *J. Colloid Interface Sci.* **2016**, *471*, 48.
[63] F. L. Graham, A. J. van der Eb, *Virology* **1973**, *52*, 456.
[64] E. H. Chowdhury, M. Kunou, M. Nagaoka, A. K. Kundu, T. Hoshiba, T. Akaike, *Gene* **2004**, *341*, 77.
[65] K. Modra, S. Dai, H. Zhang, B. Shi, J. Bi, *Eng. Life Sci.* **2015**, *15*, 489.
[66] Y. Song, T. Zhang, X. Song, L. Zhang, C. Zhang, J. Xing, X.-J. Liang, *J. Mater. Chem. B* **2015**, *3*, 911.
[67] K. Kim, W. C. W. Chen, Y. Heo, Y. Wang, *Prog. Polym. Sci.* **2016**, *60*, 18.
[68] A. Namvar, A. Bolhassani, N. Khairkhah, F. Motevalli, *Biopolymers* **2015**, *103*, 363.
[69] C. Tasdelen, S. Aktas, E. Acma, Y. Guvenilir, *Hydrometallurgy* **2009**, *96*, 253.
[70] J. Dennig, E. Duncan, *Rev. Mol. Biotechnol.* **2002**, *90*, 339.
[71] G. Sessa, G. Weissmann, *J. Lipid Res.* **1968**, *9*, 310.
[72] A. T. L. Young, J. R. T. Lakey, A. G. Murray, R. B. Moore, *Cell Transplant.* **2002**, *11*, 573.
[73] R. Fraley, S. Subramani, P. Berg, D. Papahadjopoulos, *J. Biol. Chem.* **1980**, *255*, 10431.
[74] W. Tai-Kin, C. Nicolau, P. H. Hofschneider, *Gene* **1980**, *10*, 87.
[75] A. R. Teagle, J. C. Birchall, R. Hargest, *Skin Pharmacol. Physiol.* **2016**, *29*, 119.
[76] E. Dodds, M. G. Dunckley, K. Naujoks, U. Michaelis, G. Dickson, *Gene Ther.* **1998**, *5*, 542.
[77] M. Lee, K. Chea, R. Pyda, M. Chua, I. Dominguez, *J. Biomol. Tech.* **2017**, *28*, 67.
[78] Z. Fekete, P. Nagy, G. Huszka, F. Tolner, A. Pongrácz, P. Fürjes, *Sens. Actuators, B* **2012**, *162*, 89.
[79] B. Li, L. Deng, M. Liu, Y. Zeng, *Molecules* **2017**, *22*, 406.
[80] M. P. Stewart, R. Langer, K. F. Jensen, *Chem. Rev.* **2018**, *118*, 7409.
[81] S. Delin, F. Jan, E. W. Clifford, *Curr. Top. Med. Chem.* **2016**, *16*, 170.
[82] A. Makky, M. Tanaka, *J. Phys. Chem. B* **2015**, *119*, 5857.
[83] K. Medepalli, B. W. Alphenaar, R. S. Keynton, P. Sethu, *Nanotechnology* **2013**, *24*, 205101.
[84] A. L. van de Ven, K. Adler-Storthz, R. Richards-Kortum, *J. Biomed. Opt.* **2009**, *14*, 021012.
[85] D. Koley, A. J. Bard, *Proc. Natl. Acad. Sci. USA* **2010**, *107*, 16783.
[86] A. A. Gurtovenko, J. Anwar, *J. Phys. Chem. B* **2007**, *111*, 10453.
[87] A. C. Williams, B. W. Barry, *Adv. Drug Delivery Rev.* **2004**, *56*, 603.
[88] Z.-W. Yu, P. J. Quinn, *Biophys. Chem.* **1998**, *70*, 35.
[89] A. A. Gurtovenko, J. Anwar, *J. Phys. Chem. B* **2009**, *113*, 1983.
[90] K. A. Riske, T. P. Sudbrack, N. L. Archilha, A. F. Uchoa, A. P. Schroder, C. M. Marques, M. S. Baptista, R. Itri, *Biophys. J.* **2009**, *97*, 1362.
[91] L. Yan, J. Zhang, C.-S. Lee, X. Chen, *Small* **2014**, *10*, 4487.
[92] T. M. Klein, E. D. Wolf, R. Wu, J. C. Sanford, *Nature* **1987**, *327*, 70.
[93] S. Mehier-Humbert, R. H. Guy, *Adv. Drug Delivery Rev.* **2005**, *57*, 733.
[94] K. E. Matthews, G. B. Mills, W. Horsfall, N. Hack, K. Skorecki, A. Keating, *Exp. Hematol.* **1993**, *21*, 697.
[95] M. Uchida, H. Natsume, D. Kobayashi, K. Sugibayashi, Y. Morimoto, *Biol. Pharm. Bull.* **2002**, *25*, 690.
[96] S. Wang, S. Joshi, S. Lu, *Methods Mol. Biol.* **2004**, *245*, 185.
[97] B. I. Loehr, P. Willson, L. A. Babiuk, H. van Drunen Littel-van den, *J. Virol.* **2000**, *74*, 6077.
[98] T. Ajiki, T. Murakami, Y. Kobayashi, Y. Hakamata, J. Wang, S. Inoue, M. Ohtsuki, H. Nakagawa, Y. Kariya, Y. Hoshino, E. Kobayashi, *Cancer Gene Ther.* **2003**, *10*, 318.
[99] R. Muangmoonchai, S. C. Wong, D. Smirlis, I. R. Phillips, E. A. Shephard, *Mol. Biotechnol.* **2002**, *20*, 145.
[100] Y. Matsuno, H. Iwata, Y. Umeda, H. Takagi, Y. Mori, J. Miyazaki, A. Kosugi, H. Hirose, *ASAIO J.* **2003**, *49*, 641.
[101] G. Zhang, M. E. Selzer, *Exp. Neurol.* **2001**, *167*, 304.
[102] H. P. Lauritzen, C. Reynet, P. Schjerling, E. Ralston, S. Thomas, H. Galbo, T. Ploug, *Pflügers Archiv.* **2002**, *444*, 710.
[103] C. Théry, S. Amigorena, G. Raposo, A. Clayton, in *Current Protocols in Cell Biology* (Ed: J. S. Bonifacino), Wiley, New York **2006**, Chap. 3, Unit 3.22.
[104] P. L. McNeil, R. F. Murphy, F. Lanni, D. L. Taylor, *J. Cell Biol.* **1984**, *98*, 1556.
[105] N. Altan, Y. Chen, M. Schindler, S. M. Simon, *Proc. Natl. Acad. Sci. USA* **1999**, *96*, 4432.
[106] R. L. Bernat, G. G. Borisy, N. F. Rothfield, W. C. Earnshaw, *J. Cell Biol.* **1990**, *111*, 1519.
[107] N. Araki, T. Hatae, T. Yamada, S. Hirohashi, *J. Cell Sci.* **2000**, *113*, 3329.
[108] T. H. Steinberg, A. S. Newman, J. A. Swanson, S. C. Silverstein, *J. Cell Biol.* **1987**, *105*, 2695.
[109] M. Fechheimer, J. F. Boylan, S. Parker, J. E. Sisken, G. L. Patel, S. G. Zimmer, *Proc. Natl. Acad. Sci. USA* **1987**, *84*, 8463.
[110] P. L. McNeil, E. Warder, *J. Cell Sci.* **1987**, *88*, 669.
[111] S. Besteiro, A. Michelin, J. Poncet, J.-F. Dubremetz, M. Lebrun, *PLoS Pathog.* **2009**, *5*, e1000309.
[112] N. T. Emerson, C.-H. Hsia, I. U. Rafalska-Metcalf, H. Yang, *Nanoscale* **2014**, *6*, 4538.
[113] S. Memedula, A. S. Belmont, *Curr. Biol.* **2003**, *13*, 241.

[114] T. Morisaki, K. Lyon, K. F. DeLuca, J. G. DeLuca, B. P. English, Z. Zhang, L. D. Lavis, J. B. Grimm, S. Viswanathan, L. L. Looger, T. Lionnet, T. J. Stasevich, *Science* **2016**, *352*, 1425.
[115] M. S. F. Clarke, P. L. McNeil, in *Cell Biology* (Ed: J. E. Celis), Academic Press, San Diego, CA, USA **1994**, p. 30.
[116] M. S. Clarke, P. L. McNeil, *J. Cell Sci.* **1992**, *102*, 533.
[117] A. S. Waldman, B. C. Waldman, *Anal. Biochem.* **1998**, *258*, 216.
[118] C. Laudanna, J. J. Campbell, E. C. Butcher, *Science* **1996**, *271*, 981.
[119] C. J. Meyer, F. J. Alenghat, P. Rim, J. H.-J. Fong, B. Fabry, D. E. Ingber, *Nat. Cell Biol.* **2000**, *2*, 666.
[120] P. J. Hollenbeck, *J. Cell Biol.* **1993**, *121*, 305.
[121] K. Tachibana, T. Sato, N. D'Avirro, C. Morimoto, *J. Exp. Med.* **1995**, *182*, 1089.
[122] G. T. Van Nhieu, E. S. Krukonis, A. A. Reszka, A. F. Horwitz, R. R. Isberg, *J. Biol. Chem.* **1996**, *271*, 7665.
[123] R. L. Shoeman, C. Hüttermann, R. Hartig, P. Traub, *Mol. Biol. Cell* **2001**, *12*, 143.
[124] T. L. Steck, in *Methods in Membrane Biology*, Vol. *2* (Ed: E. D. Korn), Springer, Boston, MA, USA **1974**, p. 245.
[125] J. Gruber, G. Boese, T. Tuschl, M. Osborn, K. Weber, *BioTechniques* **2004**, *37*, 96.
[126] N. J. Leidenheimer, R. A. Harris, *J. Neurosci. Methods* **1991**, *40*, 233.
[127] R. Chakrabarti, N. E. Pfeiffer, D. E. Wylie, S. M. Schuster, *J. Biol. Chem.* **1989**, *264*, 8214.
[128] D. S. D'Astolfo, R. J. Pagliero, A. Pras, W. R. Karthaus, H. Clevers, V. Prasad, R. J. Lebbink, H. Rehmann, N. Geijsen, *Cell* **2015**, *161*, 674.
[129] H. B. Bosmann, A. Hagopian, E. H. Eylar, *Arch. Biochem. Biophys.* **1968**, *128*, 51.
[130] D. L. Gill, E. F. Grollman, L. D. Kohn, *J. Biol. Chem.* **1981**, *256*, 184.
[131] N. D. Andersen, A. Chopra, T. S. Monahan, J. Y. Malek, M. Jain, L. Pradhan, C. Ferran, F. W. LoGerfo, *J. Vasc. Surg.* **2010**, *52*, 1608.
[132] H. J. Kim, J. F. Greenleaf, R. R. Kinnick, J. T. Bronk, M. E. Bolander, *Hum. Gene Ther.* **1996**, *7*, 1339.
[133] F. Scherer, M. Anton, U. Schillinger, J. Henke, C. Bergemann, A. Krüger, B. Gänsbacher, C. Plank, *Gene Ther.* **2002**, *9*, 102.
[134] T.-H. W. Chou, S. Biswas, S. Lu, in *Gene Delivery to Mammalian Cells: Nonviral Gene Transfer Techniques*, Vol. *1* (Ed: W. C. Heiser), Humana Press, Totowa, NJ, USA **2004**, p. 147.
[135] W. J. Greenleaf, M. E. Bolander, G. Sarkar, M. B. Goldring, J. F. Greenleaf, *Ultrasound Med. Biol.* **1998**, *24*, 587.
[136] D. L. Miller, M. A. Averkiou, A. A. Brayman, E. C. Everbach, C. K. Holland, J. H. Wible Jr., J. Wu, *J. Ultrasound Med.* **2008**, *27*, 611.
[137] M. W. Miller, D. L. Miller, A. A. Brayman, *Ultrasound Med. Biol.* **1996**, *22*, 1131.
[138] M. Ward, J. Wu, J.-F. Chiu, *J. Acoust. Soc. Am.* **1999**, *105*, 2951.
[139] M. Tomizawa, F. Shinozaki, Y. Motoyoshi, T. Sugiyama, S. Yamamoto, M. Sueishi, *World J. Methodol.* **2013**, *3*, 39.
[140] M. Fechheimer, C. Denny, R. F. Murphy, D. L. Taylor, *Eur. J. Cell Biol.* **1986**, *40*, 242.
[141] M. Fechheimer, D. L. Taylor, *Methods Cell Biol.* **1987**, *28*, 179.
[142] R. Furukawa, J. E. Wampler, M. Fechheimer, *J. Cell Biol.* **1988**, *107*, 2541.
[143] Y. S. Li, E. Davidson, C. N. Reid, A. P. McHale, *Cancer Lett.* **2009**, *273*, 62.
[144] L. J. M. Juffermans, P. A. Dijkmans, R. J. P. Musters, C. A. Visser, O. Kamp, *Am. J. Physiol.: Heart Circ. Physiol.* **2006**, *291*, H1595.
[145] S. Herbert, H. Anita, S. Reinhard, S. L. S. Wolfgang, L. Marco, S. Michael, *J. Biomed. Opt.* **2002**, *7*, 410.
[146] R. Xiong, S. K. Samal, J. Demeester, A. G. Skirtach, S. C. De Smedt, K. Braeckmans, *Adv. Phys.: X* **2016**, *1*, 596.
[147] L. E. Barrett, J.-Y. Sul, H. Takano, E. J. Van Bockstaele, P. G. Haydon, J. H. Eberwine, *Nat. Methods* **2006**, *3*, 455.
[148] M. Tsukakoshi, S. Kurata, Y. Nomiya, Y. Ikawa, T. Kasuya, *Appl. Phys. B* **1984**, *35*, 135.
[149] X. Du, J. Wang, Q. Zhou, L. Zhang, S. Wang, Z. Zhang, C. Yao, *Drug Delivery* **2018**, *25*, 1516.
[150] M. Patience, D. Kishan, G.-M. Frank James, *J. Biomed. Opt.* **2010**, *15*, 041507.
[151] M. Lei, H. Xu, H. Yang, B. Yao, *J. Neurosci. Methods* **2008**, *174*, 215.
[152] E. Zeira, A. Manevitch, A. Khatchatouriants, O. Pappo, E. Hyam, M. Darash-Yahana, E. Tavor, A. Honigman, A. Lewis, E. Galun, *Mol. Ther.* **2003**, *8*, 342.
[153] C. Yao, Z. Zhang, R. Rahmanzadeh, G. Huettmann, *IEEE Trans. NanoBiosci.* **2008**, *7*, 111.
[154] U. K. Tirlapur, K. König, *Nature* **2002**, *418*, 290.
[155] D. J. Stevenson, F. J. Gunn-Moore, P. Campbell, K. Dholakia, *J. R. Soc., Interface* **2010**, *7*, 863.
[156] C. McDougall, D. J. Stevenson, C. T. A. Brown, F. Gunn-Moore, K. Dholakia, *J. Biophotonics* **2009**, *2*, 736.
[157] M. Waleed, S.-U. Hwang, J.-D. Kim, I. Shabbir, S.-M. Shin, Y.-G. Lee, *Biomed. Opt. Express* **2013**, *4*, 1533.
[158] K. Jacobson, D. Papahadjopoulos, *Biochemistry* **1975**, *14*, 152.
[159] D. Hanahan, *J. Mol. Biol.* **1983**, *166*, 557.
[160] J. P. Huff, B. J. Grant, C. A. Penning, K. F. Sullivan, *BioTechniques* **1990**, *9*, 570.
[161] M. Das, H. Raythata, S. Chatterjee, *Annu. Res. Rev. Biol.* **2017**, *16*, 1.
[162] X. He, A. A. Amin, A. Fowler, M. Toner, *Cell Preserv. Technol.* **2006**, *4*, 178.
[163] G. Boheim, W. Hanke, H. Eibl, *Proc. Natl. Acad. Sci. USA* **1980**, *77*, 3403.
[164] V. F. Antonov, V. V. Petrov, A. A. Molnar, D. A. Predvoditelev, A. S. Ivanov, *Nature* **1980**, *283*, 585.
[165] C. Plank, J. Rosenecker, *Cold Spring Harbor Protoc.* **2009**, *2009*, 5230.
[166] Y. Wang, H. Cui, K. Li, C. Sun, W. Du, J. Cui, X. Zhao, W. Chen, *PLoS One* **2014**, *9*, e102886.
[167] S. Smolders, S. Kessels, S. M.-T. Smolders, F. Poulhes, O. Zelphati, C. Sapet, B. Brône, *J. Neurosci. Methods* **2018**, *293*, 169.
[168] F. M. Kievit, O. Veiseh, N. Bhattarai, C. Fang, J. W. Gunn, D. Lee, R. G. Ellenbogen, J. M. Olson, M. Zhang, *Adv. Funct. Mater.* **2009**, *19*, 2244.
[169] P. Reimer, T. Balzer, *Eur. Radiol.* **2003**, *13*, 1266.
[170] Y.-X. J. Wang, *Quant. Imaging Med. Surg.* **2011**, *1*, 35.
[171] K. J. Widder, R. M. Morris, G. Poore, D. P. Howard Jr., A. E. Senyei, *Proc. Natl. Acad. Sci. USA* **1981**, *78*, 579.
[172] K. J. Widder, R. M. Morris, G. A. Poore, D. P. Howard, A. E. Senyei, *Eur. J. Cancer Clin. Oncol.* **1983**, *19*, 135.
[173] C. Plank, U. Schillinger, F. Scherer, C. Bergemann, J. S. Rémy, F. Krötz, M. Anton, J. Lausier, J. Rosenecker, *Biol. Chem.* **2003**, *384*, 737.
[174] J. C. Weaver, *Radio Sci.* **1995**, *30*, 205.
[175] J. Gehl, *Acta Physiol. Scand.* **2003**, *177*, 437.
[176] T. S. Santra, F. G. Tseng, *Micromachines* **2013**, *4*, 333.
[177] U. Zimmermann, G. Pilwat, F. Riemann, in *Membrane Transport in Plants* (Eds: U. Zimmermann, J. Dainty), Springer, Berlin, Germany **1974**, p. 146.
[178] T. Kotnik, P. Kramar, G. Pucihar, D. Miklavcic, M. Tarek, *IEEE Electr. Insul. Mag.* **2012**, *28*, 14.
[179] M. S. Venslauskas, S. Šatkauskas, *Eur. Biophys. J.* **2015**, *44*, 277.
[180] S. A. Akimov, P. E. Volynsky, T. R. Galimzyanov, P. I. Kuzmin, K. V. Pavlov, O. V. Batishchev, *Sci. Rep.* **2017**, *7*, 12509.
[181] D. Rabussay, N. B. Dev, J. Fewell, L. C. Smith, G. Widera, L. Zhang, *J. Phys. D: Appl. Phys.* **2003**, *36*, 348.
[182] F. Hoover, J. Magne Kalhovde, *Anal. Biochem.* **2000**, *285*, 175.
[183] T. Muramatsu, Y. Mizutani, Y. Ohmori, J.-i. Okumura, *Biochem. Biophys. Res. Commun.* **1997**, *230*, 376.
[184] R. Heller, M. Jaroszeski, A. Atkin, D. Moradpour, R. Gilbert, J. Wands, C. Nicolau, *FEBS Lett.* **1996**, *389*, 225.

[185] M.-P. Rols, C. Delteil, M. Golzio, P. Dumond, S. Cros, J. Teissie, *Nat. Biotechnol.* **1998**, *16*, 168.
[186] H. Aihara, J.-I. Miyazaki, *Nat. Biotechnol.* **1998**, *16*, 867.
[187] D. J. Wells, *Gene Ther.* **2004**, *11*, 1363.
[188] E. Sokołowska, A. U. Błachnio-Zabielska, *Int. J. Mol. Sci.* **2019**, *20*, 2776.
[189] O. Gresch, F. B. Engel, D. Nesic, T. T. Tran, H. M. England, E. S. Hickman, I. Körner, L. Gan, S. Chen, S. Castro-Obregon, R. Hammermann, J. Wolf, H. Müller-Hartmann, M. Nix, G. Siebenkotten, G. Kraus, K. Lun, *Methods* **2004**, *33*, 151.
[190] M. Zeitelhofer, J. P. Vessey, Y. Xie, F. Tübing, S. Thomas, M. Kiebler, R. Dahm, *Nat. Protoc.* **2007**, *2*, 1692.
[191] A. Hamm, N. Krott, I. Breibach, R. Blindt, A. K. Bosserhoff, *Tissue Eng.* **2002**, *8*, 235.
[192] H.-I. Trompeter, S. Weinhold, C. Thiel, P. Wernet, M. Uhrberg, *J. Immunol. Methods* **2003**, *274*, 245.
[193] J. W. Gordon, G. A. Scangos, D. J. Plotkin, J. A. Barbosa, F. H. Ruddle, *Proc. Natl. Acad. Sci. USA* **1980**, *77*, 7380.
[194] V. B. Lu, D. J. Williams, Y.-J. Won, S. R. Ikeda, *J. Visualized Exp.* **2009**, *34*, 1614.
[195] S. E. Anderson, H. H. Bau, *Nanotechnology* **2014**, *25*, 245102.
[196] M. A. Barber, *J. Infect. Dis.* **1911**, *8*, 348.
[197] C. M. Feldherr, *J. Cell Biol.* **1962**, *12*, 159.
[198] M. Fischberg, J. B. Gurdon, T. R. Elsdale, *Nature* **1958**, *181*, 424.
[199] R. Briggs, T. J. King, *Proc. Natl. Acad. Sci. USA* **1952**, *38*, 455.
[200] I. Wilmut, A. E. Schnieke, J. McWhir, A. J. Kind, K. H. S. Campbell, *Nature* **1997**, *385*, 810.
[201] C. Liu, W. Xie, C. Gui, Y. Du, in *Lipoproteins and Cardiovascular Disease* (Ed: L. A. Freeman), Springer, New York **2013**, p. 217.
[202] L. Craven, H. A. Tuppen, G. D. Greggains, S. J. Harbottle, J. L. Murphy, L. M. Cree, A. P. Murdoch, P. F. Chinnery, R. W. Taylor, R. N. Lightowlers, M. Herbert, D. M. Turnbull, *Nature* **2010**, *465*, 82.
[203] M. Tachibana, M. Sparman, H. Sritanaudomchai, H. Ma, L. Clepper, J. Woodward, Y. Li, C. Ramsey, O. Kolotushkina, S. Mitalipov, *Nature* **2009**, *461*, 367.
[204] G. Palermo, H. Joris, P. Devroey, A. C. Van Steirteghem, *Lancet* **1992**, *340*, 17.
[205] Y. Hiramoto, *Exp. Cell Res.* **1962**, *27*, 416.
[206] D. O. Co, A. H. Borowski, J. D. Leung, J. van der Kaa, S. Hengst, G. J. Platenburg, F. R. Pieper, C. F. Perez, F. R. Jirik, J. I. Drayer, *Chromosome Res.* **2000**, *8*, 183.
[207] D. P. Monteith, J. D. Leung, A. H. Borowski, T. Praznovszky, F. R. Jirik, G. Hadlaczky, C. F. Perez, in *Mammalian Artificial Chromosomes* (Eds: V. Sgaramella, S. Eridani), Springer, New York **2004**, p. 227.
[208] C. R. White, J. A. Frangos, *Philos. Trans. R. Soc., B* **2007**, *362*, 1459.
[209] D. M. Hallow, R. A. Seeger, P. P. Kamaev, G. R. Prado, M. C. LaPlaca, M. R. Prausnitz, *Biotechnol. Bioeng.* **2008**, *99*, 846.
[210] M. E. Kizer, Y. Deng, G. Kang, P. E. Mikael, X. Wang, A. J. Chung, *Lab Chip* **2019**, *19*, 1747.
[211] G. Kang, D. W. Carlson, T. H. Kang, S. Lee, S. J. Haward, I. Choi, A. Q. Shen, A. J. Chung, *ACS Nano* **2020**, *14*, 3048.
[212] J. A. Jarrell, A. A. Twite, K. H. W. J. Lau, M. N. Kashani, A. A. Lievano, J. Acevedo, C. Priest, J. Nieva, D. Gottlieb, R. S. Pawell, *Sci. Rep.* **2019**, *9*, 3214.
[213] S. Li, L. Meadow Anderson, J.-M. Yang, L. Lin, H. Yang, *Appl. Phys. Lett.* **2007**, *91*, 013902.
[214] S. Panja, P. Aich, B. Jana, T. Basu, *Mol. Membr. Biol.* **2008**, *25*, 411.
[215] M. N. Kavaldzhiev, J. E. Perez, R. Sougrat, P. Bergam, T. Ravasi, J. Kosel, *Sci. Rep.* **2018**, *8*, 9918.
[216] M. Kinoshita, K. Hynynen, *Biochem. Biophys. Res. Commun.* **2007**, *359*, 860.
[217] S. Le Gac, E. Zwaan, A. van den Berg, C.-D. Ohl, *Lab Chip* **2007**, *7*, 1666.
[218] M. Thein, A. Cheng, P. Khanna, C. Zhang, E.-J. Park, D. Ahmed, C. J. Goodrich, F. Asphahani, F. Wu, N. B. Smith, C. Dong, X. Jiang, M. Zhang, J. Xu, *Biosens. Bioelectron.* **2011**, *27*, 25.
[219] Y. H. Lee, C. A. Peng, *Gene Ther.* **2005**, *12*, 625.
[220] S. Rodamporn, N. R. Harris, S. P. Beeby, R. J. Boltryk, T. Sanchez-Elsner, *IEEE Trans. Bio-Med. Eng.* **2011**, *58*, 927.
[221] D. Carugo, D. N. Ankrett, P. Glynne-Jones, L. Capretto, R. J. Boltryk, X. Zhang, P. A. Townsend, M. Hill, *Biomicrofluidics* **2011**, *5*, 044108.
[222] J. N. Belling, L. K. Heidenreich, Z. Tian, A. M. Mendoza, T.-T. Chiou, Y. Gong, N. Y. Chen, T. D. Young, N. Wattanatorn, J. H. Park, L. Scarabelli, N. Chiang, J. Takahashi, S. G. Young, A. Z. Stieg, S. De Oliveira, T. J. Huang, P. S. Weiss, S. J. Jonas, *Proc. Natl. Acad. Sci. USA* **2020**, *117*, 10976.
[223] A. R. Williams, S. Bao, D. L. Miller, *Biotechnol. Bioeng.* **1999**, *65*, 341.
[224] J. Yen, M. Fiorino, Y. Liu, S. Paula, S. Clarkson, L. Quinn, W. R. Tschantz, H. Klock, N. Guo, C. Russ, *Sci. Rep.* **2018**, *8*, 16304.
[225] A. Sharei, N. Cho, S. Mao, E. Jackson, R. Poceviciute, A. Adamo, J. Zoldan, R. Langer, K. F. Jensen, *J. Vis. Exp.* **2013**, *81*, e50980.
[226] A. Sharei, R. Poceviciute, E. L. Jackson, N. Cho, S. Mao, G. C. Hartoularos, D. Y. Jang, S. Jhunjhunwala, A. Eyerman, T. Schoettle, *Integr. Biol.* **2014**, *6*, 470.
[227] J. Lee, A. Sharei, W. Y. Sim, A. Adamo, R. Langer, K. F. Jensen, M. G. Bawendi, *Nano Lett.* **2012**, *12*, 6322.
[228] A. Sharei, R. Trifonova, S. Jhunjhunwala, G. C. Hartoularos, A. T. Eyerman, A. Lytton-Jean, M. Angin, S. Sharma, R. Poceviciute, S. Mao, M. Heimann, S. Liu, T. Talkar, O. F. Khan, M. Addo, U. H. von Andrian, D. G. Anderson, R. Langer, J. Lieberman, K. F. Jensen, *PLoS One* **2015**, *10*, e0118803.
[229] G. L. Szeto, D. Van Egeren, H. Worku, A. Sharei, B. Alejandro, C. Park, K. Frew, M. Brefo, S. Mao, M. Heimann, R. Langer, K. Jensen, D. J. Irvine, *Sci. Rep.* **2015**, *5*, 10276.
[230] M. Griesbeck, S. Ziegler, S. Laffont, N. Smith, L. Chauveau, P. Tomezsko, A. Sharei, G. Kourjian, F. Porichis, M. Hart, C. D. Palmer, M. Sirignano, C. Beisel, H. Hildebrandt, C. Cénac, A. C. Villani, T. J. Diefenbach, S. Le Gall, O. Schwartz, J. P. Herbeuval, B. Autran, J. C. Guéry, J. J. Chang, M. Altfeld, *J. Immunol.* **2015**, *195*, 5327.
[231] C. Tu, L. Santo, Y. Mishima, N. Raje, Z. Smilansky, J. Zoldan, *Integr. Biol.* **2016**, *8*, 645.
[232] J. Li, B. Wang, B. M. Juba, M. Vazquez, S. W. Kortum, B. S. Pierce, M. Pacheco, L. Roberts, J. W. Strohbach, L. H. Jones, E. Hett, A. Thorarensen, J.-B. Telliez, A. Sharei, M. Bunnage, J. B. Gilbert, *ACS Chem. Biol.* **2017**, *12*, 2970.
[233] A. Kollmannsperger, A. Sharei, A. Raulf, M. Heilemann, R. Langer, K. F. Jensen, R. Wieneke, R. Tampé, *Nat. Commun.* **2016**, *7*, 10372.
[234] M. T. Saung, A. Sharei, V. A. Adalsteinsson, N. Cho, T. Kamath, C. Ruiz, J. Kirkpatrick, N. Patel, M. Mino-Kenudson, S. P. Thayer, R. Langer, K. F. Jensen, A. S. Liss, J. C. Love, *Small* **2016**, *12*, 5873.
[235] T. DiTommaso, J. M. Cole, L. Cassereau, J. A. Buggé, J. L. S. Hanson, D. T. Bridgen, B. D. Stokes, S. M. Loughhead, B. A. Beutel, J. B. Gilbert, K. Nussbaum, A. Sorrentino, J. Toggweiler, T. Schmidt, G. Gyuelveszi, H. Bernstein, A. Sharei, *Proc. Natl. Acad. Sci. USA* **2018**, *115*, E10907.
[236] X. Han, Z. Liu, M. C. Jo, K. Zhang, Y. Li, Z. Zeng, N. Li, Y. Zu, L. Qin, *Sci. Adv.* **2015**, *1*, e1500454.
[237] X. Han, Z. Liu, Y. Ma, K. Zhang, L. Qin, *Adv. Biosyst.* **2017**, *1*, 1600007.
[238] Z. Liu, X. Han, Q. Zhou, R. Chen, S. Fruge, M. C. Jo, Y. Ma, Z. Li, K. Yokoi, L. Qin, *Adv. Biosyst.* **2017**, *1*, 1700054.
[239] Y. Ma, X. Han, O. Quintana Bustamante, R. Bessa de Castro, K. Zhang, P. Zhang, Y. Li, Z. Liu, X. Liu, M. Ferrari, Z. Hu, J. Carlos Segovia, L. Qin, *Integr. Biol.* **2017**, *9*, 548.
[240] X. Xing, Y. Pan, L. Yobas, *Anal. Chem.* **2018**, *90*, 1836.
[241] Y. Deng, M. Kizer, M. Rada, J. Sage, X. Wang, D.-J. Cheon, A. J. Chung, *Nano Lett.* **2018**, *18*, 2705.

[242] L. Chang, L. Li, J. Shi, Y. Sheng, W. Lu, D. Gallego-Perez, L. J. Lee, *Lab Chip* **2016**, *16*, 4047.
[243] Y.-C. Lin, C.-M. Jen, M.-Y. Huang, C.-Y. Wu, X.-Z. Lin, *Sens. Actuators, B* **2001**, *79*, 137.
[244] A. Adamo, A. Arione, A. Sharei, K. F. Jensen, *Anal. Chem.* **2013**, *85*, 1637.
[245] Y. S. Shin, K. Cho, J. K. Kim, S. H. Lim, C. H. Park, K. B. Lee, Y. Park, C. Chung, D.-C. Han, J. K. Chang, *Anal. Chem.* **2004**, *76*, 7045.
[246] C. Xie, Z. Lin, L. Hanson, Y. Cui, B. Cui, *Nat. Nanotechnol.* **2012**, *7*, 185.
[247] M. M. Bahi, M. N. Tsaloglou, M. Mowlem, H. Morgan, *J. R. Soc., Interface* **2011**, *8*, 601.
[248] C. d. L. Rosa, P. A. Tilley, J. D. Fox, K. K. V. I. Kaler, *IEEE Trans. Biomed. Eng.* **2008**, *55*, 2426.
[249] H. Huang, Z. Wei, Y. Huang, D. Zhao, L. Zheng, T. Cai, M. Wu, W. Wang, X. Ding, Z. Zhou, Q. Du, Z. Li, Z. Liang, *Lab Chip* **2011**, *11*, 163.
[250] H. Lu, M. A. Schmidt, K. F. Jensen, *Lab Chip* **2005**, *5*, 23.
[251] T. Geng, Y. Zhan, J. Wang, C. Lu, *Nat. Protoc.* **2011**, *6*, 1192.
[252] D. Shah, M. Steffen, L. Lilge, *Biomicrofluidics* **2012**, *6*, 014111.
[253] W. G. Lee, U. Demirci, A. Khademhosseini, *Integr. Biol.* **2009**, *1*, 242.
[254] I. Zudans, A. Agarwal, O. Orwar, S. G. Weber, *Biophys. J.* **2007**, *92*, 3696.
[255] J. A. Kim, K. Cho, M. S. Shin, W. G. Lee, N. Jung, C. Chung, J. K. Chang, *Biosens. Bioelectron.* **2008**, *23*, 1353.
[256] S. Wang, L. J. Lee, *Biomicrofluidics* **2013**, *7*, 011301.
[257] W. Kang, J. P. Giraldo-Vela, S. S. P. Nathamgari, T. McGuire, R. L. McNaughton, J. A. Kessler, H. D. Espinosa, *Lab Chip* **2014**, *14*, 4486.
[258] L. Przybyla, J. Voldman, *Annu. Rev. Anal. Chem.* **2012**, *5*, 293.
[259] L. Chang, M. Howdyshell, W. C. Liao, C. L. Chiang, D. Gallego-Perez, Z. Yang, W. Lu, J. C. Byrd, N. Muthusamy, L. J. Lee, *Small* **2015**, *11*, 1818.
[260] Z. Fei, X. Hu, H.-w. Choi, S. Wang, D. Farson, L. J. Lee, *Anal. Chem.* **2010**, *82*, 353.
[261] Z. Fei, S. Wang, Y. Xie, B. E. Henslee, C. G. Koh, L. J. Lee, *Anal. Chem.* **2007**, *79*, 5719.
[262] Z. Fei, Y. Wu, S. Sharma, D. Gallego-Perez, N. Higuita-Castro, D. Hansford, J. J. Lannutti, L. J. Lee, *Anal. Chem.* **2013**, *85*, 1401.
[263] Y. Xu, H. Yao, L. Wang, W. Xing, J. Cheng, *Lab Chip* **2011**, *11*, 2417.
[264] M. Ouyang, W. Hill, J. H. Lee, S. C. Hur, *Sci. Rep.* **2017**, *7*, 44757.
[265] Z. Dong, Y. Jiao, B. Xie, Y. Hao, P. Wang, Y. Liu, J. Shi, C. Chitrakar, S. Black, Y.-C. Wang, L. J. Lee, M. Li, Y. Fan, L. Chang, *Microsyst. Nanoeng.* **2020**, *6*, 2.
[266] T. Zhu, C. Luo, J. Huang, C. Xiong, Q. Ouyang, J. Fang, *Biomed. Microdevices* **2010**, *12*, 35.
[267] M. Zheng, J. W. Shan, H. Lin, D. I. Shreiber, J. D. Zahn, *Microfluid. Nanofluid.* **2016**, *20*, 16.
[268] H. Yun, S. C. Hur, *Lab Chip* **2013**, *13*, 2764.
[269] J. Wang, Y. Zhan, V. M. Ugaz, C. Lu, *Lab Chip* **2010**, *10*, 2057.
[270] J. E. Bestman, R. C. Ewald, S.-L. Chiu, H. T. Cline, *Nat. Protoc.* **2006**, *1*, 1267.
[271] S. J. Singer, G. L. Nicolson, *Science* **1972**, *175*, 720.
[272] M. Golzio, J. Teissié, M.-P. Rols, *Proc. Natl. Acad. Sci. USA* **2002**, *99*, 1292.
[273] Y. Huang, B. Rubinsky, *Biomed. Microdevices* **1999**, *2*, 145.
[274] Y. Huang, B. Rubinsky, *Sens. Actuators, A* **2001**, *89*, 242.
[275] Y. Huang, B. Rubinsky, *Sens. Actuators, A* **2003**, *104*, 205.
[276] M. Khine, A. Lau, C. Ionescu-Zanetti, J. Seo, L. P. Lee, *Lab Chip* **2005**, *5*, 38.
[277] M. Khine, C. Ionescu-Zanetti, A. Blatz, L.-P. Wang, L. P. Lee, *Lab Chip* **2007**, *7*, 457.
[278] A. Valero, J. N. Post, J. W. van Nieuwkasteele, P. M. ter Braak, W. Kruijer, A. van den Berg, *Lab Chip* **2008**, *8*, 62.
[279] M. Punjiya, H. R. Nejad, J. Mathews, M. Levin, S. Sonkusale, *Sci. Rep.* **2019**, *9*, 11988.
[280] A. Valero, J. N. Post, J. W. van Nieuwkasteele, P. M. ter Braak, W. Kruijer, A. van den Berg, *Lab Chip* **2008**, *8*, 62.
[281] S. Köster, F. E. Angile, H. Duan, J. J. Agresti, A. Wintner, C. Schmitz, A. C. Rowat, C. A. Merten, D. Pisignano, A. D. Griffiths, *Lab Chip* **2008**, *8*, 1110.
[282] S.-Y. Teh, R. Lin, L.-H. Hung, A. P. Lee, *Lab Chip* **2008**, *8*, 198.
[283] A. Huebner, S. Sharma, M. Srisa-Art, F. Hollfelder, J. B. Edel, A. J. Demello, *Lab Chip* **2008**, *8*, 1244.
[284] R. Seemann, M. Brinkmann, T. Pfohl, S. Herminghaus, *Rep. Prog. Phys.* **2012**, *75*, 016601.
[285] T. Thorsen, R. W. Roberts, F. H. Arnold, S. R. Quake, *Phys. Rev. Lett.* **2001**, *86*, 4163.
[286] S. L. Anna, N. Bontoux, H. A. Stone, *Appl. Phys. Lett.* **2003**, *82*, 364.
[287] C. Cramer, P. Fischer, E. J. Windhab, *Chem. Eng. Sci.* **2004**, *59*, 3045.
[288] Y. Zhan, J. Wang, N. Bao, C. Lu, *Anal. Chem.* **2009**, *81*, 2027.
[289] F. Chen, Y. Zhan, T. Geng, H. Lian, P. Xu, C. Lu, *Anal. Chem.* **2011**, *83*, 8816.
[290] L. Digiacomo, S. Palchetti, D. Pozzi, A. Amici, G. Caracciolo, C. Marchini, *Biochem. Biophys. Res. Commun.* **2018**, *503*, 508.
[291] X. Li, M. Aghaamoo, S. Liu, D.-H. Lee, A. P. Lee, *Small* **2018**, *14*, 1802055.
[292] A. Tay, *ACS Nano* **2020**, *14*, 7714.
[293] T. Da Ros, A. Ostric, F. Andreola, M. Filocamo, M. Pietrogrande, F. Corsolini, M. Stroppiano, S. Bruni, A. Serafino, S. Fiorito, *Nanoscale* **2018**, *10*, 657.
[294] I.-J. Fang, B. G. Trewyn, in *Nanomedicine: Cancer, Diabetes, and Cardiovascular, Central Nervous System, Pulmonary and Inflammatory Diseases, Methods in Enzymology*, Vol. *508*, (Ed: N. Düzgüneş), Academic Press **2012**, p. 41.
[295] P. Ghosh, G. Han, M. De, C. K. Kim, V. M. Rotello, *Adv. Drug Delivery Rev.* **2008**, *60*, 1307.
[296] C. Chiappini, J. O. Martinez, E. De Rosa, C. S. Almeida, E. Tasciotti, M. M. Stevens, *ACS Nano* **2015**, *9*, 5500.
[297] A. K. Shalek, J. T. Gaublomme, L. Wang, N. Yosef, N. Chevrier, M. S. Andersen, J. T. Robinson, N. Pochet, D. Neuberg, R. S. Gertner, I. Amit, J. R. Brown, N. Hacohen, A. Regev, C. J. Wu, H. Park, *Nano Lett.* **2012**, *12*, 6498.
[298] C. Klumpp, K. Kostarelos, M. Prato, A. Bianco, *Biochim. Biophys. Acta, Biomembr.* **2006**, *1758*, 404.
[299] Z. Liu, S. Tabakman, K. Welsher, H. Dai, *Nano Res.* **2009**, *2*, 85.
[300] H. Li, X. Fan, X. Chen, *ACS Appl. Mater. Interfaces* **2016**, *8*, 4500.
[301] D. Cai, J. M. Mataraza, Z.-H. Qin, Z. Huang, J. Huang, T. C. Chiles, D. Carnahan, K. Kempa, Z. J. N. M. Ren, *Nat. Methods* **2005**, *2*, 449.
[302] X. Xu, S. Hou, N. Wattanatorn, F. Wang, Q. Yang, C. Zhao, X. Yu, H.-R. Tseng, S. J. Jonas, P. S. Weiss, *ACS Nano* **2018**, *12*, 4503.
[303] I. I. Slowing, B. G. Trewyn, V. S.-Y. Lin, *J. Am. Chem. Soc.* **2007**, *129*, 8845.
[304] M. Oishi, J. Nakaogami, T. Ishii, Y. Nagasaki, *Chem. Lett.* **2006**, *35*, 1046.
[305] A. Verma, J. M. Simard, J. W. Worrall, V. M. Rotello, *J. Am. Chem. Soc.* **2004**, *126*, 13987.
[306] D. R. Bhumkar, H. M. Joshi, M. Sastry, V. B. Pokharkar, *Pharm. Res.* **2007**, *24*, 1415.
[307] S. Gopal, C. Chiappini, J. Penders, V. Leonardo, H. Seong, S. Rothery, Y. Korchev, A. Shevchuk, M. M. Stevens, *Adv. Mater.* **2019**, *31*, 1806788.
[308] S. Ohta, K. Yamura, S. Inasawa, Y. Yamaguchi, *Chem. Commun.* **2015**, *51*, 6422.
[309] W. Kang, R. L. McNaughton, F. Yavari, M. Minary-Jolandan, A. Safi, H. D. Espinosa, *J. Lab. Autom.* **2014**, *19*, 100.
[310] Y. Cao, E. Ma, S. Cestellos-Blanco, B. Zhang, R. Qiu, Y. Su, J. A. Doudna, P. Yang, *Proc. Natl. Acad. Sci. USA* **2019**, *116*, 7899.

[311] J. J. VanDersarl, A. M. Xu, N. A. Melosh, *Nano Lett.* **2012**, *12*, 3881.
[312] Y. Cao, M. Hjort, H. Chen, F. Birey, S. A. Leal-Ortiz, C. M. Han, J. G. Santiago, S. P. Paşca, J. C. Wu, N. A. Melosh, *Proc. Natl. Acad. Sci. USA* **2017**, *114*, E1866.
[313] X. Xie, A. M. Xu, S. Leal-Ortiz, Y. Cao, C. C. Garner, N. A. Melosh, *ACS Nano* **2013**, *7*, 4351.
[314] A. M. Xu, D. S. Wang, P. Shieh, Y. Cao, N. A. Melosh, *ChemBioChem* **2017**, *18*, 623.
[315] Y. Cao, H. Chen, R. Qiu, M. Hanna, E. Ma, M. Hjort, A. Zhang, R. S. Lewis, J. C. Wu, N. A. Melosh, *Sci. Adv.* **2018**, *4*, eaat8131.
[316] R. Wen, A.-h. Zhang, D. Liu, J. Feng, J. Yang, D. Xia, J. Wang, C. Li, T. Zhang, N. Hu, T. Hang, G. He, X. Xie, *ACS Appl. Mater. Interfaces* **2019**, *11*, 43936.
[317] W. Kang, F. Yavari, M. Minary-Jolandan, J. P. Giraldo-Vela, A. Safi, R. L. McNaughton, V. Parpoil, H. D. Espinosa, *Nano Lett.* **2013**, *13*, 2448.
[318] A. Safi, W. Kang, D. Czapleski, R. Divan, N. Moldovan, H. D. Espinosa, *J. Micromech. Microeng.* **2013**, *23*, 125014.
[319] K. H. Kim, R. G. Sanedrin, A. M. Ho, S. W. Lee, N. Moldovan, C. A. Mirkin, H. D. Espinosa, *Adv. Mater.* **2008**, *20*, 330.
[320] O. Y. Loh, A. M. Ho, J. E. Rim, P. Kohli, N. A. Patankar, H. D. Espinosa, *Proc. Natl. Acad. Sci. USA* **2008**, *105*, 16438.
[321] N. Moldovan, K.-H. Kim, H. D. Espinosa, *J. Microelectromech. Syst.* **2006**, *15*, 204.
[322] R. Yang, V. Lemaître, C. Huang, A. Haddadi, R. McNaughton, H. D. Espinosa, *Small* **2018**, *14*, 1702495.
[323] K. Riaz, S.-F. Leung, Z. Fan, Y.-K. Lee, *Sens. Actuators, A* **2017**, *255*, 10.
[324] L. Chang, D. Gallego-Perez, C. L. Chiang, P. Bertani, T. Kuang, Y. Sheng, F. Chen, Z. Chen, J. Shi, H. Yang, *Small* **2016**, *12*, 5971.
[325] X. Zhao, X. Huang, X. Wang, Y. Wu, A.-K. Eisfeld, S. Schwind, D. Gallego-Perez, P. E. Boukany, G. I. Marcucci, L. J. Lee, *Adv. Sci.* **2015**, *2*, 1500111.
[326] P. E. Boukany, A. Morss, W.-C. Liao, B. Henslee, H. Jung, X. Zhang, B. Yu, X. Wang, Y. Wu, L. Li, *Nat. Nanotechnol.* **2011**, *6*, 747.
[327] L. Chang, P. Bertani, D. Gallego-Perez, Z. Yang, F. Chen, C. Chiang, V. Malkoc, T. Kuang, K. Gao, L. J. Lee, W. Lu, *Nanoscale* **2016**, *8*, 243.
[328] D. Gallego-Perez, D. Pal, S. Ghatak, V. Malkoc, N. Higuita-Castro, S. Gnyawali, L. Chang, W.-C. Liao, J. Shi, M. Sinha, K. Singh, E. Steen, A. Sunyecz, R. Stewart, J. Moore, T. Ziebro, R. G. Northcutt, M. Homsy, P. Bertani, W. Lu, S. Roy, S. Khanna, C. Rink, V. B. Sundaresan, J. J. Otero, L. J. Lee, C. K. Sen, *Nat. Nanotechnol.* **2017**, *12*, 974.
[329] Z. Yang, J. Shi, J. Xie, Y. Wang, J. Sun, T. Liu, Y. Zhao, X. Zhao, X. Wang, Y. Ma, V. Malkoc, C. Chiang, W. Deng, Y. Chen, Y. Fu, K. J. Kwak, Y. Fan, C. Kang, C. Yin, J. Rhee, P. Bertani, J. Otero, W. Lu, K. Yun, A. S. Lee, W. Jiang, L. Teng, B. Y. S. Kim, L. J. Lee, *Nat. Biomed. Eng.* **2020**, *4*, 69.
[330] J. M. Escoffre, K. Kaddur, M. P. Rols, A. Bouakaz, *Ultrasound Med. Biol.* **2010**, *36*, 1746.
[331] Y.-I. Yamashita, M. Shimada, K. Tachibana, N. Harimoto, E. Tsujita, K. Shirabe, J.-I. Miyazaki, K. Sugimachi, *Hum. Gene Ther.* **2002**, *13*, 2079.
[332] W. Longsine-Parker, H. Wang, C. Koo, J. Kim, B. Kim, A. Jayaraman, A. Han, *Lab Chip* **2013**, *13*, 2144.
[333] J. M. Meacham, K. Durvasula, F. L. Degertekin, A. G. Fedorov, *Sci. Rep.* **2018**, *8*, 3727.
[334] X. Ding, M. P. Stewart, A. Sharei, J. C. Weaver, R. S. Langer, K. F. Jensen, *Nat. Biomed. Eng.* **2017**, *1*, 0039.
[335] T.-H. Wu, T. Teslaa, S. Kalim, C. T. French, S. Moghadam, R. Wall, J. F. Miller, O. N. Witte, M. A. Teitell, P.-Y. Chiou, *Anal. Chem.* **2011**, *83*, 1321.
[336] N. Kashaninejad, M. J. A. Shiddiky, N.-T. Nguyen, *Adv. Biosyst.* **2018**, *2*, 1700197.
[337] H. Hufnagel, A. Huebner, C. Gülch, K. Güse, C. Abell, F. Hollfelder, *Lab Chip* **2009**, *9*, 1576.
[338] P. Skafte-Pedersen, M. Hemmingsen, D. Sabourin, F. S. Blaga, H. Bruus, M. Dufva, *Biomed. Microdevices* **2012**, *14*, 385.
[339] W. Raimes, M. Rubi, A. Super, M. P. Marques, F. Veraitch, N. Szita, *Process Biochem.* **2017**, *59*, 297.
[340] M. T. Vitor, S. Sart, A. Barizien, L. G. de la Torre, C. N. Baroud, *Sci. Rep.* **2018**, *8*, 1225.
[341] D. Luo, W. M. Saltzman, *Nat. Biotechnol.* **2000**, *18*, 893.
[342] M. Giacca, S. Zacchigna, *J. Controlled Release* **2012**, *161*, 377.
[343] D. Ibraheem, A. Elaissari, H. Fessi, *Int. J. Pharm.* **2014**, *459*, 70.
[344] L. Guo, L. Wang, R. Yang, R. Feng, Z. Li, X. Zhou, Z. Dong, G. Ghartey-Kwansah, M. Xu, M. Nishi, Q. Zhang, W. Isaacs, J. Ma, X. Xu, *Saudi J. Biol. Sci.* **2017**, *24*, 622.
[345] Y. W. Cho, J. D. Kim, K. Park, *J. Pharm. Pharmacol.* **2003**, *55*, 721.
[346] A. Kabanov, V. Kabanov, *Bioconjugate Chem.* **1995**, *6*, 7.
[347] X. Gao, L. Huang, *Biochemistry* **1996**, *35*, 1027.
[348] P. L. Felgner, T. R. Gadek, M. Holm, R. Roman, H. W. Chan, M. Wenz, J. P. Northrop, G. M. Ringold, M. Danielsen, *Proc. Natl. Acad. Sci. USA* **1987**, *84*, 7413.
[349] D. Luo, W. M. Saltzman, *Nat. Biotechnol.* **2000**, *18*, 33.
[350] F. Krötz, C. De Wit, H.-Y. Sohn, S. Zahler, T. Gloe, U. Pohl, C. Plank, *Mol. Ther.* **2003**, *7*, 700.
[351] R. E. Hammer, V. G. Pursel, C. E. Rexroad Jr., R. J. Wall, D. J. Bolt, K. M. Ebert, R. D. Palmiter, R. L. Brinster, *Nature* **1985**, *315*, 680.
[352] M. T. Lin, L. Pulkkinen, J. Uitto, K. Yoon, *Int. J. Dermatol.* **2000**, *39*, 161.
[353] W. Walther, U. Stein, I. Fichtner, L. Malcherek, M. Lemm, P. Schlag, *Gene Ther.* **2001**, *8*, 173.
[354] D. L. Miller, S. V. Pislaru, J. F. Greenleaf, *Somatic Cell Mol. Genet.* **2002**, *27*, 115.
[355] C.-D. Ohl, M. Arora, R. Ikink, N. De Jong, M. Versluis, M. Delius, D. Lohse, *Biophys. J.* **2006**, *91*, 4285.
[356] K. A. Jinturkar, M. N. Rathi, A. Misra, in *Challenges in Delivery of Therapeutic Genomics and Proteomics* (Ed: A. Misra), Elsevier, Amsterdam, The Netherlands **2011**, p. 83.
[357] J. S. Soughayer, T. Krasieva, S. C. Jacobson, J. M. Ramsey, B. J. Tromberg, N. L. Allbritton, *Anal. Chem.* **2000**, *72*, 1342.
[358] A. A. Davis, M. J. Farrar, N. Nishimura, M. M. Jin, C. B. Schaffer, *Biophys. J.* **2013**, *105*, 862.
[359] P. Soman, W. Zhang, A. Umeda, Z. J. Zhang, S. Chen, *J. Biomed. Nanotechnol.* **2011**, *7*, 334.
[360] H. Nakamura, J. Funahashi, *Dev., Growth Differ.* **2013**, *55*, 15.
[361] C. Kalli, W. C. Teoh, E. Leen, in *Anticancer Genes*, (Ed: S. Grimm) Springer, New York **2014**, p. 231.
[362] J. J. Escobar-Chávez, D. Bonilla-Martínez, M. A. Villegas-González, A. L. Revilla-Vázquez, *J. Clin. Pharmacol.* **2009**, *49*, 1262.
[363] T. Jain, J. Muthuswamy, *Lab Chip* **2007**, *7*, 1004.
[364] J. A. Brown, V. Pensabene, D. A. Markov, V. Allwardt, M. D. Neely, M. Shi, C. M. Britt, O. S. Hoilett, Q. Yang, B. M. Brewer, *Biomicrofluidics* **2015**, *9*, 054124.
[365] F. M. Wurm, *Nat. Biotechnol.* **2004**, *22*, 1393.
[366] A. Pfeifer, I. M. Verma, *Annu. Rev. Genomics Hum. Genet.* **2001**, *2*, 177.
[367] L. Song, L. Chau, Y. Sakamoto, J. Nakashima, M. Koide, R. S. Tuan, *Mol. Ther.* **2004**, *9*, 607.
[368] Z. Zhou, X. Sun, J. Ma, C. Man, A. Wong, A. Leung, A. Ngan, *Sci. Rep.* **2016**, *6*, 22824.
[369] N. P. Restifo, M. E. Dudley, S. A. Rosenberg, *Nat. Rev. Immunol.* **2012**, *12*, 269.
[370] S. L. Maude, N. Frey, P. A. Shaw, R. Aplenc, D. M. Barrett, N. J. Bunin, A. Chew, V. E. Gonzalez, Z. Zheng, S. F. Lacey, *N. Engl. J. Med.* **2014**, *371*, 1507.
[371] C. Sheridan, *Nat. Biotechnol.* **2017**, *35*, 691.
[372] E. C. Svensson, D. J. Marshall, K. Woodard, H. Lin, F. Jiang, L. Chu, J. M. Leiden, *Circulation* **1999**, *99*, 201.

[373] R. L. Klein, E. M. Meyer, A. L. Peel, S. Zolotukhin, C. Meyers, N. Muzyczka, M. A. King, *Exp. Neurol.* **1998**, *150*, 183.
[374] L. Naldini, *Nature* **2015**, *526*, 351.
[375] L. Naldini, *Nat. Rev. Genet.* **2011**, *12*, 301.
[376] C. E. Thomas, A. Ehrhardt, M. A. Kay, *Nat. Rev. Genet.* **2003**, *4*, 346.
[377] T. Niidome, L. Huang, *Gene Ther.* **2002**, *9*, 1647.
[378] Y. Zhang, L. C. Yu, *BioEssays* **2008**, *30*, 606.
[379] M. Pisharodi, H. J. Nauta, *Stereotactic Funct. Neurosurg.* **1985**, *48*, 226.
[380] C. Galli, A. Perota, D. Brunetti, I. Lagutina, G. Lazzari, F. Lucchini, *Xenotransplantation* **2010**, *17*, 397.
[381] A. V. Kabanov, *Pharm. Sci. Technol. Today* **1999**, *2*, 365.
[382] S. C. De Smedt, J. Demeester, W. E. Hennink, *Pharm. Res.* **2000**, *17*, 113.
[383] M. E. Davis, *Curr. Opin. Biotechnol.* **2002**, *13*, 128.
[384] R. Duncan, *Nat. Rev. Drug Discovery* **2003**, *2*, 347.
[385] M. E. Davis, D. M. Shin, *Nat. Rev. Drug Discovery* **2008**, *7*, 771.
[386] M. E. Gindy, R. K. Prud'homme, *Expert Opin. Drug Delivery* **2009**, *6*, 865.
[387] V. J. Bruce, B. R. McNaughton, *Cell Chem. Biol.* **2017**, *24*, 924.
[388] K.-W. Kim, S.-H. Kim, J.-H. Jang, E.-Y. Lee, S.-W. Park, J.-H. Um, Y.-J. Lee, C.-H. Lee, S. Yoon, S.-Y. Seo, *Cancer Immunol. Immunother.* **2004**, *53*, 461.
[389] J. M. Weiss, C. Allen, R. Shivakumar, S. Feller, L.-H. Li, L. N. Liu, *J. Immunother.* **2005**, *28*, 542.
[390] T. Kamigaki, T. Kaneko, K. Naitoh, M. Takahara, T. Kondo, H. Ibe, E. Matsuda, R. Maekawa, S. Goto, *Anticancer Res.* **2013**, *33*, 2971.
[391] L. A. Wolfraim, M. Takahara, A. M. Viley, R. Shivakumar, M. Nieda, R. Maekawa, L. N. Liu, M. V. Peshwa, *Int. Immunopharmacol.* **2013**, *15*, 488.
[392] T. Conroy, F. Desseigne, M. Ychou, O. Bouché, R. Guimbaud, Y. Bécouarn, A. Adenis, J.-L. Raoul, S. Gourgou-Bourgade, C. de la Fouchardière, *N. Engl. J. Med.* **2011**, *364*, 1817.
[393] A. Neesse, P. Michl, K. K. Frese, C. Feig, N. Cook, M. A. Jacobetz, M. P. Lolkema, M. Buchholz, K. P. Olive, T. M. Gress, *Gut* **2011**, *60*, 861.
[394] W. S. Loc, S. S. Linton, Z. R. Wilczynski, G. L. Matters, C. O. McGovern, T. Abraham, T. Fox, C. M. Gigliotti, X. Tang, A. Tabakovic, *Nanomed.: Nanotechnol., Biol. Med.* **2017**, *13*, 2313.
[395] J. H. Adair, M. P. Parette, E. I. Altınoglu, M. Kester, *ACS Nano* **2010**, *4*, 4967.
[396] E. İ. Altınoğlu, J. H. Adair, *Future Oncol.* **2009**, *5*, 279.
[397] K. M. Gschweng, *J. Postdoct. Res.* **2018**, *23*, 25.
[398] H. Wang, Q. Li, J. Yang, J. Guo, X. Ren, Y. Feng, W. Zhang, *J. Mater. Chem. B* **2017**, *5*, 1408.
[399] J.-F. Paré, C. J. Martyniuk, M. Levin, *NPJ Regener. Med.* **2017**, *2*, 15.
[400] A. M. Xu, A. Aalipour, S. Leal-Ortiz, A. H. Mekhdjian, X. Xie, A. R. Dunn, C. C. Garner, N. A. Melosh, *Nat. Commun.* **2014**, *5*, 3613.
[401] P. Buttgereit, S. Weineck, G. Röpke, A. Märten, K. Brand, T. Heinicke, W. H. Caselmann, D. Huhn, I. G. Schmidt-Wolf, *Cancer Gene Ther.* **2000**, *7*, 1145.
[402] N. Ma, P. Ashok, D. Stevenson, F. Gunn-Moore, K. Dholakia, *Biomed. Opt. Express* **2010**, *1*, 694.
[403] Y. H. Li, L. F. Jin, L.-F. Du, Q. S. Shi, L. Liu, X. Jia, Y. Wu, F. Li, H. H. Wang, *Int. J. Oncol.* **2013**, *43*, 151.
[404] K. Ishiguro, O. Watanabe, M. Nakamura, T. Yamamura, M. Matsushita, H. Goto, Y. Hirooka, *BioTechniques* **2017**, *63*, 37.

Dorsa Morshedi Rad is a Ph.D. candidate of biomedical engineering at the University of Technology Sydney. She received her bachelor's degree as a first rank student in cell and molecular biology from the Ferdowsi University of Mashhad, Iran, in 2015. Afterward, she completed her master's degree with honors in medical genetics at Mashhad University of Medical Sciences, Iran, in 2018. Her current research interest focuses on design and development of novel microfluidic devices for intracellular delivery of various biomolecules inside the different cell types.

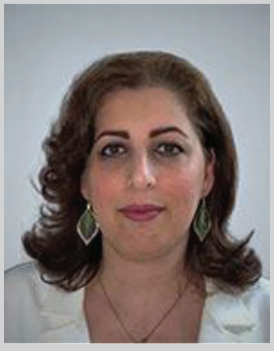

Maryam Alsadat Rad received her first Ph.D. in solid-state physics from University Science Malaysia in 2014. She was appointed as a postdoctoral researcher over two years at Sharif University of Technology in Iran and University of Technology Malaysia (UTM). She has conducted research on cancer cells in the microfluidic environment. She is currently working toward her second Ph.D. in biomedical engineering at the University of Technology Sydney. She is conducting a multidisciplinary project on the hydrogel scaffolds for the study of 3D in vitro spinal-cord injury models.

Sajad Razavi Bazaz received his M.Sc. degree as a first rank student in biomedical engineering from University of Tehran, Iran, in 2017. He currently holds a position as a Ph.D. candidate in School of Biomedical Engineering at University of Technology Sydney. His main research interest is to investigate fundamentals of inertial microfluidics in hard chips and design and fabricate functional 3D printed inertial microfluidic devices for particles/cells separation and intracellular delivery.

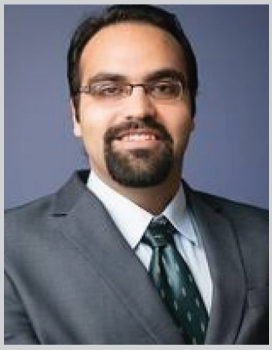

Navid Kashaninejad received his B.Sc. and M.Sc. degrees in mechanical engineering, energy conversion. In 2013, he obtained his Ph.D. degree from the Division of Thermal and Fluid Engineering, Nanyang Technological University (NTU), Singapore. His Ph.D. studies mainly focused on design and fabrication of microfluidic devices. He is currently a research fellow at Queensland Micro- and Nanotechnology Centre (QMNC), Griffith University, Australia.

Dayong Jin is a distinguished professor in the School of Mathematical and Physical Sciences and director of IBMD at the University of Technology Sydney. He specializes in physics, biophotonics, and nanotechnology to develop the next-generation technologies for multifunctional hybrid biomaterials, rapid diagnostics, point-of-care sensing, targeted delivery systems, and biomedical device engineering. He is currently the science director of ARC Research Hub for integrated device for end-user analysis and the co-director of Australia–China Science and Research fund joint research center for point of care testing.

Majid Ebrahimi Warkiani is an associate professor in biomedical engineering at University of Technology Sydney. He completed his Ph.D. program at Nanyang Technological University and subsequently undertook postdoctoral training at the Singapore–MIT Alliance for Research and Technology (SMART) center. He is an NHMRC-CD fellow and also a member of Institute for Biomedical Materials & Devices (IBMD) and Center for Health Technologies (CHT) at UTS. His current research activities focus on microfluidic devices for particle and cell sorting and intracellular delivery, 3D Printing, and organs-on-a-chip.